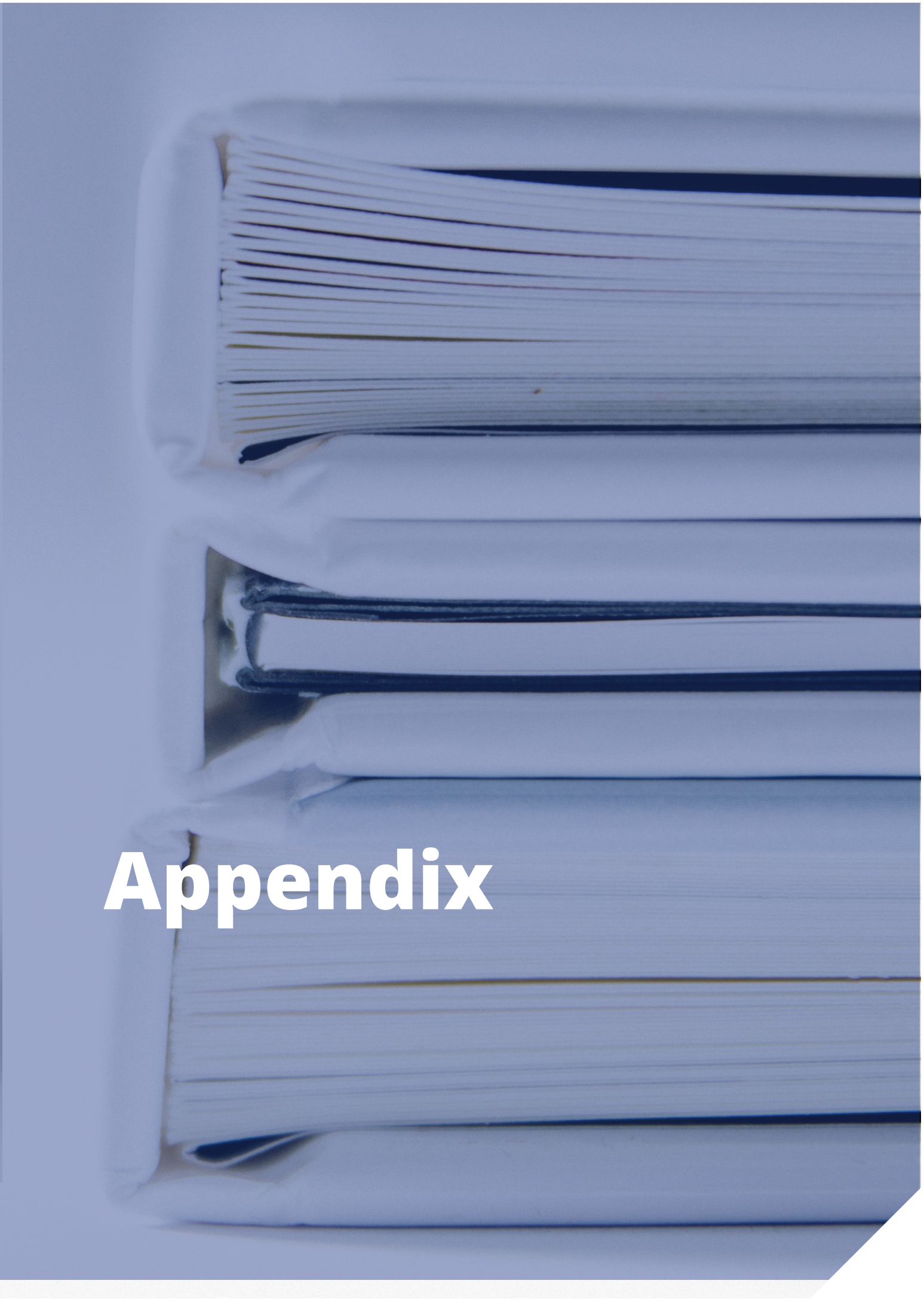

# Appendix

# 1. Additive manufacturing

*The general additive manufacturing process*

The general process of creating objects with additive manufacturing consists of 8 steps which can be divided into three main phases; the preparation, process and the post processing phase(see figure 74). The preparation phase consists of the actual digital modeling of the desired object to be produced by additive manufacturing, for this a CAD model is required. This modeling step can be done with different CAD software programs available. For this step there are no design limitations, the only limitation is the file extension of the CAD file. The output file should be suitable for import in the slicing software. The standard file used for example in rapid prototyping is the tessellated model, also known as the stereolithography file or STL file (Kai et al., 2000). In this file the 3D object is described with a coordinate list of vertices of triangles which approximate the actual surface of the model (figure 75).

Slicing is the process of converting the digital tessellated 3D model into horizontal slices(layers). Due to the intersection of the triangulated surfaces and the horizontal slices, a closed horizontal polygon is defined for each slice (Pandey et al., 2003). This closed horizontal polygon will act as the toolpath of the printer. The height of these slices can be altered in the slicing software as well as other settings like the printing temperature, printing speed, infill etc. By decreasing the height of the slice, also known as the layer height, the approximation of the actual model surface will be more accurate and smoother (figure 76).

When all settings are set accordingly to the desired combination, the next phase of the process starts. This is the actual process phase where the 3D object is built layer upon layer according to input file. The material is deposited across the toolpath according to the closed polygons in the horizontal slices. For FDM technologies, the first layer will be built on a building platform and after finishing the deposition toolpath of the first layer, the build platform moves one layer height distance in the z-direction in order to deposit the second layer on top of the first layer. This process continues until all layers are deposited.

The final phase of the process is the post-processing of the build 3D object. For some additive manufacturing technologies it is necessary to remove any support material.

*Advantages*

The advantage of RP is the ability to create complex shapes without geometric restrictions. It allows more form freedom compared to subtractive processes as milling, turning, carving, grinding etc. Its simplicity and easy usage, the wide variety of nontoxic materials and cost effective maintenance and repair contributes to its popularity. The main advantage of rapid prototyping is being able to produce prototypes in a timeframe of hours instead of days, weeks or even months.

*Applications*

RP is commonly used as an iterative process in order to test form, fit, function or user interaction in design or development related industries.

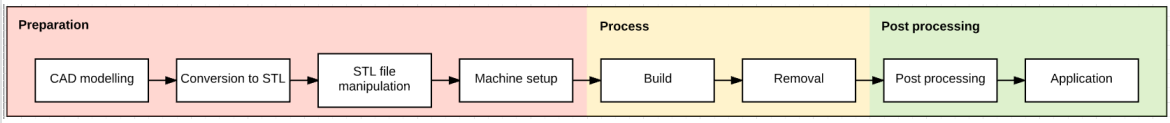


*Figure 74*

*Figure 74 Overall additive manufacturing procedure*

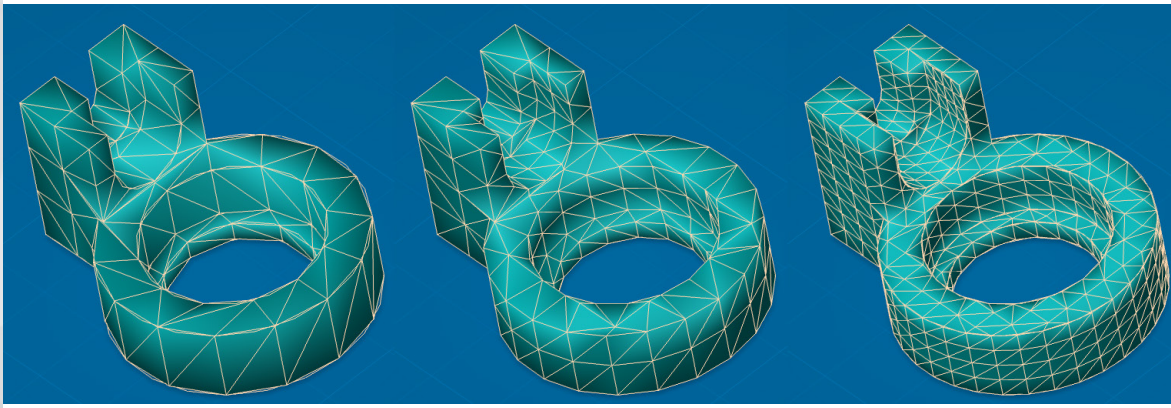

*Figure 75*

*Figure 75 Tesselation of 3D model*

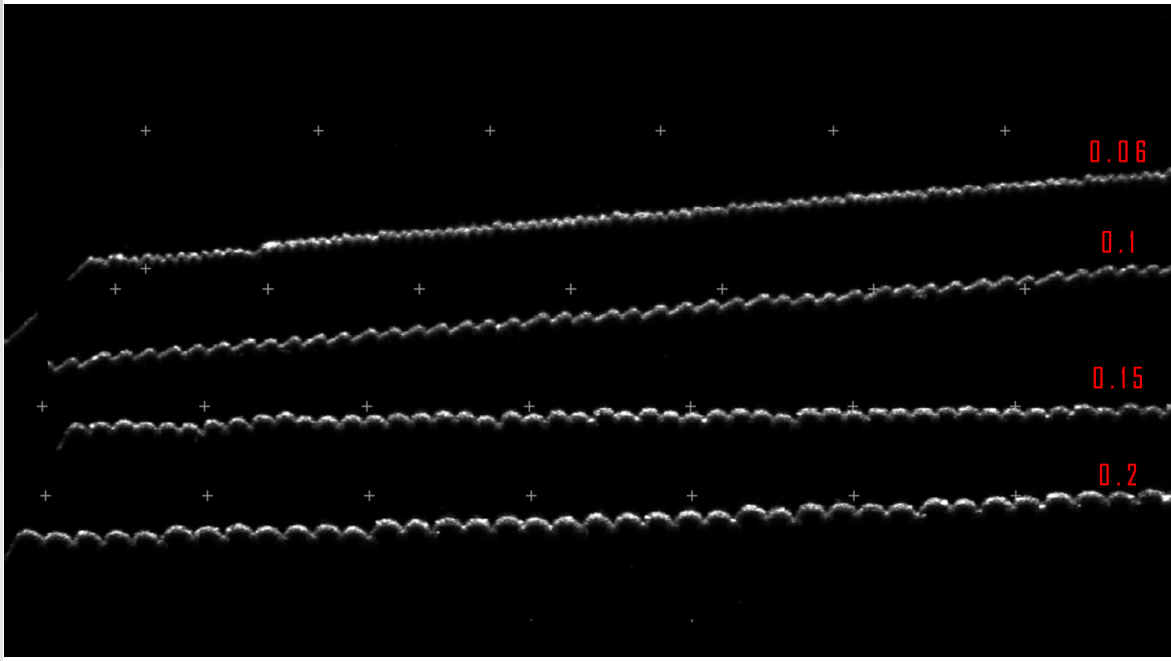


*Figure 76*

*Figure 76 Overview different layer height settings with respect to surface profile*

# 2. Fused Deposition Modelling

As mentioned before, Fused Deposition modelling(FDM), is one of the current existing additive manufacturing technologies. The basic principle of the FDM process is the buildup of a 3D model layer-by-layer by melting, extruding and solidifying thermoplastic material in the form of filament. In this section the FDM technology will be covered considering all aspects belonging to this technology. These aspects consist of the material, material transport, the extruder head, the extruding process and the deposition.

For the FDM process a similar preparation process is required mentioned in appendix 1 on rapid prototyping. A prepared file is required for the 3D printer in order to enable the build process. The machine setup for the FDM technology is different than the other rapid prototyping technologies.

*Filament material*

The FDM technology requires a material in the form of filament, basicly a spool of a thermoplastic wire. Nowadays there is a wide variety of 3D printable filaments available to use for the FDM process. The most popular used materials for FDM are Polylactic acid(PLA) and Acrylonitrile-Butadiene-Styrene(ABS). PLA is known for its reliability and high surface quality finish. This material is produced from organic and renewable sources as corn starch and sugarcane and is a biodegradable thermoplastic. ABS is a common used material in the manufacturing industry and has good mechanical properties as hardness, toughness and electrical isolation. Other engineering materials suitable for 3D printing include Nylon, Polycarbonate(PC), co-polyester(CPE), thermoplastic polyurethane (TPE 95A) (see figure 77) and some material combination filaments.

Nylon is known for its durability, flexibility, corrosion resistance to alkalis and organic chemicals and high strength. Because of these properties this material is suitable for engineering purposes as the creation of functional parts and tools.

PC, polycarbonate, is also an engineering plastic and has good mechanical and thermal properties when it comes to strength, toughness and temperature stability. This material retains its dimensional properties when exposed to high temperatures up to 110 °C (Ultimaker,2017). These properties allow this material to be used for example functional parts and tools which will be used in varying temperature conditions.

Another material suitable for applications where temperature plays an important role is CPE(co-polyester). Especially the CPE+ filament version which provides a higher temperature resistance than the regular CPE. Both can resist chemicals and have good mechanical properties.

TPU 95A, thermoplastic polyurethane, is a printable flexible material which can offer properties similar to rubber and plastic. This material has good mechanical properties for wear and tear resistance. In combination of its high impact strength makes this material a good engineering plastic for functional prototype parts such as drive belts.

The filament is being transported to the extruder head in order to be extruded. This transportation is done by the feeder, often referred as the cold end of the extruder, as no heat is required. There are different methods for transporting filament to the extruder head in FDM printing. Two main methods used for filament transportation are the bowden tube and direct drive. Both of the methods include an feeder stepper motor to push the filament forward, however there is a difference in the location of this feeder stepper motor.

*Figure 77 Overview available ultimaker materials*

*Figure 77*

In the case of the bowden tube method the filament has to travel a certain distance through a teflon tube, used by ultimaker prtinters, before reaching the extruder head. This feeder stepper motor is fixed on the frame of the 3D printer. The main advantage of a bowden tube extruder is the weight reduction of the extruder head which allows the extruder head to move faster, increasing print speed.

For the direct drive extrusion, the feeder stepper motor is placed above the extruder head. The distance the filament needs to travel from the feeder to the extruder is significantly less than the bowden tube extrusion. This enables direct drive printers to print flexible materials such as TPU more easily than bowden extruders. However the addition of the weight of the feeder motor to the extruder head can lead to visible surface defects due to the inertia during rapid movement changes (see figure 78).

The filament is pushed to the hotend of the extruder head in which it is melted till a semi liquid state is achieved. The hotend of the extruder consists of several parts namely the heat sink, heat break, heat block containing the thermistor or thermocouple and heater cartridge. At the end there's the nozzle from which filament is extruded. The filament enters the hotend of the extruder through the heat sink which is in most cases extra ventilated in order to minimize the heat transfer from the heat block into the heat sink. Excess heat from the heat block in the heat sink could lead to clogging due to filament losing its rigidity.
The heat block is heated by the heater cartridge and the temperature is measured with a thermistor or thermocouple.

The nozzle is located at the heat block and is automatically heated by the heat of the heat block. Filament is melted in the nozzle and extruded by the controlled pressure on the filament by the cold end of the extruder.

The extruded filament is deposited on the build plate on which the 3D object is build layer-by-layer. The extruder head is moved according to the toolpath from the G-code file and after finishing the horizontal path the build plate or the extruder head moves in the z-direction. This process continues until all layers are extruded and the complete 3D object is build.

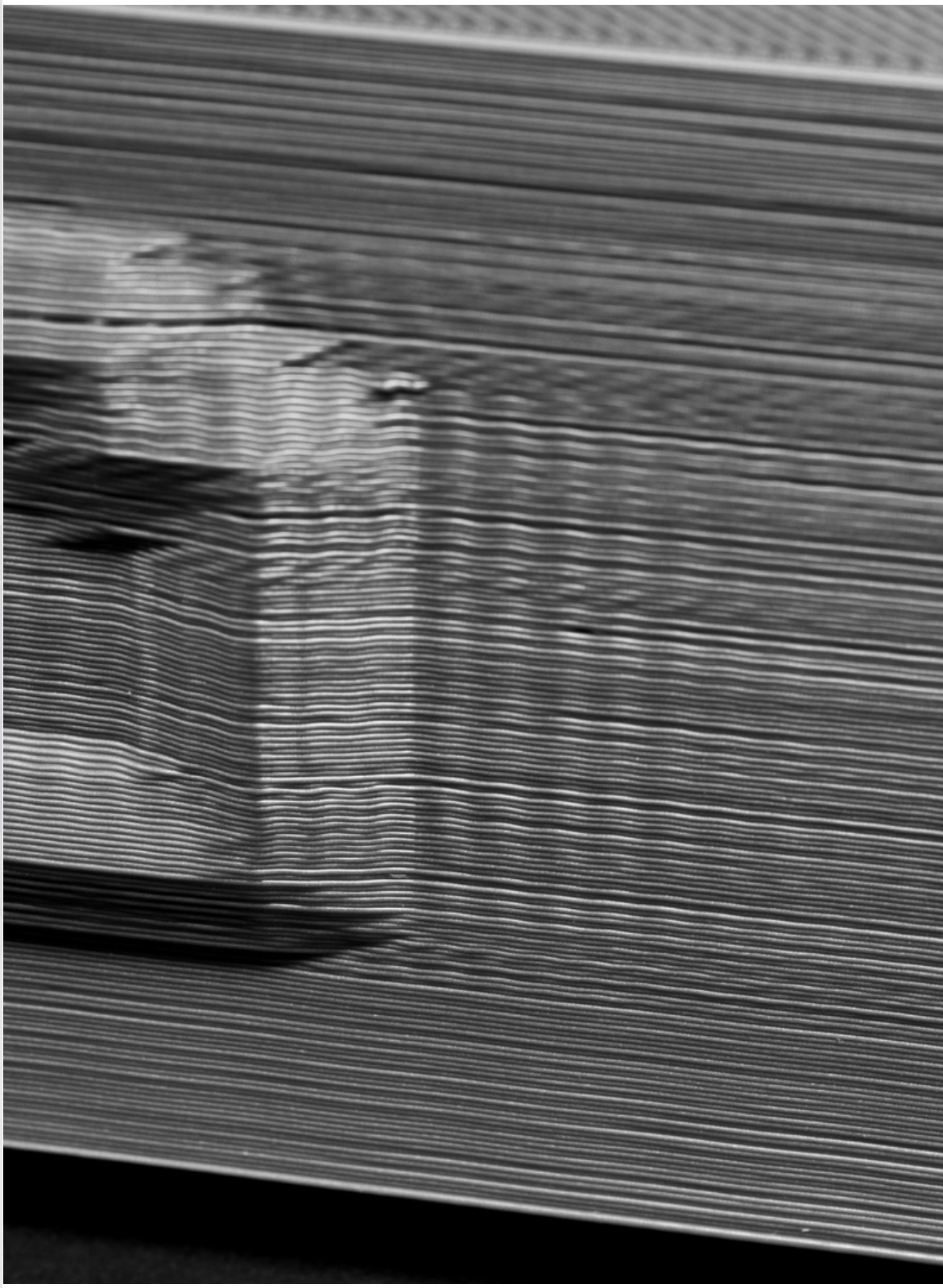

*Figure 78*

*Figure 78  Surface defects due to vibrations*

# 3. Ultimaker 3

The Ultimaker 3 is the newest 3D printer from Ultimaker and was introduced the 18th of October 2016. This new version of the Ultimaker features a dual extrusion extruder with auto nozzle-lifting system. This auto nozzle-lifting system excludes the problem of the second nozzle interfering with the primary printing nozzle which affect the printing quality.

The print head exists of two independent swappable print cores for a high uptime and fast maintenance. Auto leveling is integrated in terms of a sensor which measures the height of the print bed and calculated how much tilt the print bed has. All electronics of the extruders, thermistor and heater, are integrated in the print cores which can be accessed by lowering the front fan lid.

During printing, the objects are cooled by 2 fans with greater pressure build-up and optimized airflow. This enables better bridging and smooth surface prints. The filaments for the Ultimaker 3 are embedded with NFC chip in order for the system to automatically recognize the material and color, adjusting the print settings accordingly.

Next to the NFC technology, wireless connectivity is also incorporated. It is possible to connect to the printer with mobile devices and monitor the 3D printing process with the build in camera. (Ultimaker, 2017)

All features of the Ultimaker 3 3D printer can be seen in figure 79.

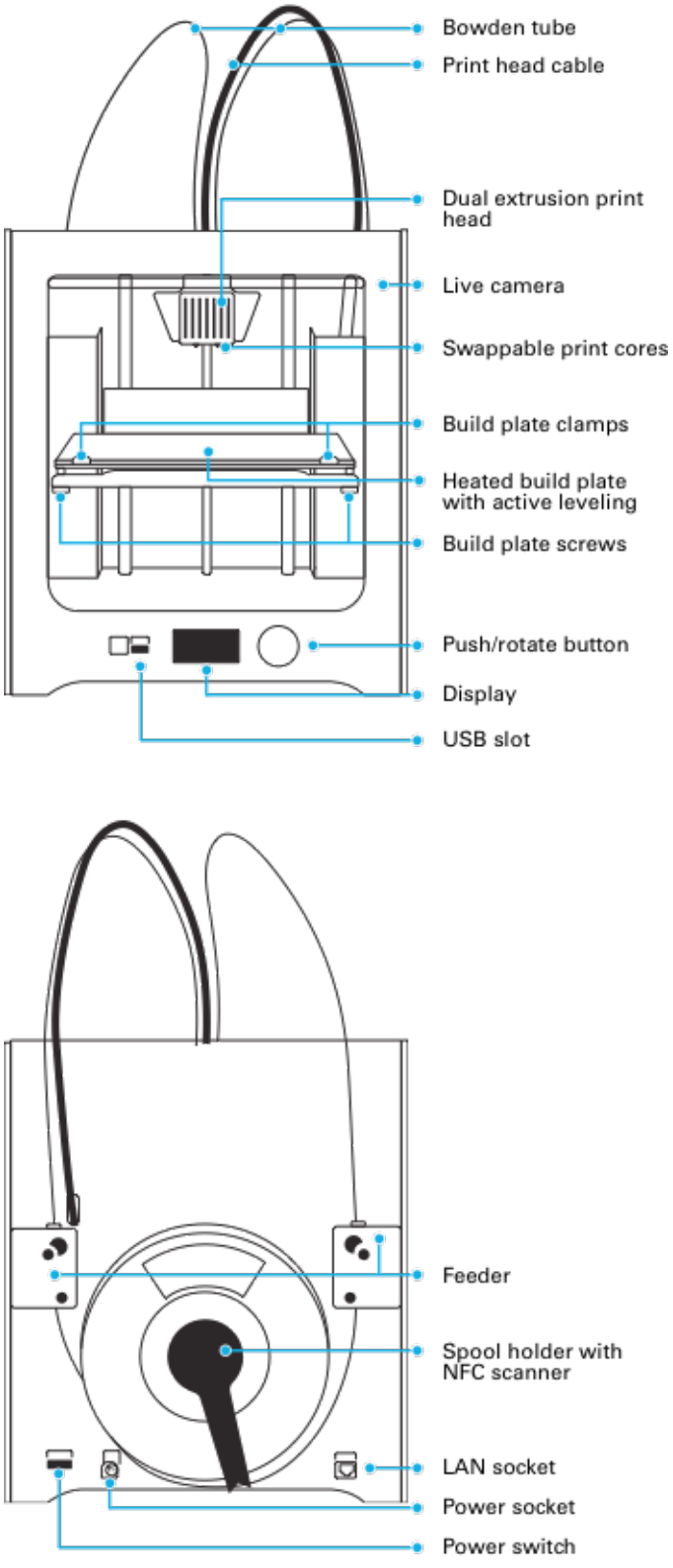


*Figure 79*

*Figure 79 Schematic overview of features Ultimaker 3*

# 4. Cura slicing software

To be able to 3D print the designed model, the 3D printer has to be able to identify the required settings and toolpath of the deposition of the material. This process is done by a slicing software in which the user can import a STL, OBJ or 3MF file of the 3D model and create the desired file; a G-code. This G-code file contains the code that informs the 3D printer what toolpath to follow, how fast to move and where to move to.

Ultimaker has its own slicing software called Cura. Cura's interface shows a preview of the 3D model and a sidebar with print settings which can be altered. Loading in a 3D model will automatically start the real time slicing process and informs the user on the required build time and material usage (figure 80). The Cura software has two different modes; the recommended and the custom mode. In each mode the general printer settings can be changed consisting of settings to specify the selection of print cores, materials for the two extruders and layer thickness.

The recommended mode gives the user predescribed profiles to choose from which have been provided and optimized by Ultimaker. These profiles are categorized by their layer height and named Draft print(0.2 mm), Fast print(0.15 mm), Normal quality(0.1 mm) and High quality(0.06 mm) respectively based on Cura 2.5. In the recommended mode the infill density can be altered with two options to include; enabling support and enabling build plate adhesion.

In the custom mode, the predescribed profiles can be altered accordingly to the users preference. New profiles can be created by users for specific 3D printing purposes or applications. In newer versions of Cura the user can alter categories such as quality, shell, infill, material, speed, travel, cooling, support, adhesion, dual extrusion and some experimental and special modes. Figure 81 shows an overview of general settings which can be altered per category.

Each change in the printing settings has influence on the final 3D printed model. Cura has integrated feedback to the user on what setting can be influenced by changing one another. By enabling this the user gains more insight in the expected end result and prevents the occurrence of settings override each other.

After adjusting the settings according to the preference of the user, the file can be transferred to the ultimaker 3D printer. The ultimaker 3 features multiple options to acquire the g-code from the slicing software Cura. This can be done with the use of an USB stick and with WIFI or LAN connection. Now the 3D printer is able to recognize the required information and incorporate the preferred settings in the FDM process.

In newer versions of Cura it is possible to import image files(jpg,jpeg,png,bmp and gif) and transform it into a 3D printable surface. The difference in darker and lighter colors is taken as a reference in order to create a 3D surface. The user is able to choose whether the darker colors are higher/lower and vice versa. An example of a wood texture image converted to a 3D surface can be seen in figure 82.

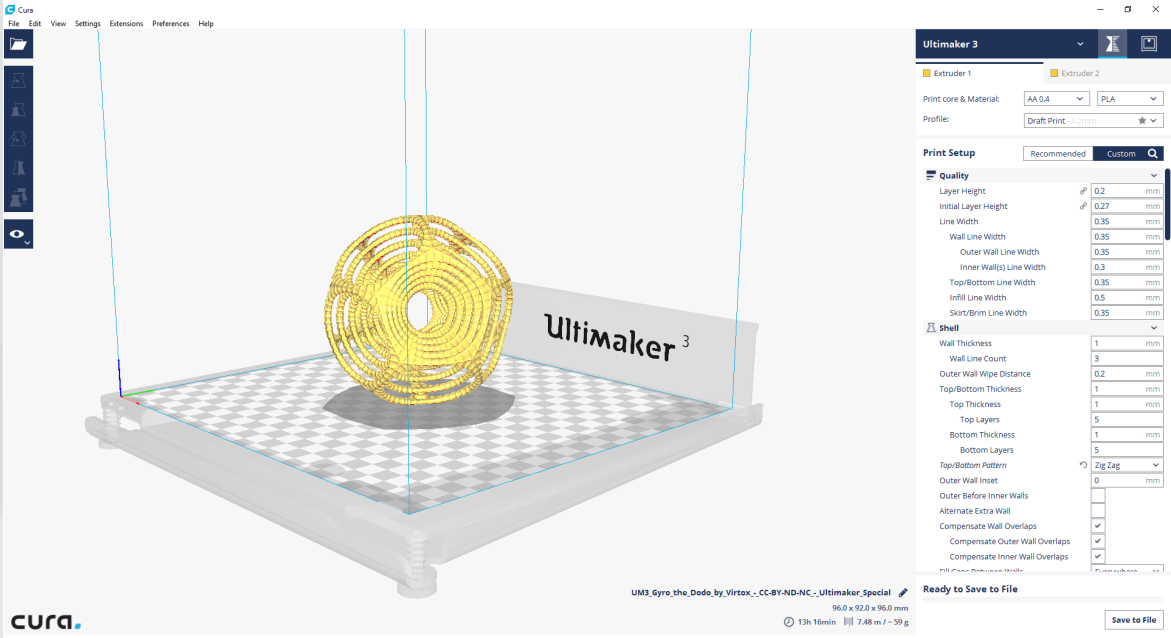


*Figure 80 Cura 2.4 overview*

*Figure 80*

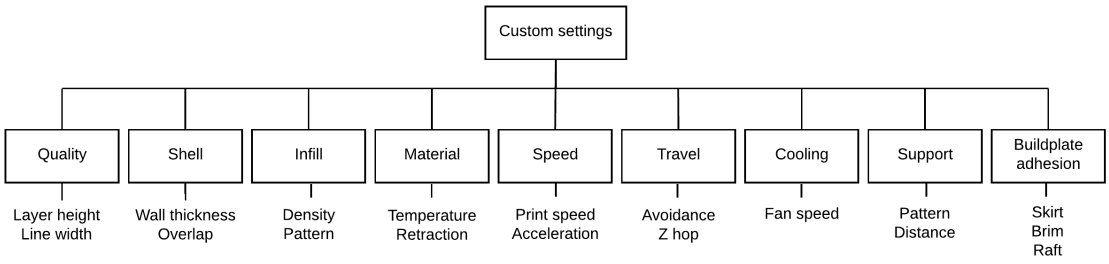


*Figure 81 Overview of different settings per category*

*Figure 81*

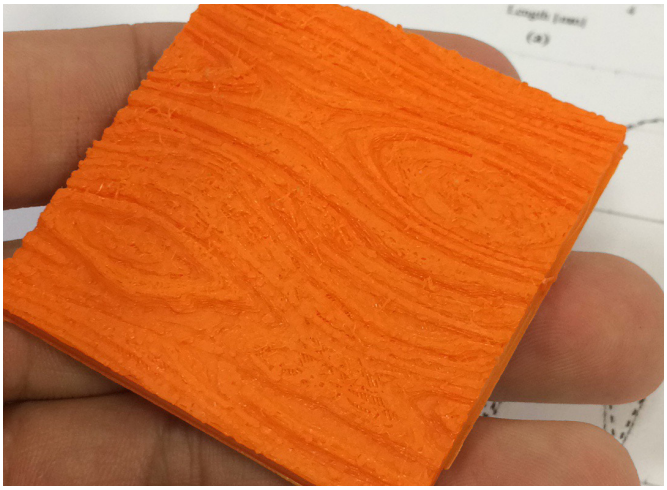

*Figure 82 Example of immitation of wood surface texture*

*Figure 82*

# 5. Surface roughness

Roughness is one of the 5 quality attributes for manufacturing processes such as additive manufacturing. The roughness attribute refers to the surface roughness of a part, which can be smooth or coarse and has a link to how the surface is perceived with the eye and touch(Tempelman, 2014). Of the other attributes - tolerance, defects, properties and reproducibility - defects also refers to the quality of surfaces as surface imperfections such as extrusion errors influence the roughness.

As FDM manufactured objects are build up from layers upon layers, the surface finish is significantly rough compared to other manufacturing processes such as injection molding, where the surface finish could be incorporated in the mold.

There are different terms used for defining the roughness of a certain surface. The most used term in surface roughness research is the Ra, defined as being the arithmetic average height of peak heights and valleys from the mean line, measured along a certain distance (figure 83). The Ra value gives an overall impression on the surface roughness, however surface defects or irregularities are not taken into account. To incorporate the surface irregularities the term Rq is used which can be defined as geometric average height of surface irregularities from the mean line measured along a certain distance (figure 83). The main difference between the Ra and the Rq is the fact that the Rq amplifies the peaks and valleys, taking irregularities more into account.

In order to measure the surface roughness the surface profile has to be mapped to identify the peaks and valleys. This can be done by profilometers, rugosimeters or optical laser systems. Most of the profilometers and rugosimeters available use a fine stylus which moves across a certain surface in order to calculate the surface roughness. The optical laser system projects a laser light beam on the surface which is scattered/reflected and projected onto a sensor in order to obtain the surface profile (Appendix 6 p.100).

Perfect buildup of layers

An actual measured surface profile is used to mathematically model the surface and calculate the surface roughness. Figure 84a shows the scanned surface profile used for this modelling and was printed with an angle of 90 degrees from the horizontal plane. So the mathematical approach will be for the build up of a surface printed with an angle of 90 degrees. For viewing convenience the surface is displayed flat. On top of the measured surface profile a build up of layers is placed, figure 84b. What can be see is that each layer has an overlap with the adjacent layers.

For the surface profile the top part, from the overlap to the tops, is necessary to be able to calculate the surface roughness. These tops show similarities with peaks of parabolic functions till the point the other layers meet. For the modelling of the peak the basic formula of a parabolic has been used; y=ax^2+bx+c. With the use of the mathematical web application Desmos, the corresponding values for a, b and c have been calculated for line width 0.4 mm and layer heights of 0.2 mm, 0.1 mm and 0.06 mm. This has led to 3 different formulas namely; y=-20x^2+x+0.2 for 0.2 mm layer height, y= -80x^2=x+0.2 for 0.1 mm layer height and y=-222.22x^2+x+0.2 for the layer height of 0.06mm. The 0.2 mm layer height function was taken over a domain of (-0.1, 0.1), 0.1 mm layer height over (-0.05, 0.05) and the 0.06 mm layer height over a domain of (-0.03, 0.03).

$$Ra = \frac{1}{\ell}\int_0^{\ell} |Z(x)|\,dx$$

$$Rq = \sqrt{\frac{1}{\ell}\int_0^{\ell} Z^2(x)\,dx}$$

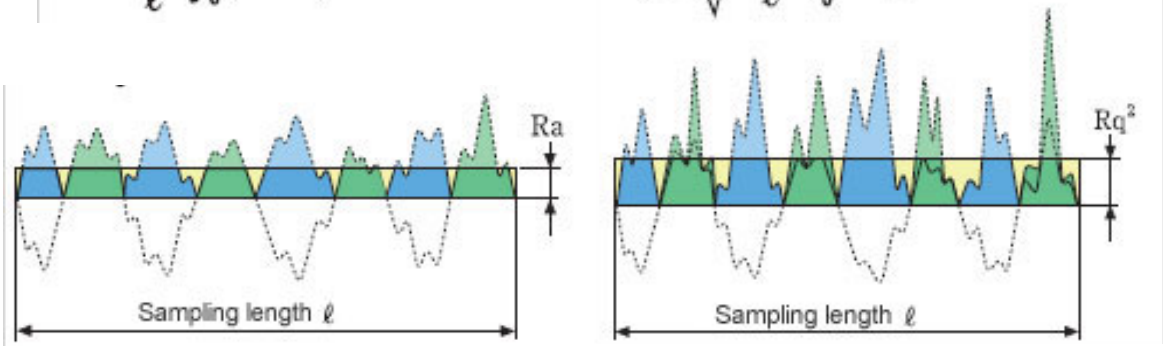


*Figure 83 Mathematical models for Ra and Rq calculation*

*Figure 83*

*Figure 84a*

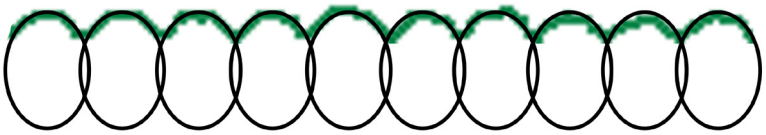

*Figure 84b*

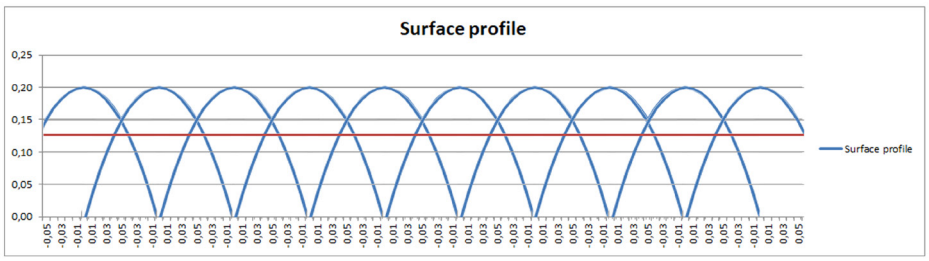


*Figure 84c*

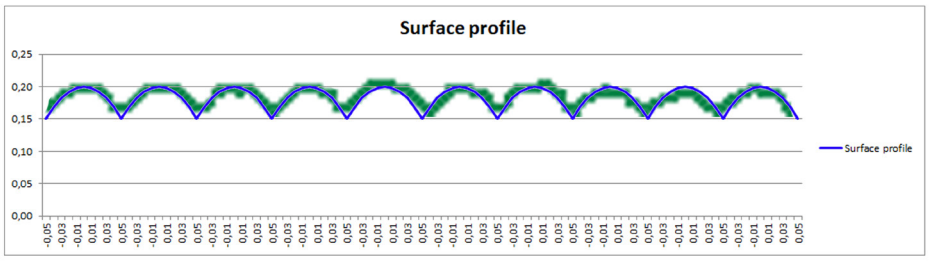


*Figure 84d*

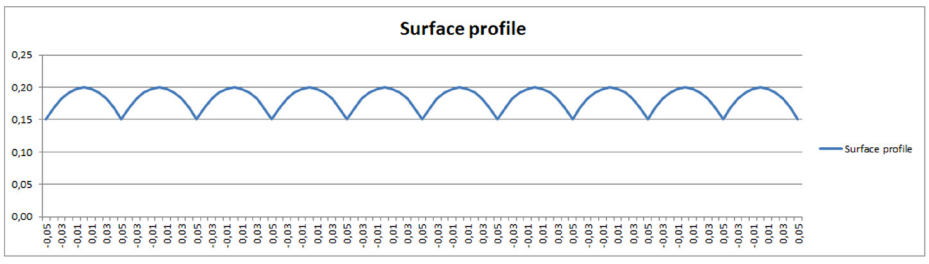


*Figure 84e*

*Figure 84 Mathematical approach for surface roughness reproduction*

These peaks with corresponding domains have been repeated for 10 times in order to create 10 layers and to incorporate the overlap the adjacent peaks are partly merged, see figure 84c. In order to complete the surface profile, the points below the layer overlap have been excluded as those will not be included in the calculation, see figure 84d. Now all data points of the model describing the surface profile can be used for surface roughness calculations. The modelled surface profile can be found in figure 84e.

All of the processing and collection of data has been done in excel. The procedure of calculating roughness values was similar for all mathematical surface profile representations. The mathematical representation graphs looked identical for all layer heights except for the domain values as this is based on the layer height. The range stays the same as a 0.4 mm nozzle is incorporated.

The results for the layer height of 0.2 mm indicate a surface roughness value Ra of 14 µm and a Rq value of 0.5 µm. The roughness values of a layer height of 0.1 mm correspond to a Ra of 13 µm and Rq of 0.5 µm. And 0.06 mm layer height resulting in a  Ra of 14 µm and a Rq of 0.5 µm.

From the results it is clear there is a difference in roughness Ra however for the Rq there is no significant change. The Rq value incorporates the errors more than in the Ra value as values are squared for Rq. But for a ideal buildup of layers there are no errors or inconsistencies which can affect the Rq value and explains the low Rq values. For the Ra there are some changes especially for the layer height of 0.06 mm. The main difference in the calculation of the roughness values is the amount of data points between the different layer height. For the layer height of 0.06 mm less data points were calculated then the calculation for layer height 0.2 and 0.1 mm. This might account for the change in the roughness Ra as the model has a lack of fit is not able to describe the surface profile accurately.

Conclusion

This section tried to mathematically calculate/ approach the surface roughness of different layer heights with an ideal buildup of layers. The roughness values Ra and Rq were calculated for 0.2, 0.1 and 0.06 mm layer heights. These roughness values were Ra=14 µm(Rq=0.5 µm), Ra=13 µm(Rq= 0.5 µm) and Ra= 14 µm(Rq= 0.5 µm) respectively. The low Rq values refer to the ideal buildup of layers without errors or inconsistencies which otherwise increase the Rq value.

# 6. Optical scanning system

For initial surface roughness scanning exploration, different "roughness cubes" were printed incorporating different printing settings and materials (figure 85). These printing settings were based on existing printing profiles provided by Ultimaker. This cube consists of 18 planes having different angles, including downward and upward facing surfaces. This to investigate the influence of the angle orientation from horizontal plane on the roughness. The model is constructed in such a manner there is always a flat surface facing upwards at similar heights for measuring.

*Scanning apparatus*

The optical scanner used for the measurements of the 3D printed surfaces is the Micro-epsilon ScanControl 2910-10/BL laser line sensor, figure 86. This laser line sensor operates with the use of a semiconductor with a wavelength of 405 nanometers which is visible blue light. It operates according to the method of optical triangulation. The laser line is displayed on the surface with the use of a linear optical system consisting of special lenses. The diffusely reflected light of the laser is captured by the highly sensitive sensor. The captured image is used to calculate the distance, the z axis, and the position , the x axis along the projected laser line. The result of this is a surface profile line which can be used for average roughness calculations(Micro epsilon,2017).

For the measurement of the surface profile of a 3D printed object the laser line of the optical scanner has to be perpendicular to the layer lines of the 3D printed surface. The width of the surface profile measurement is approximately 1 cm.

This scanning module is fixed on a frame which is able to move in the Z-direction with the use of a screw thread shaft. In order to scan a particular surface area, a movable platform is integrated which can move in the Y direction. This platform is equipped with magnetic parts to fix objects. With the use of python scripts, programmed by Oscar van de Ven, the scanning module and the platform can be adjusted. The interface of this control panel can be seen in figure 87.

*Software*

In order to operate the scanning module two programmes are required to obtain and process data. The software to obtain data from the module is Micro Epsilon scanCONTROL Configuration Tools 5.0 in which general settings can be adjusted. These settings include the exposure time, nr. of profiles and trigger modes. When scanning a surface the object should be placed in the focus area of the laser. With the display image preview a 2D surface profile can be seen if placed correctly. Adjusting the exposure time has influence on how well the measurement can be done. Over- and underexposing can lead to inaccurate results as surface points could not be identified properly. The kind of material has also significant influence on the accuracy of the surface profile. Materials which are (semi) transparent, containing reflective particles or blue pigment are difficult to measure. Figure 88 displays the difference in accuracy of the measurement between white PLA and Pearl White PLA which is shiny and semi transparent. In the case of (semi)transparent the laser light is scattered through the materials which makes it hard to be projected on the sensor. Reflective particles reflect the laser light which will result in gaps in the surface

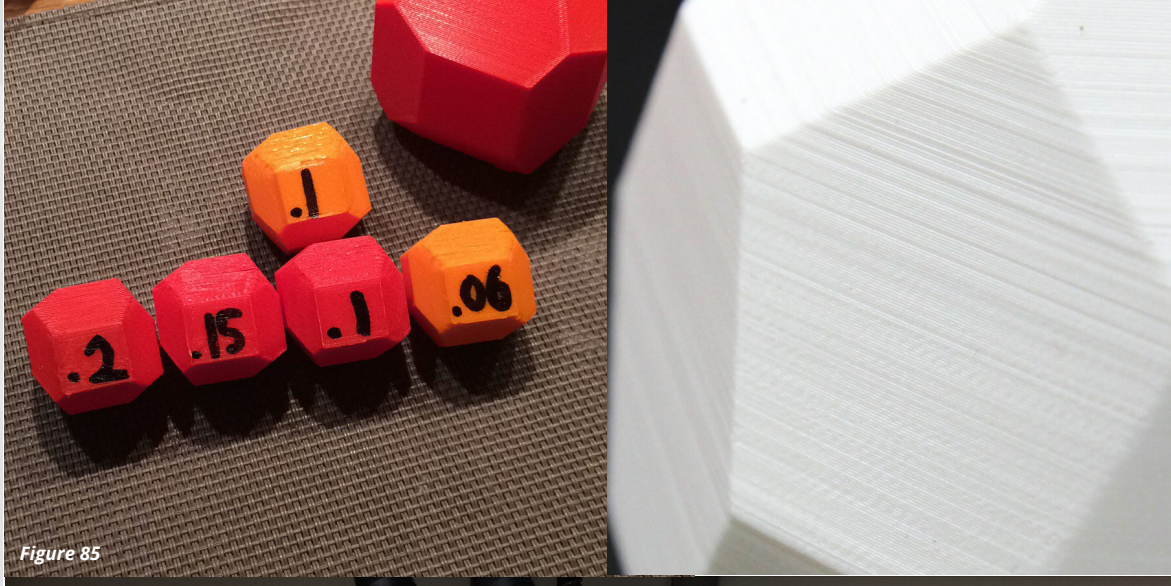


Figure 85

*Figure 85 Initial testing model; R-cube*


Figure 86

*Figure 86 Optical scanner system with scan module, sample holder and movable platform*

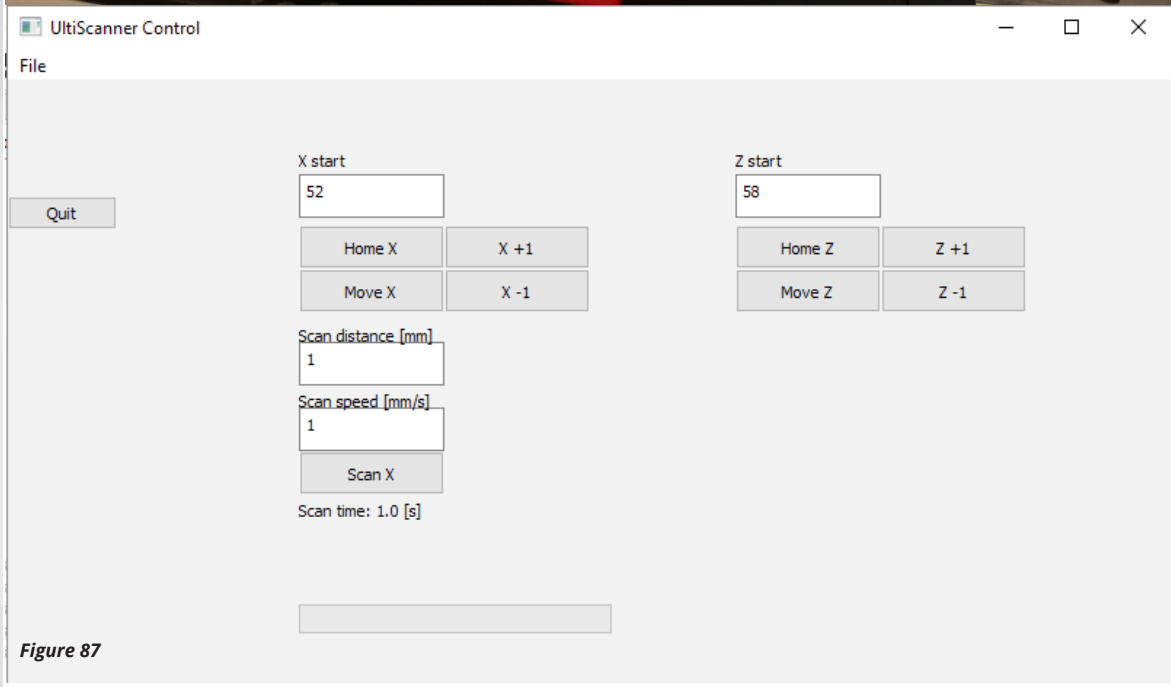


Figure 87

*Figure 87 Movable platform control interface*

profile. Blue colored surfaces can be hardly measured due to the blue laser light of the scanner.
Surface profiles can be scanned in two ways; separate or continuous measurements. The main difference is the amount of profiles which is significantly more with a continuous measurement. Any surface defects could be better identified with a continuous measurement as a particular surface area is scanned.

The saved surface profiles can be opened with Micro Epsilon scanCONTROL 3D-View 3.0 and reviewed on the quality of the measurement. The measurement profiles can be plotted as a 3D surface, see figure 89. The overall purpose of this program for this research is to export the 3D data. This 3D data can then be used for surface roughness calculations in python scripts, programmed by Oscar van de Ven, see figure 90.

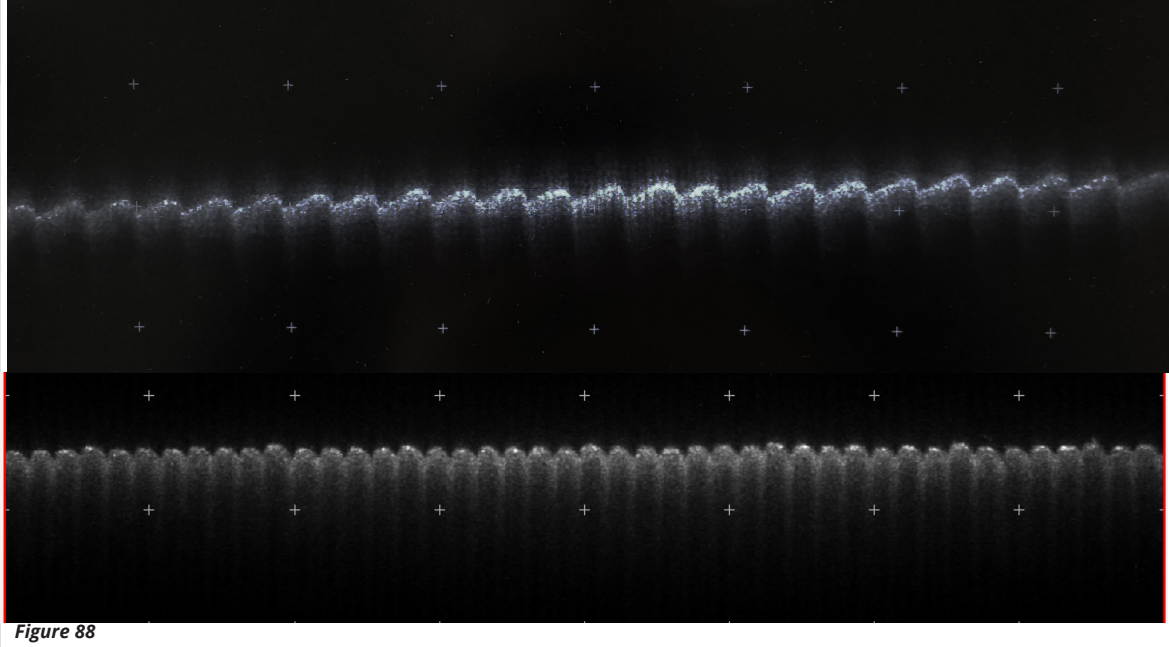

*Figure 88 Difference in accuracy between PLA white and PLA pearl white*

*Figure 88*

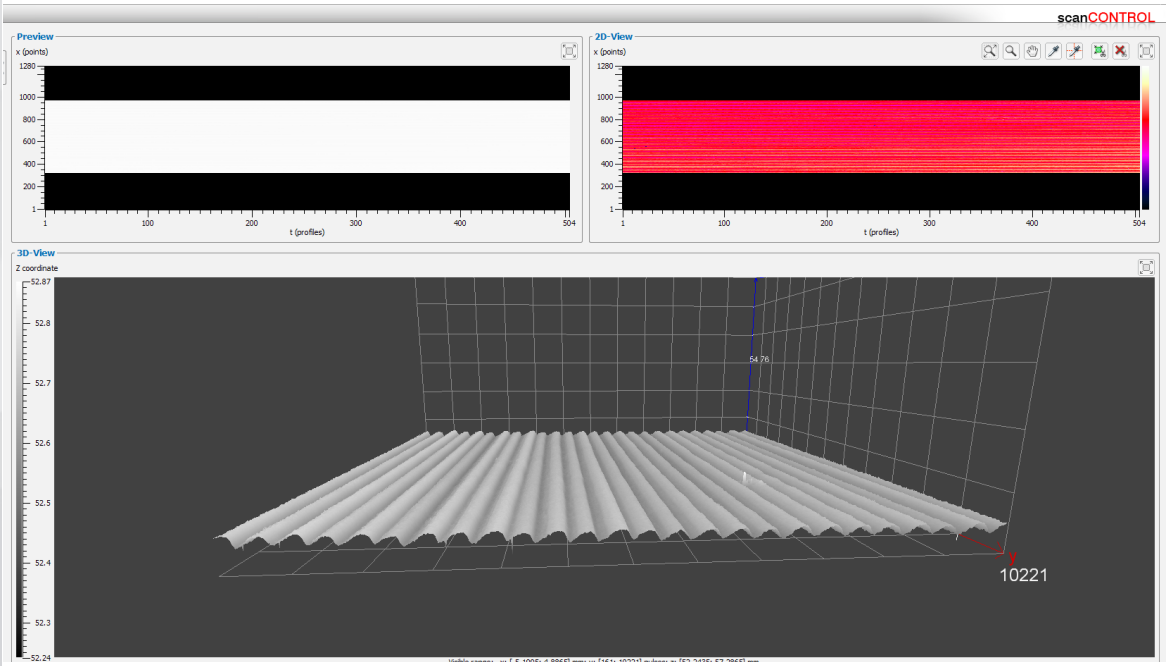


*Figure 89 3D view scanned surface*

*Figure 89*

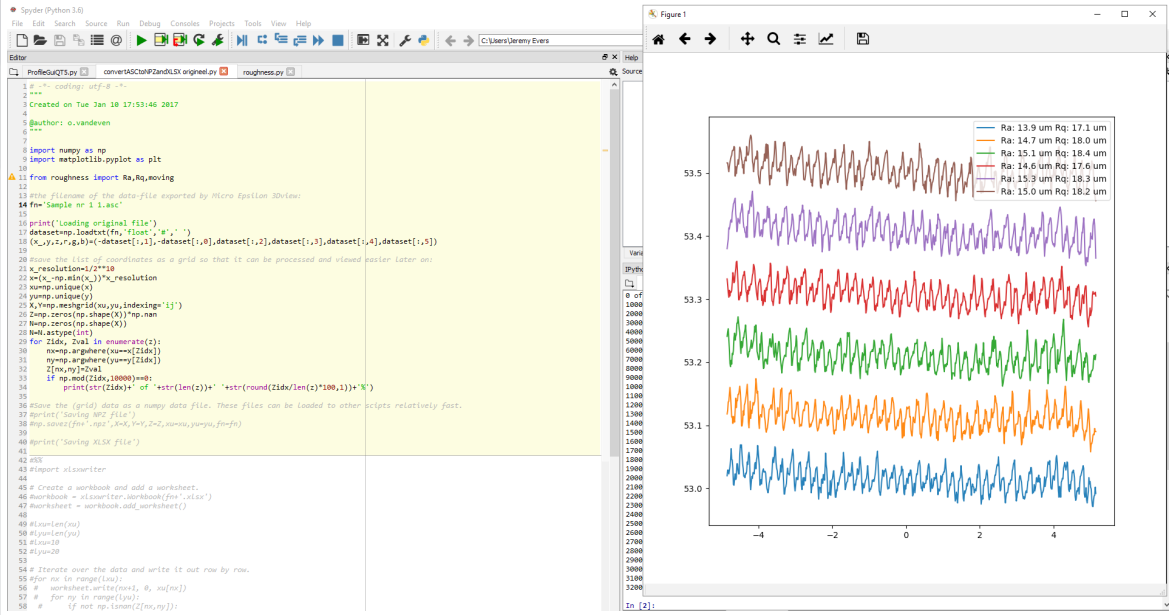


*Figure 90 Python script output*

*Figure 90*

# 7. Sample design

Due to this two-sided study on surface roughness consisting of an objective and perceptual experiment, it is important to have a suitable sample design. For the objective experiment with the optical laser system a flat and even surface is required for surface profile measurements. The beam of the blue laser light has to be projected perpendicular to the 3D printed lines.

Ultimaker B.V. provided the "R-cube" 3D model(figure 91) as a reference model for surface roughness measurements. For the initial surface roughness scanning exploration, R-cubes were printed incorporating various layer heights and materials including PLA, ABS, PC and Nylon. The initial settings were based on existing printing profiles in the slicing software Cura provided by Ultimaker. The R-cube consists of 18 surfaces having different angles(30,45,60, 90 and flat surfaces), including upward facing surfaces and overhangs. The R-cube is designed to have a flat surface facing upward in any orientation. Figure 92 shows the measurement of the surface profile of a R-cube.

The disadvantage of the R-cube is the fact that the measuring surface is quite small for the laser light beam and incorporated edges, see figure 93. Keeping in mind the sample will be used for fingertip scanning in the perception experiment, this r-cubes provides too little surface area.

From the initial exploration of the optical laser system and instructions by Ultimaker engineer Oscar van de Ven a list of requirements is formulated.

The requirements of the sample design for the optical laser system experiment are:

- The sample design needs to have sufficient area for surface profile measurement.
- The sample design needs to have a flat surface on which the laser line will be projected.
- The sample design needs to have similar height distance between the sample and the projector of the laser beam.
- The sample design needs to allow swapping samples without adjusting sample position.
- The sample design has to have sufficient space for sample coding.
- The sample design has to be printable in multiple angular orientations.

As mentioned before the sample design also has to be suitable for the perception experiment. During this experiment the samples are presented to the participants which will scan the surface of the sample with their index fingertip. The length and width of the sample should allow enough area to scan without interfering with the edges. Participants with broad fingertips should also be able to scan the surface without interference of surface edges.

Using anthropometric data from Dined, the established index finger width of percentile 95 is 20 mm(Dined, 2017). This to include participants with an above average fingertip width(see figure 94).

The length of the sample was initially based on previous literature on the roughness judgements by Drewing (2016). In this research different rectangular samples were presented to participants with different

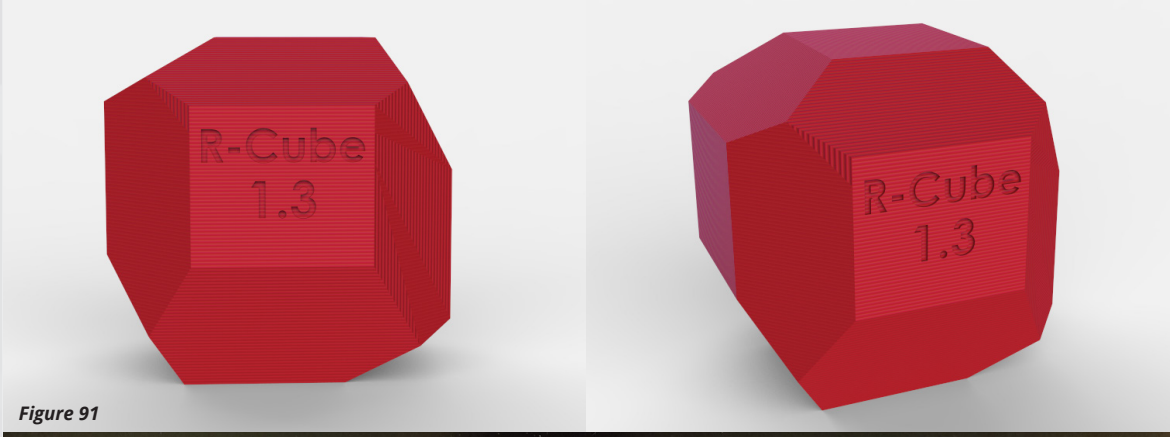


*Figure 91 Provided reference model R-cube*

*Figure 91*

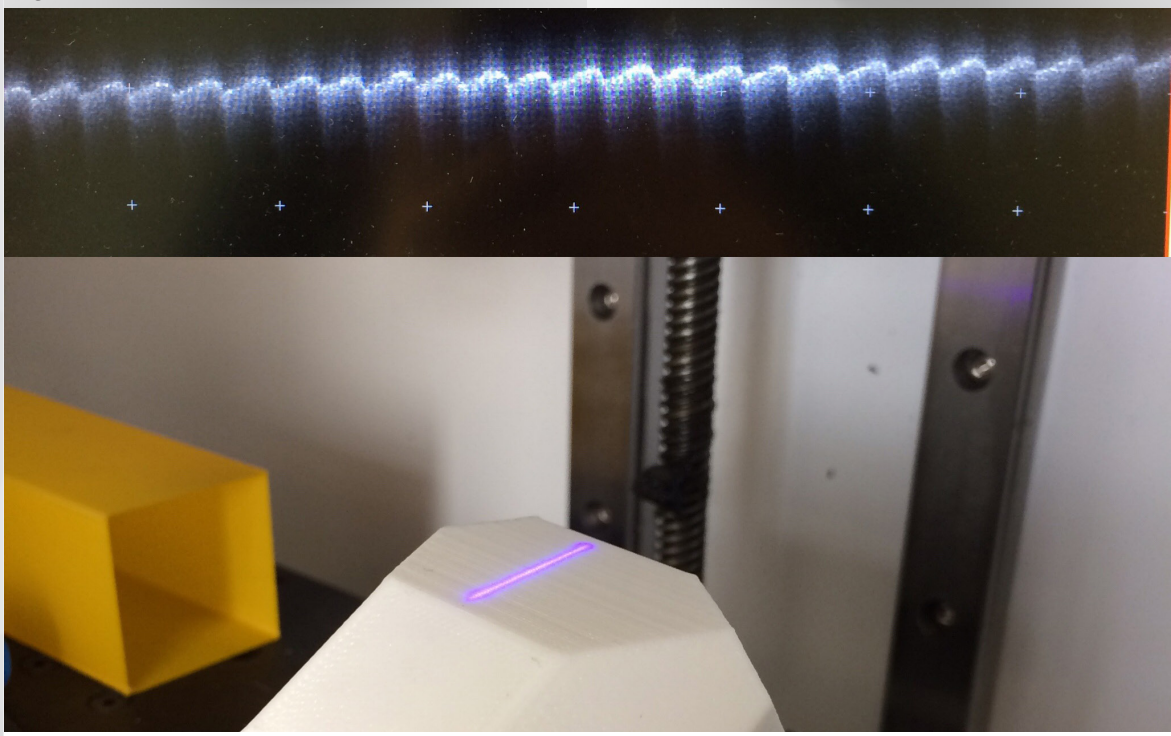

*Figure 92 Surface roughness scanning*

*Figure 92*

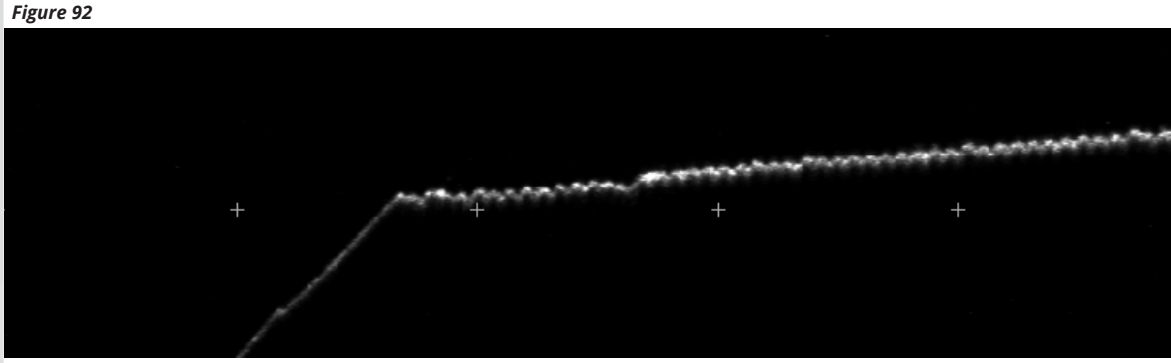

*Figure 93 Surface profile R-cube*

*Figure 93*

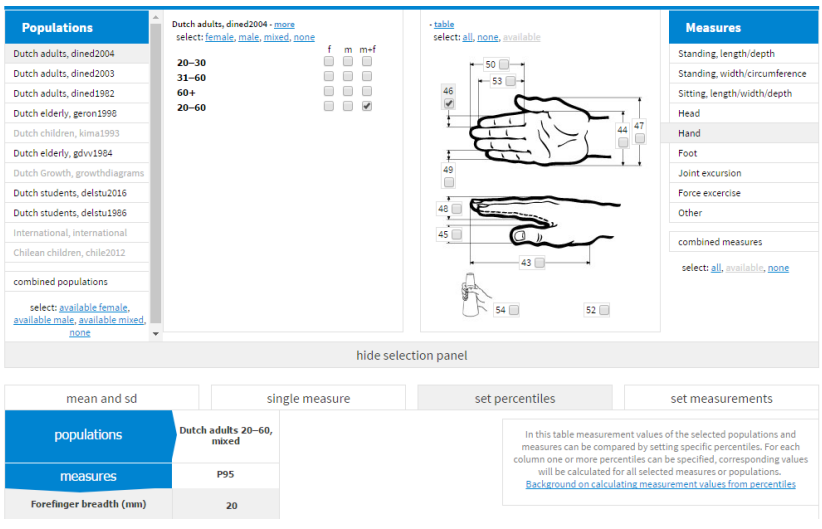


*Figure 94 Dined anthropometric database*

*Figure 94*

textures incorporated. The length of these samples were 80 mm and provided sufficient scanning surface area for texture discrimination. But to decrease the printing time the sample has been reduced to 40 mm. And instead of one translation of the finger over the surface, now multiple translations are incorporated.

From previous touch perception literature and exploration of sample dimensions, requirements for the perceptual experiment sample design were formulated:

- The sample design has to have sufficient width for index finger scanning of percentile 95 which indicates a minimum width of 20 mm.
- The sample design has to have a sufficient finger scanning length of 40 mm.
- The sample design has to have a flat scanning surface.
- The sample design has to have sufficient space for sample coding.
- The sample design has to be printable in multiple angular orientations.

As mentioned before in the literature review of section 2.1 previous studies on surface roughness used different sample designs. These sample designs can be seen in figure 95. Most common used sample design was the truncheon model which consisted of accumulated rectangles with varying angular orientations. Other models consisted of partly separated surfaces with different angular orientations.

Taking into consideration the requirements for both experiments, the final sample design has been constructed. The final design of the sample can be seen in figure 96, incorporating the specified dimensions, requirements and coding example. The specified dimensions from the perceptual experiment sample requirements fits the requirements of the objective experiment sample design with respect to the scanning area of the laser line(length 1 cm). Eventually the width of the sample was set to 30 mm to incorporate an extra margin and taking in mind an overlap of the sample holder. The length of the sample was set to 40 mm.

In the final sample design two support walls are incorporated to provide enough stability during printing, even when printing steep angles. Also this allows for some extra cooling time of the actual sample as the thickness is minimised to 2 mm to keep printing time in control. The support walls are connected to the sample with a wall thickness of 0.5 mm and can be easy broken off without leaving marks on the surface edges, see figure 97.

The advantage of this sample design is the fact that both the upward and overhang surface are printed in one sample. The samples can be easily rotated to change between upward and downward surface. By placing the coding on the upward surface, the two side can be distinguished in the case of unnoticable visual differences. This lower area of the sample will not be included in the roughness measurement by the optical laser as the heated build plate - necessary for printing most materials - transfers heat to this lower part and might influence the roughness. Which makes this unused area suitable for coding.

To make sure the samples are scanned at equal height a sample holder is designed for the optical laser scanning procedure, see figure 98. This sample holder has a slot on the side in which the samples can be slided in.The top surface is open for scanning. There is a small overlap of approximately 2 mm at each side to flatten the sample if slightly warped. The inner surface of the sample holder can be used to place magnets to fix the holder on the moving table of the optical scanner system.

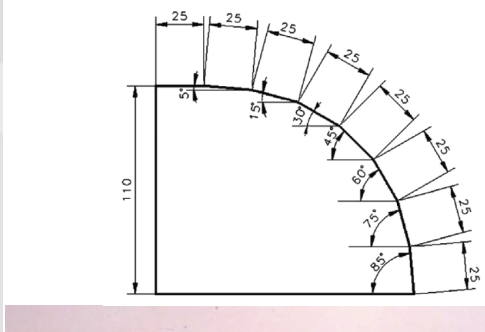


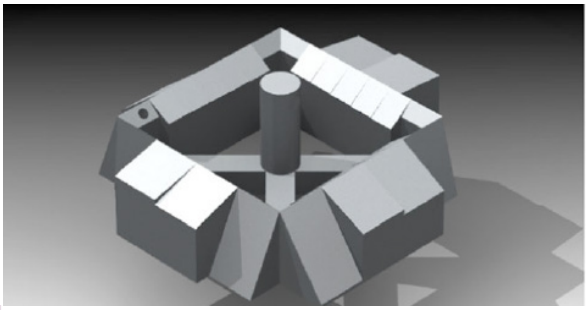

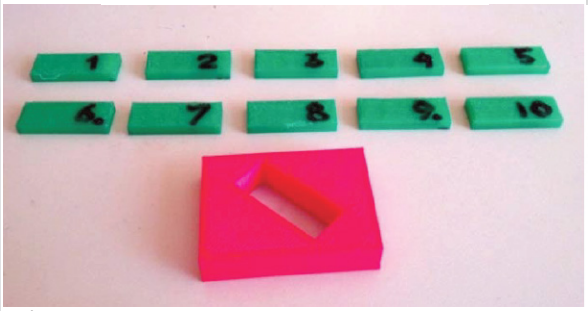


*Figure 95 Previous surface roughness research models*

*Figure 95*

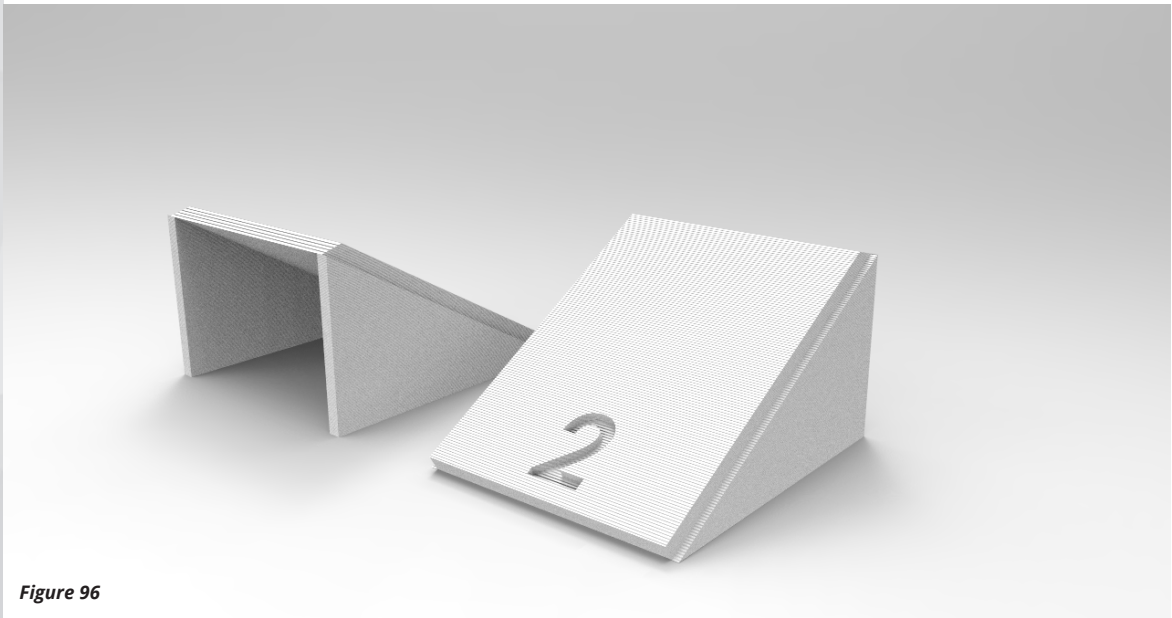


*Figure 96 Sample design for experiments*

*Figure 96*

*Figure 97 Single walled side supports broken off easily*

*Figure 97*

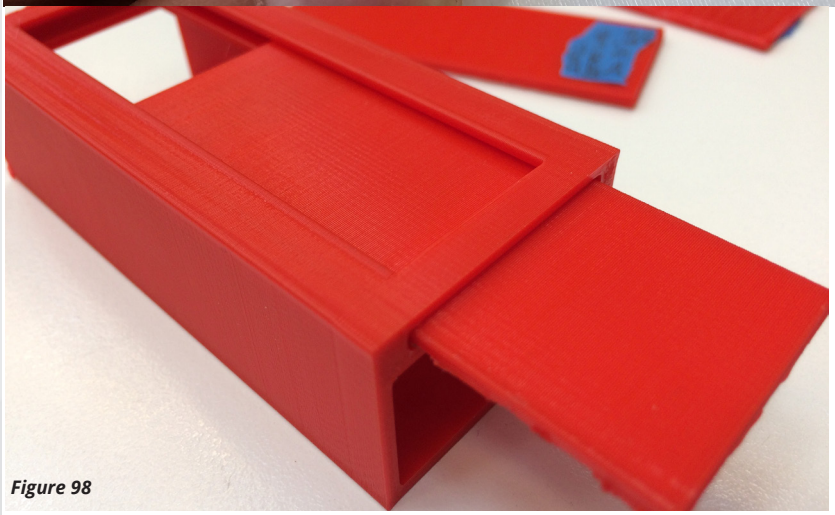

*Figure 98 Sample holder for sample scanning*

*Figure 98*

# 8. Touch perception apparatus

For the perception study the 3D printed samples will be used which were also scanned by the optical scanner system. This to collect human touch perception data and compare this with the outcome of the objective study. Previous research has been reviewed in order to gain more insight in previous touch perception research.

In the research by Libouton et al. (2010) two samples were presented and the participant was requested to scan with a sliding motion the surface of the two samples subsequently, see figure 99. This research was done with samples consisting of sandpaper with different grits. With the data from this research the tactile roughness discrimination threshold was investigated.

From previous research and consultation with Jess Hartcher-O'Brien a suitable approach for this perceptual part is determined. The main goal of this perception study is to investigate the threshold to which participants can distinguish the difference in physical and perceptual roughness. With a specially designed apparatus 2 separate samples will slide across the participant's fingertip. Two samples will be presented consecutively and participants react on which is the roughest in their perception. Next, the samples will be replaced with another sample and tested again. All of these measurements will be processed with Matlab to be able to calculate the threshold where participants cannot perceive a difference between the presented samples. This will be done for each print parameter so that the influence of print parameters on perceived roughness thresholds can be assessed.

To be able to collect data on the perceptual feel of the 3D printed surfaces an apparatus needed to be created. The main use of this apparatus is to present two different samples to participants so the apparatus should include the sample holder for two samples. These samples will be scanned horizontally with participants fingertips in order to feel and judge the surface roughness. The samples should be fixed in the sample holder in order to exclude horizontal movements which might influence touch perception.

For the design of the perception study apparatus it is chosen to automate the scanning motion in order to exclude differences in scanning speeds by participants. By this participants only need to position their fingertips on the sample and focus on the roughness when the samples are moved horizontally. The scanning speed of the samples is set to 4 cm per second as this is the standard scan speed of passive presentation of textures(Hartcher-O'Brien, 2017).

For the design of the perception study apparatus the following requirements are set up;

- The sample holder should be suitable for 2 surface roughness samples of 30mm x 40mm x 2mm.
- The samples should be fixed to exclude horizontale movements in the sample holder.
- The sample holder should enable swapping samples.
- The sample holder has a horizontal translation speed of 4 cm per second.
- The apparatus should enable only horizontal translation of the samples

Different iterations of the sample holder are produced and tested with actual sample dimensions. It was found that no horizontal movement of the samples was possible in the designed holder as samples can be slided in from the side, perpendicular to the holder's movement. This allows for convenient swapping of samples during the study, see figure 102.

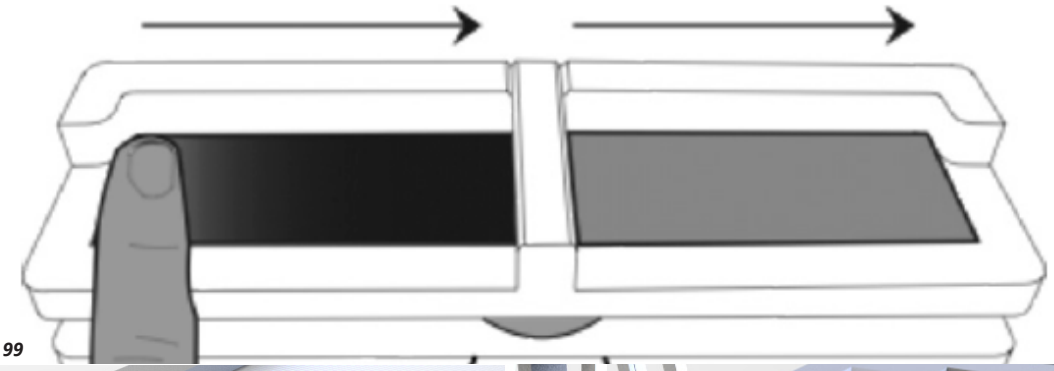

*Figure 99 Inspiration for new apparatus design*

*Figure 99*

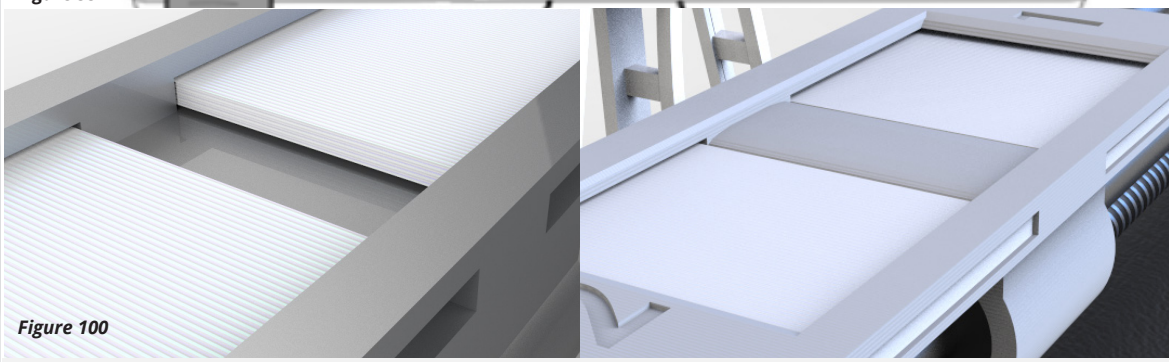

*Figure 100 Iteration mid section sample holder*

*Figure 100*

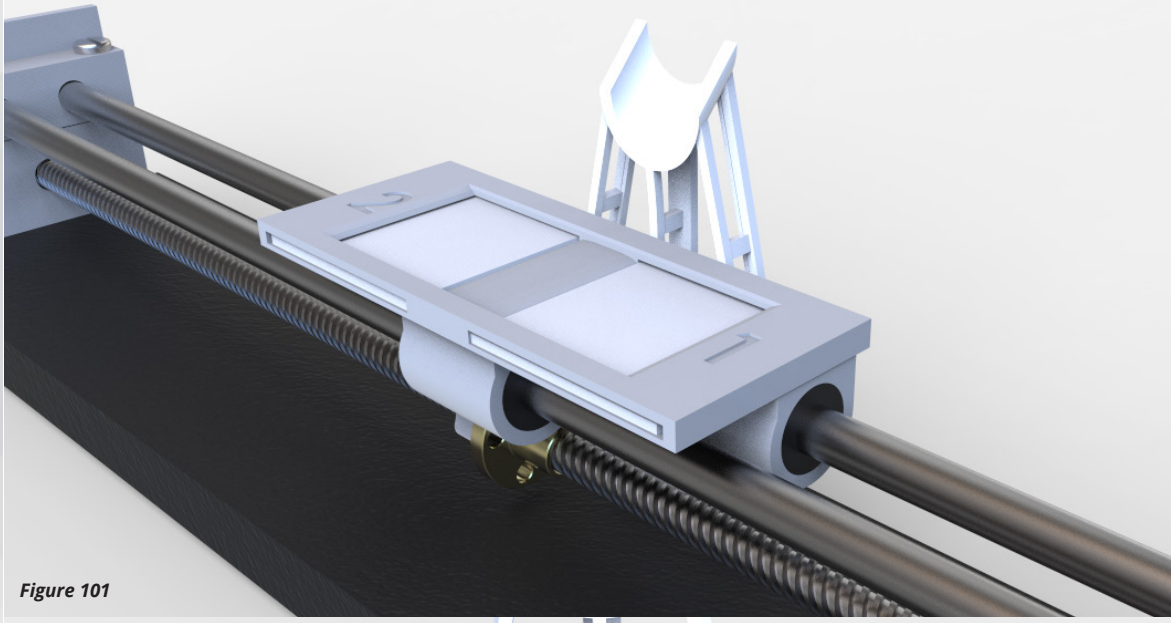


*Figure 101 Incorporated finger bracket*

*Figure 101*

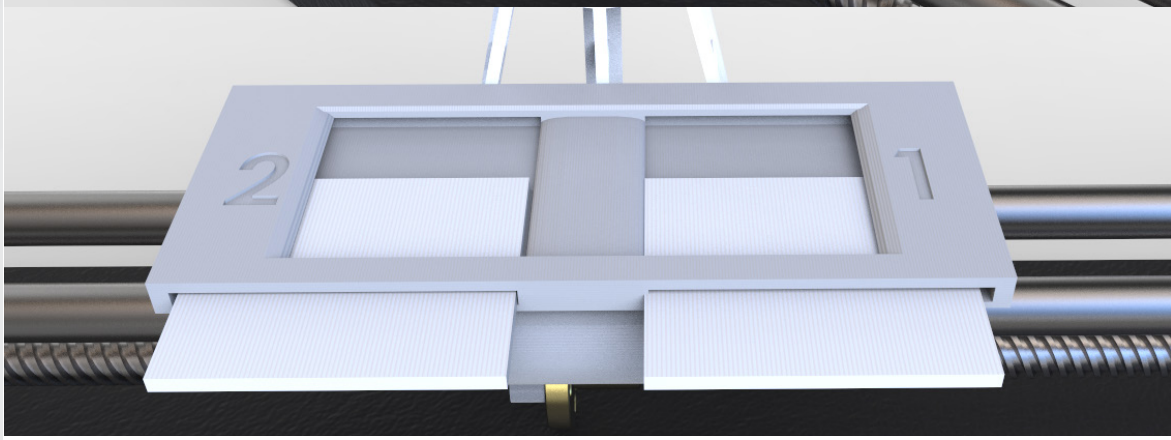


*Figure 102*

*Figure 102*

During the scanning of the samples a short pause is implemented between two samples to enable receptors to "reset" and to exclude receptor signals from previous sample to influence the subsequent sample receptor signals. Two different iterations are tested for this intermediate space, see figure 100. With a gap between the two samples the participant's finger will lower and contact the side of the second sample and the bottom of the sample holder. With no gap between the samples the participant's fingertip will rest on a flat surface before continuing to the next sample. The height of the middle section is equal to the samples and no side contact is present. This allows for a smooth transition between the samples and is the explanation why the middle section was added for the sample holder design. From a pilot with the apparatus it was found that the participant's finger would slide along with the sample holder. To prevent this from happening, a finger bracket was designed and integrated on the base plate of the apparatus, figure 101.

*Drive shaft*

To automate the scanning movement a 12 volt DC motor of 300 rpm is fixed to a lead screw which is held into position with two ball bearings. The screw thread of the lead screw allows for 8 mm movement per rotation. So for a movement of 40 mm in one second, 5 rotations per second are required. Translating this to rotations per minute results in a motor of 300 rpm. This kind of lead screw is commonly used in 3D printers as the Z axis on which the print platform or extruder is fixed. The sample holder is fixed to the lead screw using a lead screw nut and is stabilised by two rods. To allow smooth movement across the rods 3 linear bearings are attached to the sample holder. 3 Linear bearings are chosen to stabilize the full length of the sample holder.

*Electronics*

In order to precisely control the motor movement rotating the leadscrew a motor driver module is used in combination with an arduino uno board. This module is powered by 12 volts and has the possibility to power an arduino uno with the addition of a 5 volts output. An arduino uno is used to regulate the motor movement in terms of rotation speed and direction. Also a controlled pause could be easily implemented between the two samples. And the arduino reset button is used to start a new movement, see figure 103. The whole electronics system is covered by a embodiment printing in PC and indicates the side at which the participant and the observer needs to be located. The setup of the electronics can be seen in figure 104.

The final realised model of the perception sample presenter can be seen in figure 105.

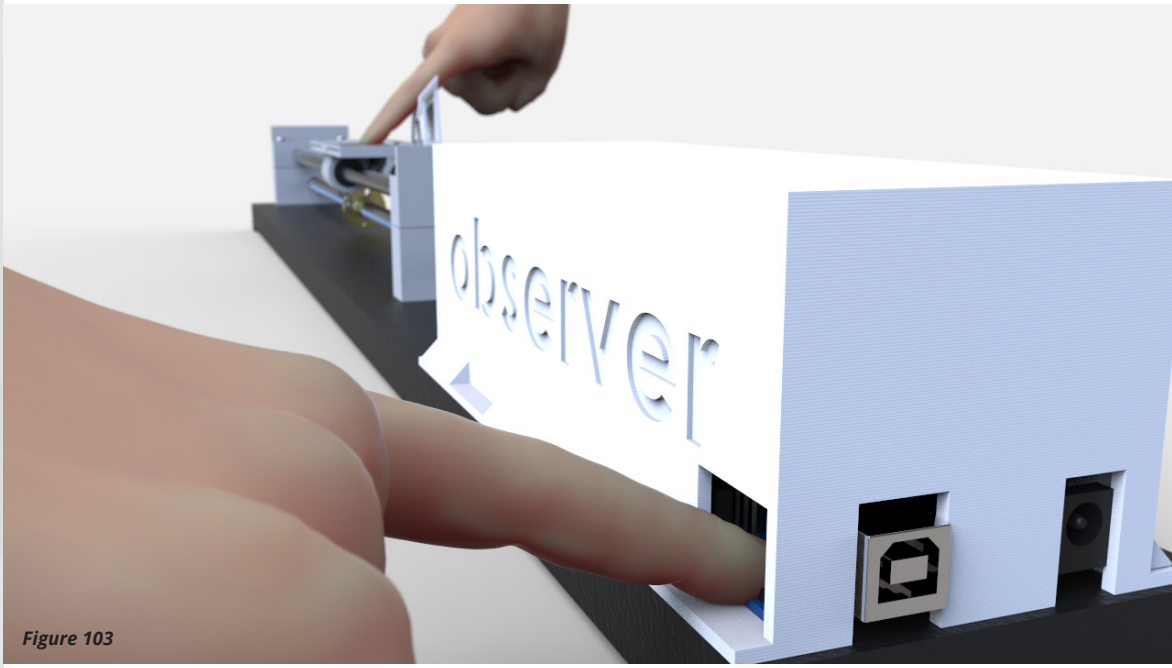


Figure 103

*Figure 103 Reset button for restarting moving cyclus*

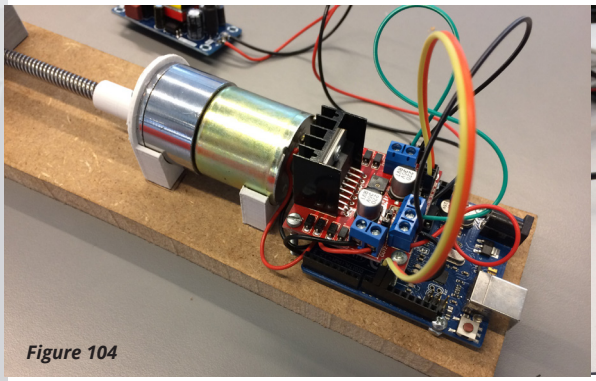

Figure 104

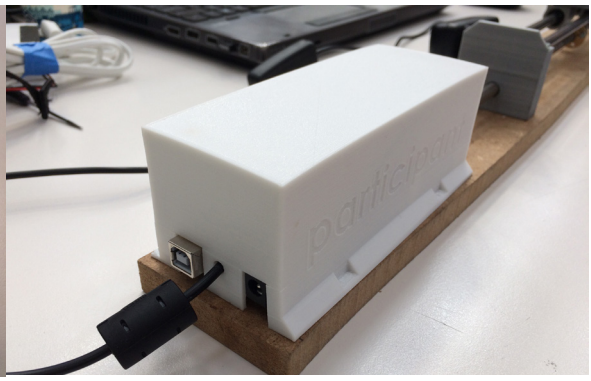

*Figure 104 Electronic setup and protective embodiment*

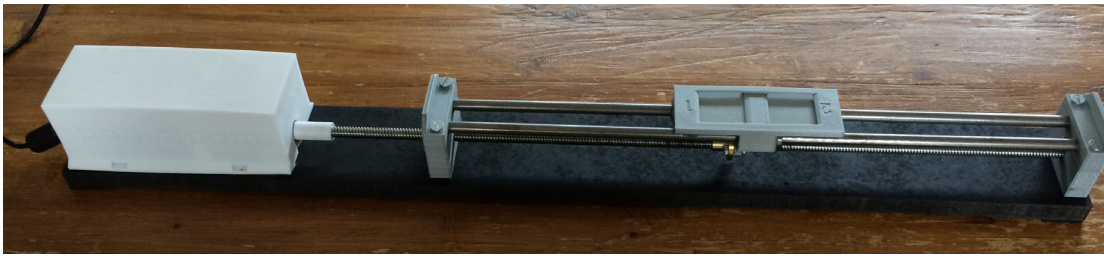

Figure 105

*Figure 105 Final model human perception apparatus*

# 9. Build plate orientation

## Introduction

3D models are placed on the build plate where users can influence the location where the model is being build. Different locations on the build plate can influence the quality of the printed 3D prints. This can be caused by several processes of the 3D printer. Because the filament is transported through a bowden tube for ultimaker3D printers, it experiences friction and influences the extrusion of the filament. Next to this the performance of the motors driving the belts which move the axis of the hot end could influence the extrusion process.

So the orientation of a 3D sample model on the build plate has been investigated to learn more about surface roughness caused by the axis used for printing the surface. In order to move the extruder hot end, it slides along an x and y axis which are driven with the use of belts. These belts have teeth and in combination with pulleys on the axis motors these belts can be moved. Figure 106 gives an overview of the system used for the movement of the extruder hot end.

## Experimental setup/ method

In total 8 samples were printed having different orientations on the build plate. The first 4 samples were printed in a manner so only one axis at the time was used for printing the surface, see figure 107. The other 4 samples were rotated 45 degrees along the Z axis in order to use both the X and the Y axis for printing the surface, see figure 108. All of the samples had coding incorporated regarding its clock position( 3, 6, 9, 12) on the build plate in order to distinguish the samples after printing and measuring with the optical scanner system.

The settings used for printing the different samples were the same for both the regular orientation and the 45 degree rotated orientation. The standard draft profile from the Cura software 2.4 was used which indicated a layer height of 0.2 mm. As this investigation was in the initial experimentation phase of the project the material white PLA, polylactic acid, was used for all build plate orientation samples. Other setting were; 205° C printing temperature, 70 mm/s printing speed, 100% cooling and 60° angle.

After printing the samples were prepared for scanning by removing the single wall supports from the surface edge. The single wall supports provide enough stability during printing and can be easily broken off without leaving inconsistencies. The scanning procedure is the same as described in appendix 6 p.100 on the optical scanner system.

Each roughness value is registered in excel sheets to provide a clear overview of the gathered data. Each sample has been scanned multiple times to minimize extreme values from the noise of the scanner which rarely occurred. If it occurred only one peak could be identified over the entire scan, see figure 108. The scanned data was checked visually for inconsistencies during scanning. If more inconsistencies were identified the sample was cleaned by air and rescanned.

## Results

The results of the build plate orientation investigation can be found in figure 110 and 111. Figure 110 shows the results for the orientation where the surface is printed with one axis at the time and figure 111 with

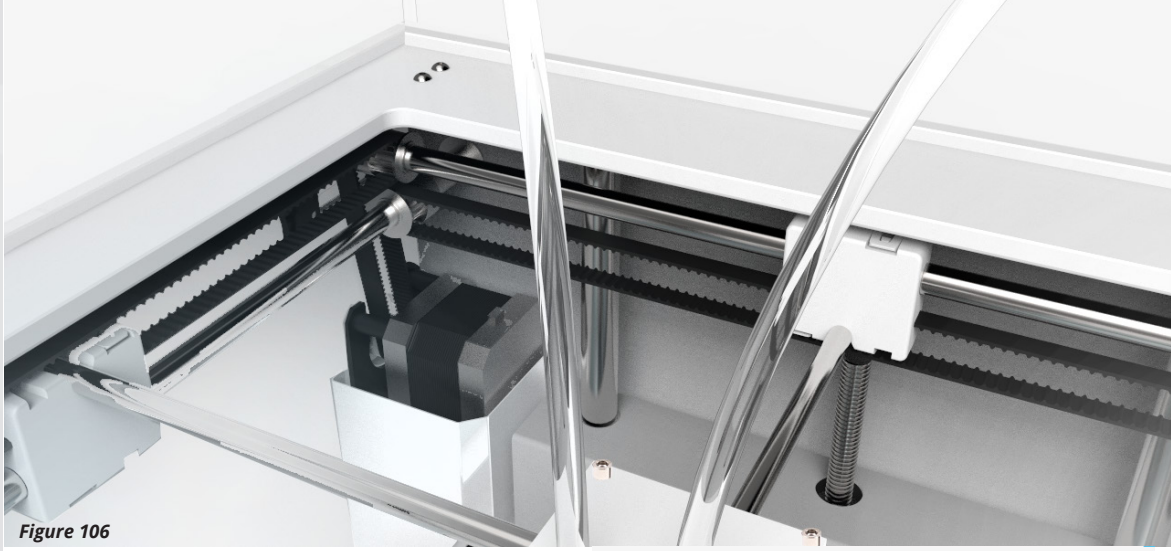

*Figure 106 Belt and pulley system for extruder movement*

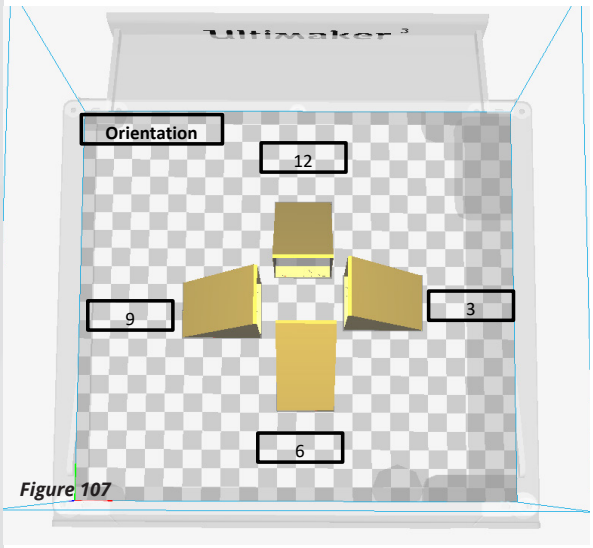


*Figure 107 Single axis position*

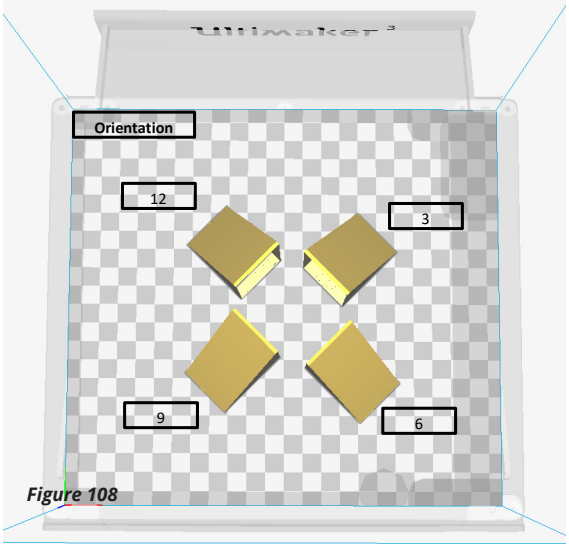


*Figure 108 Duo axis position*

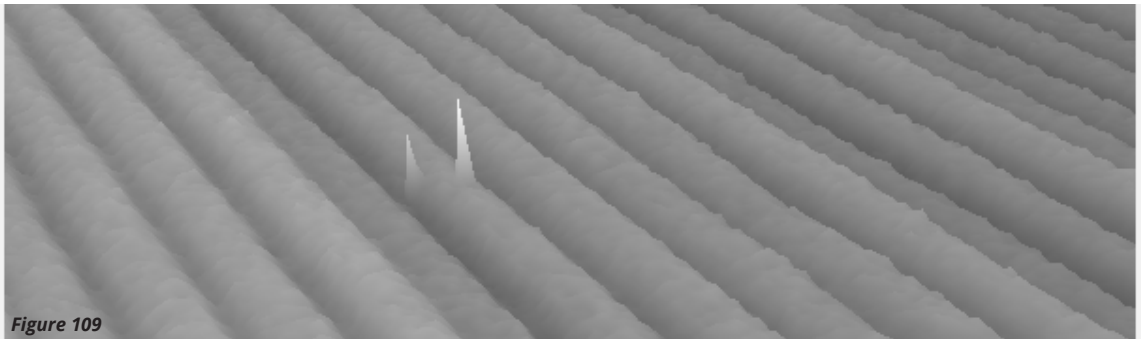

*Figure 109 Identification of noise in measurement*

| Normal orientation | Buildplate Orientation | Roughness Ra [µm] | | | | | | | | | | Roughness Rq [µm] | | | | | | | | | | Mean | | Average deviation | | Ratio |
|---|---|---|---|---|---|---|---|---|---|---|---|---|---|---|---|---|---|---|---|---|---|---|---|---|---|---|
| | clock position | Ra | Ra | Ra | Ra | Ra | Ra | Ra | Ra | Ra | | Rq | Rq | Rq | Rq | Rq | Rq | Rq | Rq | Rq | | Mean Ra [µm] | Mean Rq [µm] | Avg Dev (Ra) | Avg Dev (Rq) | Rq:Ra |
| Upward surface | 3 | 24 | 24 | 25 | 24 | 24 | 25 | 24 | 24 | 25 | | 30 | 30 | 31 | 30 | 30 | 31 | 30 | 30 | 31 | | 24 | 30 | 0,1 | 0,2 | 1,2 |
| | 6 | 28 | 28 | 29 | 28 | 28 | 29 | 28 | 28 | 29 | | 34 | 34 | 34 | 34 | 34 | 34 | 34 | 34 | 34 | | 29 | 34 | 1,6 | 0,2 | 1,2 |
| | 9 | 28 | 28 | 28 | 28 | 28 | 28 | 28 | 28 | 28 | | 33 | 33 | 33 | 33 | 33 | 33 | 33 | 33 | 33 | | 28 | 33 | 0,1 | 0,3 | 1,2 |
| | 12 | 29 | 29 | 30 | 29 | 29 | 30 | 29 | 29 | 30 | | 36 | 36 | 37 | 36 | 36 | 36 | 36 | 36 | 36 | | 29 | 36 | 0,2 | 0,3 | 1,2 |
| Downward surface | 3 | 20 | 19 | 19 | 20 | 20 | 19 | 20 | 20 | 19 | | 24 | 23 | 23 | 24 | 23 | 23 | 24 | 23 | 23 | | 20 | 23 | 0,2 | 0,1 | 1,2 |
| | 6 | 25 | 25 | 26 | 25 | 25 | 26 | 25 | 25 | 26 | | 30 | 30 | 32 | 30 | 30 | 32 | 30 | 30 | 32 | | 25 | 30 | 0,3 | 0,5 | 1,2 |
| | 9 | 23 | 23 | 24 | 23 | 23 | 24 | 23 | 23 | 24 | | 27 | 27 | 28 | 27 | 27 | 28 | 27 | 27 | 28 | | 23 | 27 | 0,1 | 0,1 | 1,2 |
| | 12 | 19 | 18 | 19 | 19 | 18 | 19 | 19 | 18 | 19 | | 23 | 22 | 23 | 23 | 22 | 23 | 23 | 22 | 23 | | 19 | 23 | 0,3 | 0,4 | 1,2 |

*Figure 110 Normal orientation roughness Ra and Rq measurements*

*Figure 110*

two axis simultaneously. Next to the roughness data, the mean and the mean deviation are incorporated. To investigate the relation between the Ra value and the Rq value, the ratio between these values has been calculated as well.

What can be seen in the results of the build plate orientation investigation is that there are some differences. Overall the upward facing surfaces of the single axis printed samples shows similar Ra roughness around 24 - 29 µm and the average deviation of the Ra show similar deviations between the samples printed with the same axis. However there is quite a difference for the 6 and 12 positions. Also the Ra of position 3(24 µm) is lower than the other measurements. As the Rq is based the same surface profile but with amplified differences it is expected to be higher than the Ra value. The Rq value was the highest for the 12 o'clock position. The overall values of the Rq were around 30 - 36 µm. This might also be caused by the difference in possible friction in the bowden tube. For the average deviation of the Rq values the deviation is the same for the 3 and 9 o'clock positions and the deviation of the 6 and 12 o'clock positions is different.

For the overhangs of the samples which were printed with one axis the Ra roughness is around 19 - 24 µm. As overhangs are more challenging to print than upward facing surfaces and depend on several factors it is expected to see more pronounced difference in roughness. There is a difference between the samples printed with one axis, 3 compared with 9 and 6 compared with 12. This same effect can be seen for the Rq values. This shows that there is a difference in roughness for overhangs when objects are placed at different locations on the build plate.

The 45° rotated samples show a Ra roughness around 23 - 27 µm for the upward surface with sample 3 having a higher roughness value Ra of 27 µm. Overall the use of two axis for printing the surface reduces the surface roughness for the upward surface as the Rq of all surface is less than the one axis printed upward surfaces.

Overhangs at 45° rotated samples have in general a lower Ra and Rq than the normal orientation overhangs. The Ra of the overhangs at 45° rotated samples are in the range of 15 - 20 µm( Rq in the range of 18 - 24 µm).

Figures 112, 113, 114, 115 show the change in Ra and Rq value between normal and 45 degree rotated samples for upward and downward facing surfaces of different positions.

| 45 degree orientation | Buildplate Orientation | Roughness Ra [µm] | | | | | | | | | Roughness Rq [µm] | | | | | | | | | Mean | | Average deviation | | Ratio |
|---|---|---|---|---|---|---|---|---|---|---|---|---|---|---|---|---|---|---|---|---|---|---|---|---|
| | clock position | Ra | Ra | Ra | Ra | Ra | Ra | Ra | Ra | Ra | Rq | Rq | Rq | Rq | Rq | Rq | Rq | Rq | Rq | Mean Ra [µm] | Mean Rq [µm] | Avg Dev (Ra) | Avg Dev (Rq) | Rq:Ra |
| Upward surface | 3 | 27 | 27 | 28 | 27 | 27 | 28 | 27 | 27 | 28 | 31 | 32 | 32 | 31 | 32 | 32 | 31 | 32 | 32 | 27 | 32 | 0,4 | 0,5 | 1,2 |
| | 6 | 25 | 24 | 25 | 25 | 24 | 25 | 25 | 24 | 25 | 30 | 29 | 29 | 30 | 29 | 29 | 30 | 29 | 29 | 26 | 30 | 0,2 | 0,1 | 1,1 |
| | 9 | 23 | 24 | 24 | 23 | 24 | 24 | 23 | 24 | 24 | 27 | 28 | 28 | 27 | 28 | 28 | 27 | 28 | 28 | 23 | 27 | 0,3 | 0,3 | 1,2 |
| | 12 | 25 | 24 | 25 | 25 | 24 | 25 | 25 | 24 | 25 | 29 | 28 | 29 | 29 | 28 | 28 | 29 | 28 | 29 | 25 | 29 | 0,4 | 0,6 | 1,2 |
| Downward surface | 3 | 20 | 20 | 19 | 20 | 20 | 19 | 20 | 20 | 19 | 24 | 24 | 23 | 24 | 24 | 23 | 24 | 24 | 23 | 20 | 23 | 0,2 | 0,4 | 1,2 |
| | 6 | 18 | 18 | 18 | 18 | 18 | 18 | 18 | 18 | 18 | 22 | 22 | 21 | 22 | 22 | 21 | 22 | 22 | 21 | 18 | 22 | 0,1 | 0,2 | 1,2 |
| | 9 | 20 | 20 | 20 | 20 | 20 | 20 | 20 | 20 | 20 | 24 | 24 | 24 | 24 | 24 | 24 | 24 | 24 | 24 | 20 | 24 | 0,2 | 0,2 | 1,2 |
| | 12 | 15 | 16 | 16 | 15 | 16 | 16 | 15 | 16 | 16 | 18 | 19 | 19 | 19 | 19 | 19 | 18 | 19 | 19 | 16 | 19 | 0,2 | 0,3 | 1,2 |

*Figure 111 45 degree orientation roughness Ra and Rq measurements*

*Figure 111*

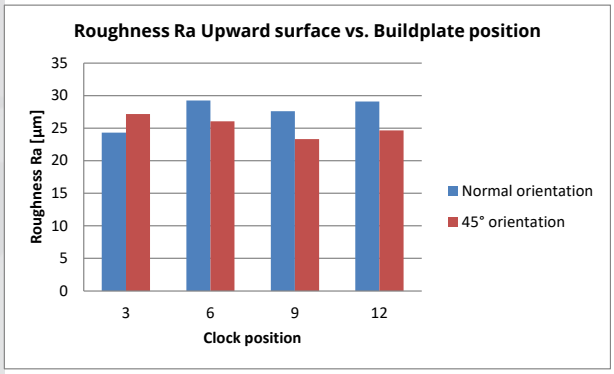


*Figure 112 Roughness Ra comparison upward surface*

*Figure 112*

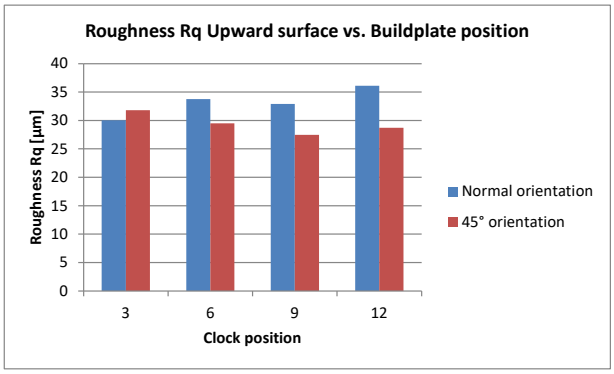


*Figure 113 Roughness Rq comparison upward surface*

*Figure 113*

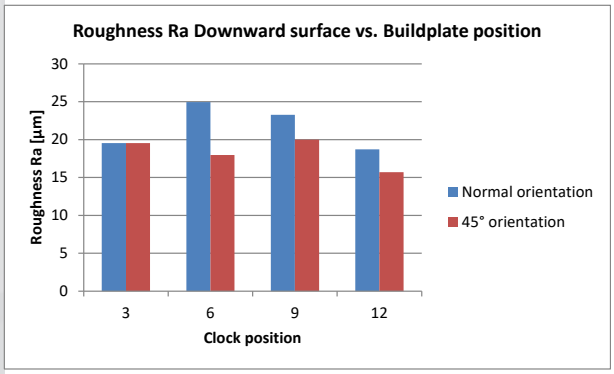


*Figure 114 Roughness Ra comparison downward surface*

*Figure 114*

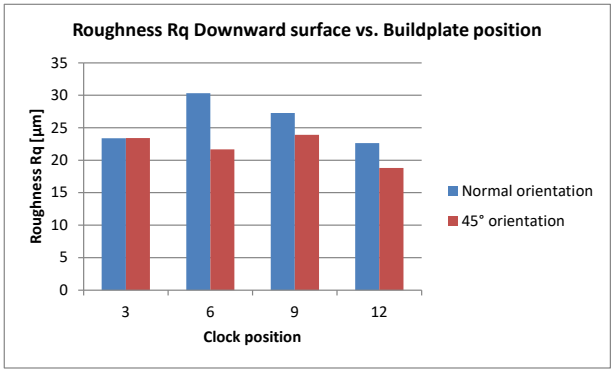


*Figure 115 Roughness Rq comparison downward surface*

*Figure 115*

# 10. Screening experiment

## Introduction

A screening experiment has been performed in order to investigate the influence of a single factor on the surface roughness of 3D printed surfaces. From the literature research several factors were identified as having influence on the surface roughness. However, as the previous research is based on other machines and materials, most factors will be included in this screening experiment. So although some reseaches might indicate a parameter not having influence, it will be taken into account for the screening. Also as this research is performed with an Ultimaker 3 desktop 3D printer with the engineering material Polycarbonate(PC).

From previous research the factors having significantly influence on the surface roughness are; layer height, printing speed, tessellation(for curved surfaces), road width and angular orientation. Factors having no significant effect or not investigated are printing temperature and cooling. In the research of Lužanin et al(2013) also a desktop 3D printer, the makerbot 2, was used to investigate the influence of printing speed and printing temperature. Even though the Ultimaker 3 is also a desktop 3D printer sharing some process similarities both parameters will be taken into account in the screening. To conclude, parameters which were selected for the screening experiment were; layer height, printing temperature, printing speed, cooling, angle orientation and line width. To compare the results and check the reliability of the experiment, 6 center points are also incorporated in the experiment.

## Experimental setup

First the technical limitations of the Ultimaker 3 were taken into account to determine the range in which the screening samples will differ from one another. Please note that lower and upper limit are determined to still deliver reliable print results. Exceeding this range is possible however it dramastically decreases the reliability of the 3D printer and the prints. For the layer height the lower limit is 0,06 mm and the upper limit is set to 0,2 mm. For printing temperature the lower limit is set to 250°C and the upper limit to 280°C. This is for the material Polycarbonate, the nozzle temperature needs to be in the range of the material's melting temperature. By lowering the temperature the flow of the material decreases and might eventually stop extruding and grind the filament at the cold end of the extruder(feeder wheel). Increasing the temperature more than 280°C might lead to degradation of the material and silicon flaps around the nozzles of the ultimaker 3. Printing speed is set to 20 mm/s for the lower limit and 100 mm/s for the upper limit. In the cura profiles for the material PC the cooling is not active, but to investigate the effect the parameter is included in steps of 25%. So the lower limit is 0% and the upper limit is 100%. The angle at which the surface is printed can significantly influence the surface roughness as it directly affects the buildup of layers. The lower limit of the angle orientation is set to 15°(from the horizontal plane). From this point the layers of the overhanging surface start to print far enough from the adjacent layers to begin to detach and form loose lines. The upper limit of the angle was set to 75°. But to investigate what the roughness will be at an angle of 90°, this is investigated as well. For the line width the lower limit is set at 0,32 mm and the upper limit at 0,38 mm. Normally the line width is not changed as it depends on the nozzle opening. For the ultimaker it is optimized and set at 0,35 mm, slightly below the nozzle diameter of 0,4 mm.

Each parameter range is divided into 5 samples to see the change of roughness per step size. However for the line width the range is divided into 3 samples, step size 0,03 mm, as the step size for 5 samples, 0,012mm, would be too little to correctly be executed by the 3D printer.

Figure 116 gives an overview of the upper and lower limits of the parameters, the step size and each centerpoint.

Each parameter range has its own unique coding incorporated to track and register the samples correctly. The coding is integrated in the sample and will be printed in the first section of the sample. The upper section of the sample will not be affected by the printing of the coding and will be used for the roughness measurement with the optical scanner. Figure 117 gives an overview of all sample variations with the coding letter corresponding to the correct parameter.

In total screening 35 samples were printed in Polycarbonate from one batch to exclude differences in material between batches. Each sample was placed in the middle of the build plate to exclude the influence of different build plate orientations. The temperature offset of the extruder was measured by placing thermistors in the nozzle and then incorporated in the slicing software Cura 2.4.

After printing the samples were prepared for scanning with the optical scanning system. As only single walled support walls were incorporated the supports could be removed without leaving any inconsistencies. To ensure proper adhesion to the build plate a raft was included in the slicing software.

The sample holder was used to keep the printed samples at the correct height for scanning. The area above the coding letters provided enough surface area for the 1 cm wide laser beam to scan 1 cm. In the program provided with the micro epsilon laser, scanCONTROL Configuration Tools 5.0, the surface profile recordings could be saved to an avi file. During scanning an exposure of 1.50 ms was used in combination with a recording speed of 25 recordings per seconds.

The avi files were then converted to an .asc file with the use of another program provided with the micro epsilon laser, scanCONTROL 3D-View 3.0. In this program the avi file can be loaded in and converted to a 3D surface containing all measurement points. During this procedure the surface can be analyzed on visual surface defects such as loose lines or dust particles.

Python is used to process all asc files in order to calculate the roughness values Ra and Rq of the measured surface profiles. The standard equations for the calculation of the Ra and Rq are used. After processing the asc files with python scripts provided by Oscar van de Ven the roughness values are collected and registered in excel sheets.

## Results

The results from the screening experiment can be found in figures 118 to 129 and visualizes the change in roughness for the Ra and Rq value with respect to changing 3D printing parameters. As models can consist of upward facing surfaces and downward facing surfaces(overhangs), both have been investigated separately.

Polycarbonate

| Printing Parameters | | Limitations | | | Variables | | | | | Center |
|---|---|---|---|---|---|---|---|---|---|---|
| Layer height | [mm] | 0,06 | - | 0,2 | 0,06 | 0,1 | 0,13 | 0,17 | 0,2 | 0,13 |
| Printing temperature | [°C] | 250 | - | 280 | 250 | 260 | 270 | 280 | 290 | 270 |
| Printing speed | [mm/s] | 20 | - | 100 | 20 | 40 | 60 | 80 | 100 | 60 |
| Cooling | [%] | 0 | - | 100 | 0 | 25 | 50 | 75 | 100 | 50 |
| Angular orientation | [°] | 10 | - | 80 | 15 | 30 | 45 | 60 | 75 | 45 |
| Line width | [mm] | 0,32 | - | 0,42 | 0,32 | 0,35 | 0,38 | | | 0,35 |

*Figure 116 Identification of technical limitations of Ultimaker 3*

*Figure 116*

Parameter **A**

| Parameter | Variables 1 | 1/2 | 2 | 2/3 | 3 |
|---|---|---|---|---|---|
| Layer height (mm) | 0,06 | 0,1 | 0,13 | 0,17 | 0,2 |
| Printing temperature (°C) | 270 | 270 | 270 | 270 | 270 |
| Printing speed (mm/s) | 60 | 60 | 60 | 60 | 60 |
| Cooling (%) | 50 | 50 | 50 | 50 | 50 |
| Angular orientation (°) | 45 | 45 | 45 | 45 | 45 |
| Line width (mm) | 0,35 | 0,35 | 0,35 | 0,35 | 0,35 |

Parameter **B**

| Parameter | Variables 1 | 2 | 3 | 4 | 5 |
|---|---|---|---|---|---|
| Layer height (mm) | 0,13 | 0,13 | 0,13 | 0,13 | 0,13 |
| Printing temperature (°C) | 250 | 260 | 270 | 280 | 290 |
| Printing speed (mm/s) | 60 | 60 | 60 | 60 | 60 |
| Cooling (%) | 50 | 50 | 50 | 50 | 50 |
| Angular orientation (°) | 45 | 45 | 45 | 45 | 45 |
| Line width (mm) | 0,35 | 0,35 | 0,35 | 0,35 | 0,35 |

Parameter **C**

| Parameter | Variables 1 | 2 | 3 | 4 | 5 |
|---|---|---|---|---|---|
| Layer height (mm) | 0,13 | 0,13 | 0,13 | 0,13 | 0,13 |
| Printing temperature (°C) | 270 | 270 | 270 | 270 | 270 |
| Printing speed (mm/s) | 20 | 40 | 60 | 80 | 100 |
| Cooling (%) | 50 | 50 | 50 | 50 | 50 |
| Angular orientation (°) | 45 | 45 | 45 | 45 | 45 |
| Line width (mm) | 0,35 | 0,35 | 0,35 | 0,35 | 0,35 |

Parameter **D**

| Parameter | Variables 1 | 2 | 3 | 4 | 5 |
|---|---|---|---|---|---|
| Layer height (mm) | 0,13 | 0,13 | 0,13 | 0,13 | 0,13 |
| Printing temperature (°C) | 270 | 270 | 270 | 270 | 270 |
| Printing speed (mm/s) | 60 | 60 | 60 | 60 | 60 |
| Cooling (%) | 0 | 25 | 50 | 75 | 100 |
| Angular orientation (°) | 45 | 45 | 45 | 45 | 45 |
| Line width (mm) | 0,35 | 0,35 | 0,35 | 0,35 | 0,35 |

Parameter **E**

| Parameter | Variables 1 | 2 | 3 | 4 | 5 |
|---|---|---|---|---|---|
| Layer height (mm) | 0,13 | 0,13 | 0,13 | 0,13 | 0,13 |
| Printing temperature (°C) | 270 | 270 | 270 | 270 | 270 |
| Printing speed (mm/s) | 60 | 60 | 60 | 60 | 60 |
| Cooling (%) | 50 | 50 | 50 | 50 | 50 |
| Angular orientation (°) | 15 | 30 | 45 | 60 | 75 |
| Line width (mm) | 0,35 | 0,35 | 0,35 | 0,35 | 0,35 |

Parameter **F**

| Parameter | Variables 1 | 2 | 3 | 4 | 5 |
|---|---|---|---|---|---|
| Layer height (mm) | 0,13 | 0,13 | 0,13 | 0,13 | 0,13 |
| Printing temperature (°C) | 270 | 270 | 270 | 270 | 270 |
| Printing speed (mm/s) | 60 | 60 | 60 | 60 | 60 |
| Cooling (%) | 50 | 50 | 50 | 50 | 50 |
| Angular orientation (°) | 45 | 45 | 45 | 45 | 45 |
| Line width (mm) | 0,32 | 0,35 | 0,38 | | |

Parameter **0** (centerpoint)

| Parameter | Variables 1 | 2 | 3 | 4 | 5 |
|---|---|---|---|---|---|
| Layer height (mm) | 0,13 | 0,13 | 0,13 | 0,13 | 0,13 |
| Printing temperature (°C) | 270 | 270 | 270 | 270 | 270 |
| Printing speed (mm/s) | 60 | 60 | 60 | 60 | 60 |
| Cooling (%) | 50 | 50 | 50 | 50 | 50 |
| Angular orientation (°) | 45 | 45 | 45 | 45 | 45 |
| Line width (mm) | 0,35 | 0,35 | 0,35 | 0,35 | 0,35 |

*Figure 117 Overview sample variations of screening experiment*

*Figure 117*

The Ra and Rq values are displayed in the same graphs in order to see if the change in one value has similar change on the other value. The results of the comparison of the ratio between Rq and Ra is described in section Rq/Ra ratio results.

*Layer height*

For the investigation of the influence of layer height 5 different samples with a layer height of 0.06 mm, 0.1 mm, 0.13 mm and 0.2 mm have been printed with single walled support and a raft. All other settings were set at baseline setting.

Results for the influence of layer height on the upward facing surface is shown in figure 118 and shows an increase in roughness with an increase in layer height. The lowest value in Ra roughness is for a layer height of 0.06 mm, having a value of 15 µm(Rq= 19 µm). And the highest roughness value Ra of a layer height 0.2 mm resulted in a roughness value of 34 µm(Rq= 41 µm). The Ra roughness values for layer heights of 0.1 mm, 0.13 mm, and 0.17 mm are respectively 17 µm(Rq= 21 µm), 27 µm(Rq= 34 µm) and 28 µm(Rq= 33 µm). As expected the Rq values are higher than the Ra as the surface inconsistencies are squared for the calculation of the Rq. Overall the Rq shows the similar pattern as the Ra values.

The downward facing surfaces show a different trend for the change in roughness values Ra and Rq, figure 119. The lowest roughness value Ra is 15 µm(Rq= 18 µm) for a layer height of 0.1 mm. The finest layer height of 0.06 mm shows a Ra roughness of 18 µm(Rq= 23 µm). So there is a decrease of roughness between a layer height of 0.06 mm and 0.1 mm but an increase of roughness from 0.1 mm layer height to 0.2 mm. Layer height 0.13 mm has a roughness of 22 µm(Rq= 26 µm), followed by layer height 0.17 mm having a roughness of 25 µm(Rq= 30 µm). The highest roughness values measured are 30 µm(Rq= 36 µm) for a layer height of 0.2 mm.

*Printing temperature*

The printing temperature has been investigated with respect to the range possible for the material Polycarbonate. This range has been set with 250 °C being the lowest printing temperature and 290 °C the highest. In this range 5 samples are printed with a temperature increase of 10 °C resulting in 250 °C, 260 °C, 270 °C, 280 °C and 290 °C. Each sample is printed with single walled supports and a raft.

Figure 120 shows the results of the change in roughness values Ra and Rq with an increase of printing temperature. What can be seen immediately is that the roughness fluctuates at a certain value showing no major increase or decrease with a change in printing temperature. The mean Ra value of 27 µm(Rq= 33 µm) for printing temperature has a standard deviation of 0,84(Rq standard deviation= 1,14). The lowest printing temperature of 250 °C resulted in a Ra roughness value of 26 µm(Rq= 32 µm), 260 °C in 28 µm(Rq= 34 µm), 270 °C in 25 µm(Rq= 31 µm), 280 °C in 28 µm(Rq= 34 µm) and the highest temperature of 290 °C in 26 µm(Rq= 33 µm).

For the downward facing surfaces the same pattern can be seen as for the upward facing surfaces, figure 121. There is no major increase or decrease in roughness with a change in printing temperature. Overall the roughness values of the downward facing surfaces are lower than the upward facing surfaces. The mean Ra value of the downward facing surfaces is 22 µm(Rq= 27 µm) with a standard deviation of 0,88(Rq standard deviation= 1,09). The lowest printing

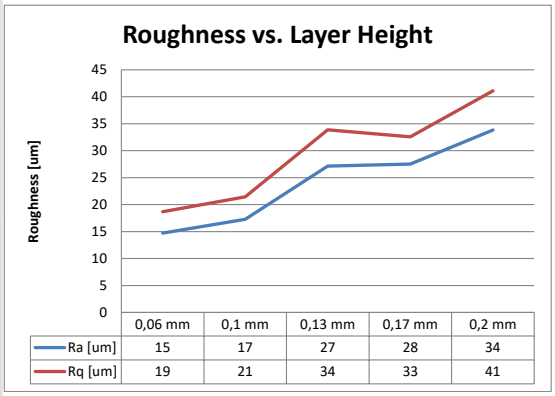


*Figure 118*

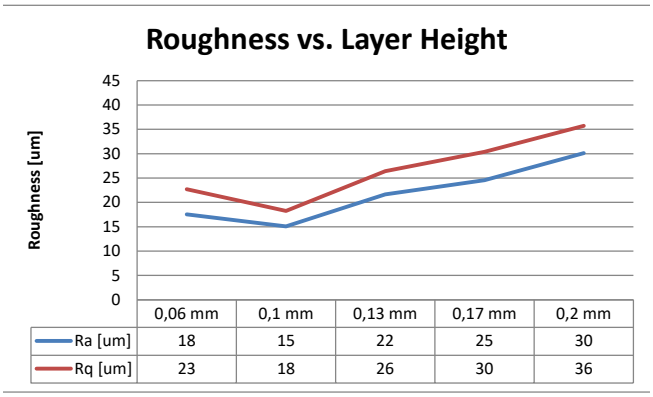


*Figure 119*

*Figure 118 Influence of layer height on upward surface roughness*

*Figure 119 Influence of layer height on downward surface roughness*

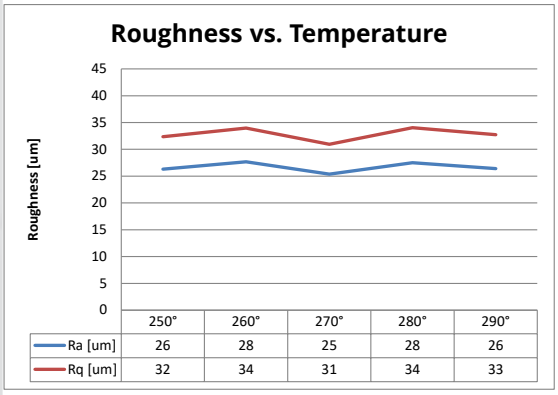


*Figure 120*

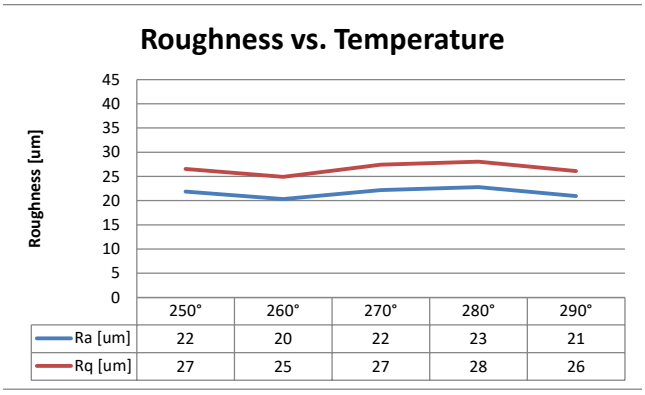


*Figure 121*

*Figure 120 Influence of temperature on upward surface roughness*

*Figure 121 Influence of temperature on downward surface roughness*

temperature of 250 °C resulted in a Ra roughness value of 22 µm(Rq= 27 µm), 260 °C in 20 µm(Rq= 25 µm), 270 °C in 22 µm(Rq= 27 µm), 280 °C in 23 µm(Rq= 28 µm) and the highest temperature of 290 °C in 21 µm(Rq= 26 µm).

*Printing speed*

To see the influence of printing speed on the surface roughness 5 samples are created incorporating different speeds. These speeds were 20 mm/s, 40 mm/s, 60 mm/s, 80 mm/s and 100 mm/s. Also, these samples were printed with single walled supports and a raft for adhesion.

The results of the roughness measurements of printing speeds for upward facing surfaces can be seen in figure 122. It seems that an increase in speeds reduces the surface roughness values Ra and Rq. There is only a small increase of roughness between a printing speed of 60 mm/s and 80 mm/s. The lowest printing speed 20 mm/s resulted in a surface roughness value Ra of 29 µm(Rq= 55 µm). The fastest printing speed resulted in a roughness Ra value of 25 µm(Rq= 31). When considering a printing speed of 60 mm/s results in a roughness Ra of 25 µm(Rq= 31 µm).

Downward facing surfaces have a lower roughness compared to the upward surfaces when investigating printing speed. The results of the influence of printing speed on the surface roughness of the downward facing surfaces can be seen in figure 123. It shows a similar trend as the upward facing surfaces; an increase of speeds decreases the surface roughness values Ra and Rq. The highest Ra value occurred at the lowest printing speed of 20 mm/s which indicated a roughness of 23 µm(Rq= 29). Also for the downward facing surface there is a small increase of roughness between 60 mm/s(Ra= 21 µm, Rq= 26 µm) and 80 mm/s(Ra= 22 µm, Rq= 27 µm).

*Cooling*

The cooling parameter is the one which is not discussed earlier in studies on FDM surface quality, but it plays a role in the solidification of the extruded filament. To investigate whether this parameter is having influence on the surface roughness, it has been incorporated in the screening experiment. In slicing software Cura 2.4 the amount of cooling can be controlled. The cooling amount can be set between 0% to 100% cooling percentage. For this experiment the range of the 5 samples is set at 0%, 25%, 50%, 75% and 100% cooling percentage respectively.
Each sample is printed with incorporated single walled supports and a raft.

What can be seen immediately from the results of roughness of the upward facing surfaces is that there is a difference when the cooling is enabled and when it is disabled, see figure 124. When the cooling is disabled, the roughness value is 23 µm(Rq= 27 µm). When enabled at 25%, the roughness increases to 26 µm(Rq= 33 µm). Although the cooling shows an increase of the roughness values Ra and Rq, it does not increase from 25% to 100% cooling percentage. The roughness values of 50% cooling is Ra= 27 µm(Rq= 33 µm), 75% a Ra of 27 µm(Rq= 34 µm) and full 100% cooling leads to a Ra of 27 µm(Rq= 33 µm).

For the downward facing surfaces the cooling plays an import role on the success of printed overhangs, as print lines are partly printed without support from below the layers. In general the same trend in roughness can be seen for the downward facing surfaces, see figure 125. However, instead of the roughness increasing between 0% and 25% cooling percentage the roughness decreases for the downward facing surfaces. No cooling for the

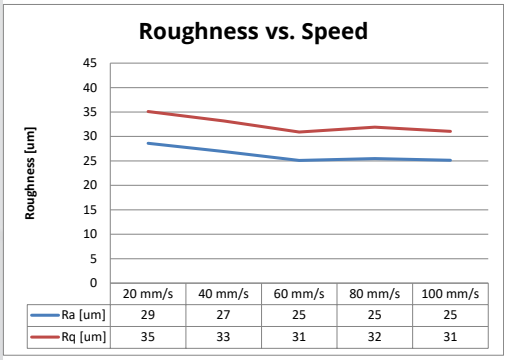


*Figure 122*

*Figure 122 Influence of speed on upward surface roughness*

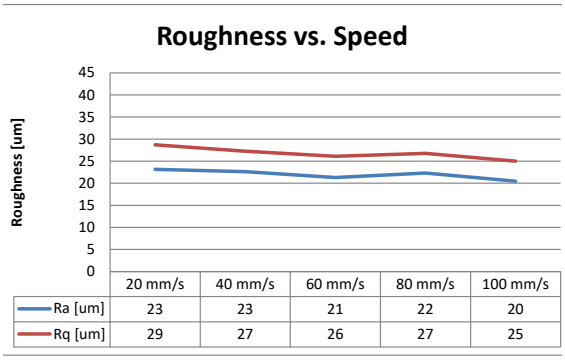


*Figure 123*

*Figure 123 Influence of speed on downward surface roughness*

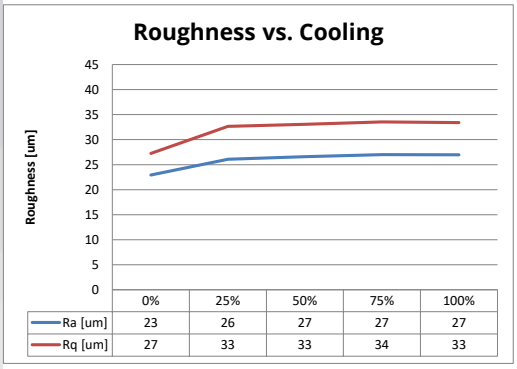


*Figure 124*

*Figure 124 Influence of cooling on upward surface roughness*

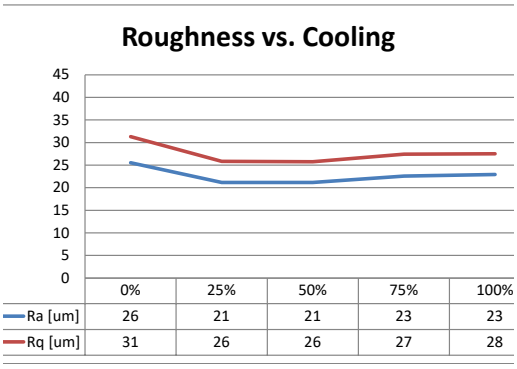


*Figure 125*

*Figure 125 Influence of cooling on downward surface roughness*

downward facing surfaces results in a Ra roughness of 26 µm(Rq= 31 µm) and decreases to 21 µm(Rq= 26 µm) for 25% cooling percentage. From 25% to 100% cooling percentage there is no significant increase of roughness. 50% cooling sample has a roughness of Ra= 21 µm(Rq= 26 µm), following 75% cooling resulting in 23 µm(Rq= 27 µm) and full cooling of 100% with a roughness of Ra= 23 µm(Rq= 28).

*Angle orientation*

With the angle orientation, the angle from the horizontal plane and the 3D printed surface is varied between specific orientations. From initial experimenting with the material Polycarbonate(PC) it was possible to print an overhang of 15° with only 2 print lines separated from the surface. However, it is not recommended to print these overhangs unsupported. The steps chosen for the angle orientation are 15°, 30°, 45°, 60° and 75°. But to gain insight in the perpendicular angle to the horizontal plane, 90° angle was also included in the experiment. All of the samples were printed with single walled side supports an a raft for better adhesion to the build plate. Other parameters were set to the centerpoint settings.

Figure 126 shows the change in roughness of upward facing surfaces for varying angles. What can be seen is that the roughness for 15° and 30° stays quite constant. The angle of 15° has a roughness value Ra of 30 µm(Rq= 35 µm) and the angle of 30° a Ra of 30 µm(Rq= 35 µm). From the 30° angle up to 90° angle the surface roughness decreases to the lowest roughness value of 11 µm(Rq= 14 µm). The lowest roughness value belongs to the perpendicular angle of 90°. The other angles; 30°, 45°, 60° and 75° have roughness values of 30 µm(Rq= 35 µm), 24 µm(Rq= 30 µm), 19 µm(Rq= 23 µm) and 14 µm(Rq= 17 µm) respectively.

As mentioned earlier, the angle of the printed surface plays an important role on the success of the unsupported overhang as bounding layers start to be printed “in the air”. Not supporting these overhang can cause loose lines across the downward facing surfaces. Figure 127 visualizes the results from the screening experiment of the downward facing surfaces with respect to the angle orientation. The 15° overhang started to show loose lines as the overhang is too steep to be correctly printed. This resulted in roughness values of Ra= 116 µm(Rq= 148 µm) primarily due to these loose lines. The 30° angle was printed successfully without loose lines and resulted in a roughness Ra of 26 µm(Rq= 31 µm). Which is almost a factor 4,5 less than the 15° angle orientation. The rest of the results show a decrease in roughness with an increasing angular orientation. With the 45° angle having a roughness value of Ra= 24 µm(Rq= 30 µm), following 60° angle a Ra= 17 µm(Rq= 21µm), 75° angle a Ra= 14 µm(Rq= 18 µm) and 90° angle a Ra of 13 µm(Rq= 16 µm).

*Line Width*

Also the line width was investigated whether it had any influence on the surface roughness. Normally the line width is not changed when printing 3D models as it is partly dependent on the nozzle opening of the extruder. For the printer used in this experiment, the ultimaker 3, this value is set to 0.35 mm. In order to explore the influence, the boundaries of this setting are incorporated. For the linewidth sample serie 3 different samples were created; one with a linewidth of 0.32 mm, followed by 0.35 mm(standard) and finally the upper limit of 0.38 mm.

Figure 128 displays the results for roughness values with a change in line width. What can be seen is that the lowest roughness is achieved with the standard line width of 0.35 mm. This line width resulted in a

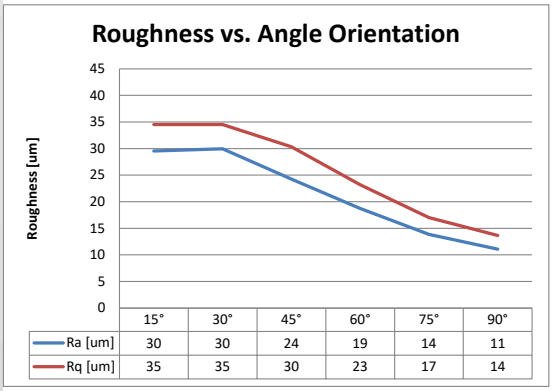


*Figure 126*

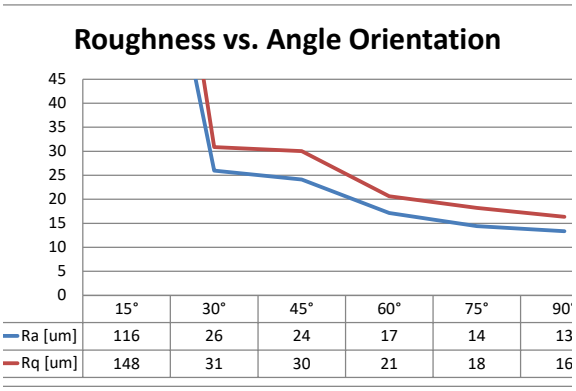


*Figure 127*

*Figure 126 Influence of angle orientation on upward surface roughness*

*Figure 127 Influence of angle orientation on downward surface roughness*

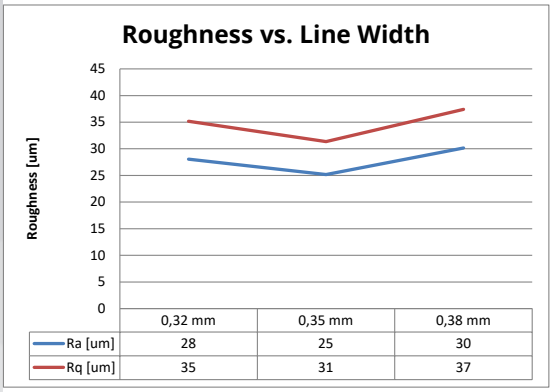


*Figure 128*

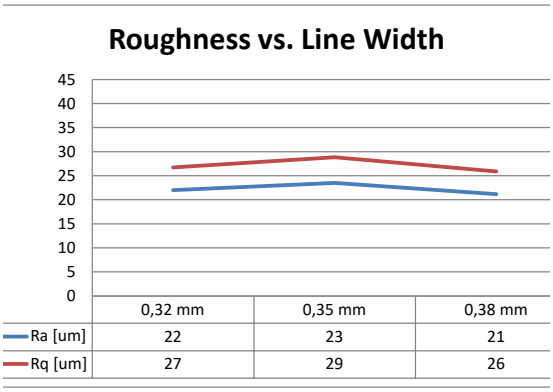


*Figure 129*

*Figure 128 Influence of line width on upward surface roughness*

*Figure 129 Influence of line width on downward surface roughness*

roughness of Ra= 25 µm(Rq= 31 µm). The upper and lower limit of the line width resulted in a higher surface roughness during this experiment. The line width of 0.32 mm resulted in a roughness of 28 µm(Rq= 35 µm) which is slightly less than the roughness of the 0.38 mm line width, namely Ra= 30 µm(Rq= 37 µm).

For the downward facing surfaces the results are the opposite compared to the upward facing surfaces. Figure 129 shows the highest roughness value of Ra= 23 µm(Rq= 29 µm) corresponding to a line width of 0.35 mm. The upper and lower limit, 0.32 mm and 0.38 mm, resulted in a roughness of 22 µm(Rq= 27 µm) and Ra= 21 µm(Rq= 26 µm) respectively.

*Center points*

The center points were printed to compare the results and to check the reliability of the experiment. In total 6 center points were printed with a layer height of 0.13 mm, printing temperature of 270 °C, printing speed 60 mm/s, 50% cooling, 45° angle orientation and a line width of 0.35 mm. These samples also had the single walled supports and raft included.
Each center point of the investigated parameters can also be seen as a center point measurement which will result in an amount of 12 center point measurements.

Figure 130 shows the upward center point measurements and show that there is no significant change across the different samples. The deviations were investigated and resulted in a standard deviation of 1.11 for the Ra and 1.41 for the Rq.

The downward surface center points are displayed in figure 131 and also show no major differences between samples. The deviations are checked and the standard deviation of the Ra is 1.12 and 1.63 for the Rq.

Overall there was no significant change or deviations between the center point measurements which means that the experiment is reliable and parameter can be checked on their influence on surface roughness values.

*Ratio Rq/Ra*

By observing the result graphs of the roughness values of all parameters, an interesting trend can be seen. Although it is known that the Rq is higher than the Ra due to the squared surface irregularities, this effect looks quite constant for all sample measurements. To investigate this relation between the Ra and the Rq the values have been compared for all samples. Figure 132 shows all mean Ra and Rq values of the screening experiment with the Rq/Ra ratio. Both the upward and downward facing surfaces are integrated in the figure. What can be seen is that the ratio of the Rq/Ra is quite constant for the upward and downward surfaces. For the upward surfaces the Rq is 23% larger than the Ra with an average mean deviation of 0,02 µm and standard deviation of 0,02. For the downward surfaces the Rq is 22% larger than the Ra with an average mean deviation of 0,02 and standard deviation of 0,02.

## Discussion

Overall the samples were printed and measured without problems and all measurements were suitable for data processing. At first sight, some parameters show a significant change in roughness when varying settings. In this section the hypotheses on the influence of the parameter will be discussed and parameters selected for further investigation on the correlation between parameters. The standard deviations of the different parameter were compared with the center point standard deviation to see whether a parameter has influence or just noise incorporated in the measurements.

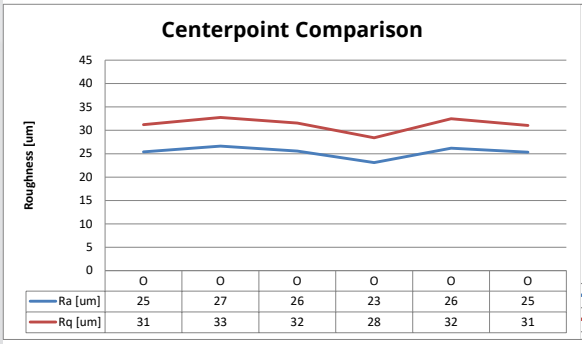


*Figure 130*

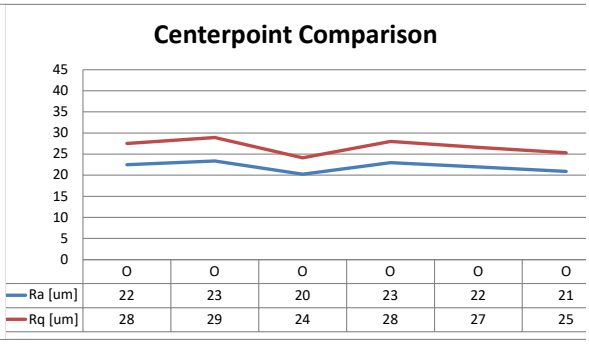


*Figure 131*

*Figure 130 Center point comparison of upward surface roughness*

*Figure 131 enter point comparison of downward surface roughness*

| | | Upward surface | | | Downward surface | | |
|---|---|---|---|---|---|---|---|
| | Parameter | Mean [um] | | Ratio | Mean [um] | | Ratio |
| | value | Mean Ra | Mean Rq | Rq/Ra | Mean Ra | Mean Rq | Rq/Ra |
| Layer height | 0,06 mm | 15 | 19 | *1,3* | 18 | 23 | *1,3* |
| | 0,1 mm | 17 | 21 | *1,2* | 15 | 18 | *1,2* |
| | 0,13 mm | 27 | 34 | *1,2* | 22 | 26 | *1,2* |
| | 0,17 mm | 28 | 33 | *1,2* | 25 | 30 | *1,2* |
| | 0,2 mm | 34 | 41 | *1,2* | 30 | 36 | *1,2* |
| Temperature | 250° | 26 | 32 | *1,2* | 22 | 27 | *1,2* |
| | 260° | 28 | 34 | *1,2* | 20 | 25 | *1,2* |
| | 270° | 25 | 31 | *1,2* | 22 | 27 | *1,2* |
| | 280° | 28 | 34 | *1,2* | 23 | 28 | *1,2* |
| | 290° | 26 | 33 | *1,2* | 21 | 26 | *1,2* |
| Speed | 20 mm/s | 29 | 35 | *1,2* | 23 | 29 | *1,2* |
| | 40 mm/s | 27 | 33 | *1,2* | 23 | 27 | *1,2* |
| | 60 mm/s | 25 | 31 | *1,2* | 21 | 26 | *1,2* |
| | 80 mm/s | 25 | 32 | *1,3* | 22 | 27 | *1,2* |
| | 100 mm/s | 25 | 31 | *1,2* | 20 | 25 | *1,2* |
| Cooling | 0% | 23 | 27 | *1,2* | 26 | 31 | *1,2* |
| | 25% | 26 | 33 | *1,3* | 21 | 26 | *1,2* |
| | 50% | 27 | 33 | *1,2* | 21 | 26 | *1,2* |
| | 75% | 27 | 34 | *1,2* | 23 | 27 | *1,2* |
| | 100% | 27 | 33 | *1,2* | 23 | 28 | *1,2* |
| Angle | 15° | 30 | 35 | *1,2* | 116 | 148 | *1,3* |
| | 30° | 30 | 35 | *1,2* | 26 | 31 | *1,2* |
| | 45° | 24 | 30 | *1,3* | 24 | 30 | *1,2* |
| | 60° | 19 | 23 | *1,2* | 17 | 21 | *1,2* |
| | 75° | 14 | 17 | *1,2* | 14 | 18 | *1,3* |
| | 90° | 11 | 14 | *1,2* | 13 | 16 | *1,2* |
| Line width | 0,32 mm | 28 | 35 | *1,3* | 22 | 27 | *1,2* |
| | 0,35 mm | 25 | 31 | *1,2* | 23 | 29 | *1,2* |
| | 0,38 mm | 30 | 37 | *1,2* | 21 | 26 | *1,2* |
| Center points | O | 25 | 31 | *1,2* | 22 | 28 | *1,2* |
| | O | 27 | 33 | *1,2* | 23 | 29 | *1,2* |
| | O | 26 | 32 | *1,2* | 20 | 24 | *1,2* |
| | O | 23 | 28 | *1,2* | 23 | 28 | *1,2* |
| | O | 26 | 32 | *1,2* | 22 | 27 | *1,2* |
| | O | 25 | 31 | *1,2* | 21 | 25 | *1,2* |
| | | | **gem** | *1,2* | | **gem** | *1,2* |
| | | | **gem dev** | *0,02* | | **gem dev** | *0,02* |
| | | | std. | *0,02* | | std. | *0,02* |

*Figure 132*

*Figure 132 Overview Ra, Rq and Rq:Ra ratio of upward and downward facing surfaces of the screening experiment*

*Layer height*

From the results on the roughness with an increase of layer height, it is clearly visible that the roughness increases. This effect can be seen for both the upward and downward facing surfaces. So the null hypotheses can be rejected as layer height has a significant influence on the surface roughness. Therefore this parameter will be taken into account for further investigation in the correlation experiment.

*Printing temperature*

The results of the influence of printing temperature were fluctuating around a specific roughness and showed no significant change across temperatures. The standard deviations of the roughness values Ra and Rq are lower than the center point comparisons, so the printing temperature has no significant influence on the surface roughness. The null hypothesis can be rejected as printing temperature has no influence regarding surface roughness. The printing temperature parameter will not be taken into account for the correlation experiment. This same outcome can also be seen in the research by Lužanin et al(2013) where printing temperature on a makerbot desktop 3D printer did not have significant influence on roughness value Ra. The limitation of the research by Lužanin is the fact that the Rq was not taken into consideration.

*Printing speed*

Although there might be no change in roughness for the different printing speeds, there is a slight decrease of 3 µm from 20 mm/s to 100 mm/s. This effect can be seen for both upward and downward facing surfaces. From this we can conclude that an increase of printing speed decreases the surface roughness. And thereby we can accept the null hypothesis and include the parameter in the correlation experiment.

*Cooling*

As mentioned in the results section there was a difference between when the cooling was enabled and when it was not enabled. For the upward surface the the enabling of the cooling resulted in a slight increase of surface roughness. However, for the downward surface this enabling of cooling resulted in a slight decrease of roughness. But when the cooling was enabled for both surfaces, there was no significant change in roughness(standard deviation of 0,35 upward and 0,83 downward). So the null hypothesis can be rejected as there is no change in roughness when cooling. And will not be taken into account for the correlation experiment.

*Angle*

The angle orientation was expected to have influence on the roughness as it directly influences the buildup of the layers. From the results it can be clearly seen that an increase of the angle from the horizontal plane resulted in a decrease of roughness values Ra and Rq. The 15° overhang has an extreme roughness value of 116 µm(Rq= 148 µm) as lines started to separate from the printed surface. An overhang of 15° is not recommended to print unsupported so for the interpretation of the results the roughness value will be excluded. The angles from 30° to 90° were successfully printed without extra supporting the overhang surface. The 15° upward facing surface printed without any problems and did not result in an extreme roughness value. To conclude, the null hypothesis can be accepted as roughness values decrease with increasing angle orientation.

Therefore the angle orientation will be taken into account in the correlation experiment.

*Line width*

The last parameter to investigate was the line width and from the screening results it can be seen that there is no clear increase or decrease. Also because this setting is not suitable for a wider range investigation only 3 different samples were analyzed. Because there is an increase in roughness for the upward facing surfaces for both the 0,32 mm and 0,38 mm (except for the standard value of 0,35 mm) there is some influence. The reversed effect can be seen for the downward facing surfaces, the 0,32 mm and 0,38 mm showed a decrease compared to the standard value of 0,35 mm. Because of this effect it is chosen to further investigate the influence of line width on surface roughness with the correlation experiment.

*Rq/Ra ratio*

From the figure on the Rq/Ra ratio it can be seen that for both upward and downward facing surfaces the Rq is 1,2 times larger than the Ra. This ratio can be seen for all measured samples of the screening experiment. The analysis of the Rq/Ra ratio for the correlation samples will be discussed in the chapter on the correlation experiment. There are few special occasions where the 1,2 increase is not suitable, primarily for angle orientations of 15° - 30°. Furthermore, this ratio could be used for prediction of the Rq value with the Ra value in the case of a successful FDM printed surface by the Ultimaker 3 in Polycarbonate(PC).

## Conclusions

The goal of this experiment was to investigate the influence of several parameters on the surface roughness values Ra and Rq. In this research 6 parameters were tested and the results processed into graphs for interpretation of the results. The results were compared with center point measurements in order to check the reliability of the experiment. The center point measurements were consistent and showed no large deviations. From this we can conclude that the chosen approach to investigate the influence of parameters is sufficient.

Also, from this screening experiment, 4 parameters were selected for further correlation investigation. The parameters chosen which had significant influence on roughness are:

- Layer height
- Printing Speed
- Angle orientation
- Line Width

Parameter proven not to have significant influence on the surface roughness are:

- Printing temperature
- Cooling

Besides the approach and investigation of parameters influencing the surface roughness, the ratio Rq/Ra has been analyzed. This experiment resulted in a ratio Rq/Ra of 1,2 for the calculation of the Rq with known value Ra. This ratio has proven to be sufficient for roughness prediction for successful FDM printed surfaces on the Ultimaker 3 desktop printer with filament material Polycarbonate(PC). Such screening investigation with respect to surface roughness Rq/Ra ratio and the influence of parameters can provide more guidance and insights in the FDM process. Especially for desktop 3D printers as professional industrial grade printers are studied in the past. More profoundly, letting users of 3D printing gain insights on the influence of machine settings on surface roughness is beneficial for better understanding the surface finish of FDM prints.

# 11. Correlation experiment

## Introduction

To take a closer look at the effect of a specific parameter and possible parameter interactions, a correlation experiment has been performed. The selected parameters from the screening experiment are used as factors which are then statistically analyzed using Design Expert 10 software by Stat-Ease. With this program the design of experiment will be set up and monitor the process of analyzing. When finished, this program can deliver a prediction model for FDM surface roughness estimation. Which can be used to calculate the surface roughness depending on the chosen parameters or even specify the parameters in order to produce a surface with a desirable surface roughness. As the last step of this experiment samples with random parameters will be printed and checked with the prediction model to confirm the fit.

From the screening experiment 4 parameter were found which had influence on the surface roughness with FDM printing technology. These parameters were layer height, printing speed, angle orientation and line width. The other parameters, printing temperature and cooling, were not found having an evident effect on the surface roughness. Even though cooling showed a clear difference in roughness when cooling was enabled or disabled, it was not changing significantly when cooling was increased from 25% to 100%.
Printing temperature resulted in a fluctuating curve at a specific roughness value of Ra= 27 µm(Rq= 33 µm). So these parameter will not be taken into account for the correlation experiment.

## Experimental setup/method

As this experiment is partly similar to the screening experiment, the same sample designs will be suitable for printing and scanning. It will be a 40 by 30 by 2 mm rectangle with a specific angle at which it is printed. Two single wall supports are added to provide stability during printing and exclude vibrations or movements of the sample. To enhance the adhesion of the polycarbonate to the build plate a raft has been used for all samples. For monitoring all samples had a new unique coding integrated in the design, see first colomn of figure 134. For the correlation experiment all samples had different numbers corresponding to their standard order, not the run order as the experiment will be randomized.

As 4 parameters will be investigated on their significance and correlation, a 2 level factorial design will be used for the experiment. In total 19 samples are printed incorporating 3 center points and all samples are randomized. This design of experiment(DOE) is set up using Design expert 10 software by Stat-Ease. The whole experimental procedure can be monitored with this statistical program. After printing and scanning the samples, the data can be analyzed immediately with the build in statistical tools.
Figure 133 shows an overview of the factors and responses included in the design of experiment with corresponding name, units and high/ low level values. The complete overview of the run sheet with the corresponding set of parameters can be found in figure 134.

The Ultimaker 3 desktop 3D printer has been used for printing the samples for the correlation experiment. During printing one batch of Ultimaker

| Factor | Name | Units | Type | Subtype | Minimum | Maximum | Coded | Values | Mean | Std. Dev. |
|---|---|---|---|---|---|---|---|---|---|---|
| A | Layer Height | mm | Numeric | Continuous | 0,06 | 0,2 | -1,000=0,06 | 1,000=0,2 | 0,13 | 0,0659966 |
| B | Speed | mm/s | Numeric | Continuous | 20 | 100 | -1,000=20 | 1,000=100 | 60 | 37,7124 |
| C | Angle | Degree | Numeric | Continuous | 30 | 75 | -1,000=30 | 1,000=75 | 52,5 | 21,2132 |
| D | Line width | mm | Numeric | Continuous | 0,32 | 0,38 | -1,000=0,32 | 1,000=0,38 | 0,35 | 0,0282843 |

| Response | Name | Units | Obs | Analysis | Minimum | Maximum | Mean | Std. Dev. | Ratio |
|---|---|---|---|---|---|---|---|---|---|
| R1 | Roughness Ra | um | 19 | Factorial | 6,9 | 133 | 30,0316 | 30,1388 | 19,2754 |
| R2 | Roughness Rq | um | 19 | Factorial | 9 | 177 | 36,6105 | 38,6982 | 19,6667 |
| R3 | Printing Time | min | 19 | Factorial | 25 | 224 | 92,3158 | 56,2841 | 8,96 |

*Figure 133 Factor and response overview of correlation analysis*

*Figure 133*

| Std | Run | Factor 1 A:Layer Height mm | Factor 2 B:Speed mm/s | Factor 3 C:Angle Degree | Factor 4 D:Line width mm |
|---|---|---|---|---|---|
| 17 | 1 | 0,13 | 60 | 52,5 | 0,35 |
| 7 | 2 | 0,06 | 100 | 75 | 0,32 |
| 12 | 3 | 0,2 | 100 | 30 | 0,38 |
| 2 | 4 | 0,2 | 20 | 30 | 0,32 |
| 9 | 5 | 0,06 | 20 | 30 | 0,38 |
| 1 | 6 | 0,06 | 20 | 30 | 0,32 |
| 4 | 7 | 0,2 | 100 | 30 | 0,32 |
| 3 | 8 | 0,06 | 100 | 30 | 0,32 |
| 15 | 9 | 0,06 | 100 | 75 | 0,38 |
| 5 | 10 | 0,06 | 20 | 75 | 0,32 |
| 11 | 11 | 0,06 | 100 | 30 | 0,38 |
| 13 | 12 | 0,06 | 20 | 75 | 0,38 |
| 19 | 13 | 0,13 | 60 | 52,5 | 0,35 |
| 14 | 14 | 0,2 | 20 | 75 | 0,38 |
| 8 | 15 | 0,2 | 100 | 75 | 0,32 |
| 16 | 16 | 0,2 | 100 | 75 | 0,38 |
| 10 | 17 | 0,2 | 20 | 30 | 0,38 |
| 6 | 18 | 0,2 | 20 | 75 | 0,32 |
| 18 | 19 | 0,13 | 60 | 52,5 | 0,35 |

*Figure 134 Run sheet overview of correlation analysis*

*Figure 134*

polycarbonate(PC) is used as material and extruder temperature offset is measured and adjusted in the slicing software Cura 2.4. All samples are placed in the center of the build plate and one sample is printed at once. As the samples are printed in polycarbonate(PC), the front enclosure and avery sheets are used for adhesion and maintaining a stable internal temperature.

When printing was finished, all samples were prepared for scanning with the optical scanner system. The single walled supports and the raft can be removed without leaving any inconsistencies on the surface. The sample holder used to position the samples in the screening experiment has also been used for the correlation experiment. No necessary changes were required for this model of the sample holder.

The procedure for scanning the 3D printed surface samples is identical to the screening experiment. The samples are placed in the sample holder and positioned under the laser beam of the scanner. It is fixed with the use of magnets to the top of the moving platform on the y-axis carriage. A python script is used to position the laser module at the correct height so the surface is in focus of the sensor. Also the distance and duration of the moving platform is adjusted to a scanning distance of 10 mm for 10 seconds in the y-direction.

For the actual scanning and capturing the surface profiles micro epsilon scanCONTROL Configuration Tools 5.0 has been used which is provided with the optical scanner module. In this program the laser module settings are changed to an exposure of 1.50 ms and 25 recording per second. Each surface is scanned 3 times for both the upward and downward facing surface. Each scan file was named according to the sample number, surface orientation and number of scan.

Further processing was done with scanCONTROL 3D-View 3.0 in which the scanned avi file was transformed to an 3D surface file and saved as a ASC file. By transforming the data file to a 3D surface it can be analyzed for any surface irregularities due to dust particles. All processed files were loaded in a python script to calculate the surface roughness values Ra and Rq. After calculation these values were compared to the second and third surface scans of the same surface and finally entered in the design expert 10 software.

## Results

In this section all results for both the upward and downward facing surfaces are presented per parameter and in the end possible interactions between parameters. All samples were printed successfully and suitable for scanning with the optical scanner system. All data is gathered in Design Expert 10 for statistical analysis and processing.

*Overall results upward facing surfaces*

The overall responses for roughness values Ra and Rq of the upward surface can be seen in figure 135 as well as the printing time which has been monitored. However printing time will not be statistically analyzed. From all roughness measurements the lowest registered value for Ra was 10 µm(Rq= 13 µm) and the highest Ra was 49 µm(Rq= 57 µm).

| | | Factor 1 | Factor 2 | Factor 3 | Factor 4 | Response 1 | Response 2 | Response 3 |
|---|---|---|---|---|---|---|---|---|
| Std | Run | A:Layer Height | B:Speed | C:Angle | D:Line width | Roughness Ra | Roughness Rq | Printing Time |
| | | mm | mm/s | Degree | mm | um | um | min |
| 17 | 1 | 0,13 | 60 | 52,5 | 0,35 | 20 | 24 | 61 |
| 7 | 2 | 0,06 | 100 | 75 | 0,32 | 12 | 16 | 90 |
| 12 | 3 | 0,2 | 100 | 30 | 0,38 | 49 | 57 | 36 |
| 2 | 4 | 0,2 | 20 | 30 | 0,32 | 37 | 43 | 106 |
| 9 | 5 | 0,06 | 20 | 30 | 0,38 | 16 | 19 | 199 |
| 1 | 6 | 0,06 | 20 | 30 | 0,32 | 15 | 18 | 224 |
| 4 | 7 | 0,2 | 100 | 30 | 0,32 | 44 | 51 | 40 |
| 3 | 8 | 0,06 | 100 | 30 | 0,32 | 16 | 20 | 106 |
| 15 | 9 | 0,06 | 100 | 75 | 0,38 | 12 | 15 | 68 |
| 5 | 10 | 0,06 | 20 | 75 | 0,32 | 12 | 15 | 177 |
| 11 | 11 | 0,06 | 100 | 30 | 0,38 | 15 | 19 | 99 |
| 13 | 12 | 0,06 | 20 | 75 | 0,38 | 10 | 13 | 137 |
| 19 | 13 | 0,13 | 60 | 52,5 | 0,35 | 16 | 19 | 61 |
| 14 | 14 | 0,2 | 20 | 75 | 0,38 | 20 | 24 | 61 |
| 8 | 15 | 0,2 | 100 | 75 | 0,32 | 21 | 25 | 33 |
| 16 | 16 | 0,2 | 100 | 75 | 0,38 | 21 | 26 | 25 |
| 10 | 17 | 0,2 | 20 | 30 | 0,38 | 41 | 47 | 93 |
| 6 | 18 | 0,2 | 20 | 75 | 0,32 | 20 | 24 | 77 |
| 18 | 19 | 0,13 | 60 | 52,5 | 0,35 | 16 | 19 | 61 |

*Figure 135 Overview response for roughness values Ra and Rq of upward facing surfaces*

*Figure 135*

| | | Factor 1 | Factor 2 | Factor 3 | Factor 4 | Response 1 | Response 2 | Response 3 |
|---|---|---|---|---|---|---|---|---|
| Std | Run | A:Layer Height | B:Speed | C:Angle | D:Line width | Roughness Ra | Roughness Rq | Printing Time |
| | | mm | mm/s | Degree | mm | um | um | min |
| 17 | 1 | 0,13 | 60 | 52,5 | 0,35 | 17 | 20 | 61 |
| 7 | 2 | 0,06 | 100 | 75 | 0,32 | 10 | 12 | 90 |
| 12 | 3 | 0,2 | 100 | 30 | 0,38 | 133 | 177 | 36 |
| 2 | 4 | 0,2 | 20 | 30 | 0,32 | 60 | 65 | 106 |
| 9 | 5 | 0,06 | 20 | 30 | 0,38 | 37 | 49 | 199 |
| 1 | 6 | 0,06 | 20 | 30 | 0,32 | 26 | 32 | 224 |
| 4 | 7 | 0,2 | 100 | 30 | 0,32 | 45 | 49 | 40 |
| 3 | 8 | 0,06 | 100 | 30 | 0,32 | 17 | 21 | 106 |
| 15 | 9 | 0,06 | 100 | 75 | 0,38 | 9 | 12 | 68 |
| 5 | 10 | 0,06 | 20 | 75 | 0,32 | 9 | 12 | 177 |
| 11 | 11 | 0,06 | 100 | 30 | 0,38 | 17 | 20 | 99 |
| 13 | 12 | 0,06 | 20 | 75 | 0,38 | 7 | 9 | 137 |
| 19 | 13 | 0,13 | 60 | 52,5 | 0,35 | 16 | 19 | 61 |
| 14 | 14 | 0,2 | 20 | 75 | 0,38 | 20 | 24 | 61 |
| 8 | 15 | 0,2 | 100 | 75 | 0,32 | 20 | 24 | 33 |
| 16 | 16 | 0,2 | 100 | 75 | 0,38 | 20 | 25 | 25 |
| 10 | 17 | 0,2 | 20 | 30 | 0,38 | 69 | 77 | 93 |
| 6 | 18 | 0,2 | 20 | 75 | 0,32 | 20 | 24 | 77 |
| 18 | 19 | 0,13 | 60 | 52,5 | 0,35 | 18 | 21 | 61 |

*Figure 136 Overview response for roughness values Ra and Rq of downward facing surfaces*

*Figure 136*

*Overall results downward facing surfaces*

For the downward facing surfaces the overview of all roughness measurements can be found in figure 136. By examining the minimum and maximum roughness values it is clear there is a large difference between the range of the upward and downward facing surface roughness. For the downward facing surface the minimum surface roughness value Ra was 7 µm(Rq= 9 µm) and the highest Ra was 133 µm(Rq= 177 µm).

*Correlation analysis*

To have an initial view on the gathered data the roughness values with respect to the changing parameters have been observed. Design Expert 10 automatically generates graphs displaying the registered responses and a correlation coefficient of the linear relation between the roughness response and the changed parameter. Figure 137 shows an overview of the graphs for layer height, printing speed, angle orientation and line width with respect to roughness values Ra and Rq for the upward and downward facing surfaces.

The correlation coefficient indicates the strength of a linear relationship between the parameter and the response and whether the linear relation is negative or positive. This value is always between -1 and +1 whereas a value 0 indicates zero linear relationship. A value of +1 indicates a strong positive linear relationship so an increase in one variable leads to an increase in the other variable. For the upward facing surfaces the correlation coefficients are as followed; layer height vs. roughness Ra 0,73(Rq= 0,73), printing speed vs. roughness Ra 0,09(Rq= 0,10), angle orientation vs. roughness Ra -0,52(Rq= -0,52) and line width vs. roughness Ra 0,03(Rq= 0,03).

For the downward facing surfaces the correlation coefficients are as followed; layer height vs. roughness Ra 0,50(Rq= 0,45), printing speed vs. roughness Ra 0,04(Rq= 0,07), angle orientation vs. roughness Ra -0,56(Rq= -0,53) and line width vs. roughness Ra 0,20(Rq= 0,23).

*Parameter influence on upward facing surface roughness Ra and Rq*

After the initial correlation analysis, the parameters are statistically checked on its significance and interactions. Figure 138 shows the half-normal plot with standardized effect of parameters and interactions. The red line in the graphs represents the error line and indicates the smallest 50% of the effects. The parameters at the far right in the graph are the largest effects and have to be separated from the likely to repeatable effects and small, possible noise effects. In this case the layer height, angle orientation and the interaction between these parameters are the largest effects on surface roughness Ra. The half-normal plot for the Rq shows the same largest effects. To confirm the results from the half-normal plots, the pareto chart is analyzed. This chart ranks the parameters according to their rank on influencing the response. Parameters above the Bonferroni limit can be seen as big effects, parameters between the Bonferroni limit and t-value limit can be seen as moderate effects and parameters below the t-value limit can be seen as small or neglectable effects. Layer height, angle orientation and their interaction are the biggest effects according to the pareto chart, figure 139. Figure 142 shows the contribution of the parameter on roughness Ra and whether it is taken into account for the prediction model(e stands for exclusion).

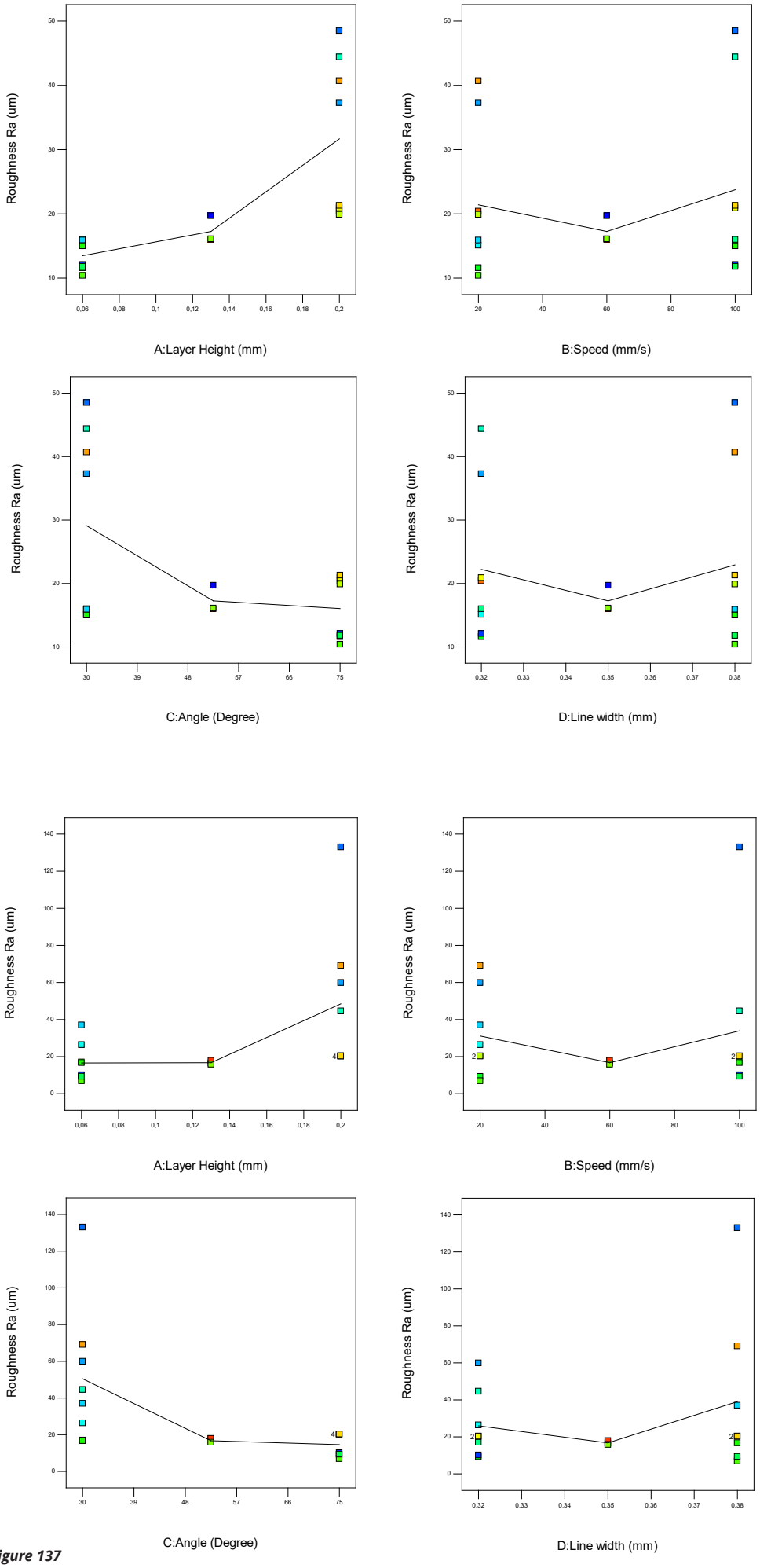


***Figure 137 Overview roughness vs. parameter graphs***

***Figure 137***

*Parameter influence on downward facing surface roughness Ra and Rq*

The same statistical analysis has been performed for the downward facing surfaces. Figure 140 shows the half-normal plot with standardized effect of parameters and interactions. In this case the angle orientation and layer height were the parameters having the biggest effect on the surface roughness value Ra. The half-normal plot for the Rq shows identical effects. The pareto chart confirms this with a significant difference between the 2 biggest effects and the rest having small effects, see figure 141. Parameters included in the prediction model and its contribution in % can be found in figure143.

*Prediction model and confirmation*

With the input of the measurements the design expert 10 software can set up a prediction model to predict surface roughness based on included parameters for the model. For the upward facing surface prediction model the layer height, angle orientation and their interaction are taken into account and resulted in the following formulas:

Ra= 0,512046 + 280,536 * Layer Height + 0,0826984 * Angle + -2,86905 * Layer Height * Angle

Rq= 2,37525 + 310,595 * Layer Height + 0,0896032 * Angle + -3,15079 * Layer Height * Angle

For the downward facing surface prediction model the layer height and angle orientation are taken into account and resulted in the following formulas:

1/Sqrt(Ra)= 0,190008 + -0,737027 * Layer Height + 0,00252369 * Angle

1/Sqrt(Rq)= 0,167806 + -0,601067 * Layer Height + 0,00217834 * Angle

The downward facing surface roughness data needed a transformation in order to fit the model, design expert 10 software has this option integrated and recommends transformations if necessary.

In order to confirm the prediction model several confirmation samples were printed incorporating random parameter variables. Confirmation sample 1( 5x printed) was printed at layer height 0,15 mm, speed 40 mm/s, angle orientation 35° and line width 0,35 mm. Confirmation sample 2(4x printed) was printed at layer height 0,1 mm, speed 55 mm/s, angle orientation 65° and line width 0,35 mm. Roughness values for the confirmation runs can be found in figure 144 for both upward and downward facing surfaces.

Both confirmation samples have roughness values which are in the range of the prediction model of the upward and downward facing surfaces. See figure 145 for the confirmation report.

## Discussion

With this correlation experiment the main goal was to further analyse the relation between 4 parameters and the surface roughness. Additionally interactions between parameters are investigated on the influence on the surface roughness. With the use of Design expert 10 the results are statistically analyzed prediction models created.

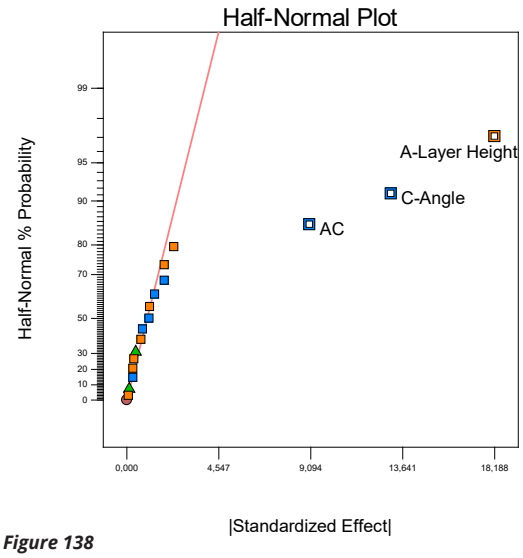


*Figure 138*

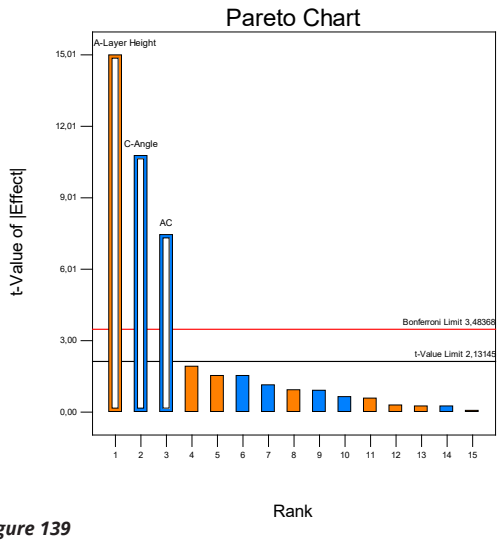


*Figure 139*

*Figure 138 Half-normal plot for Ra roughness of upward surface*

*Figure 139 Pareto chart of Ra roughness of upward surface*

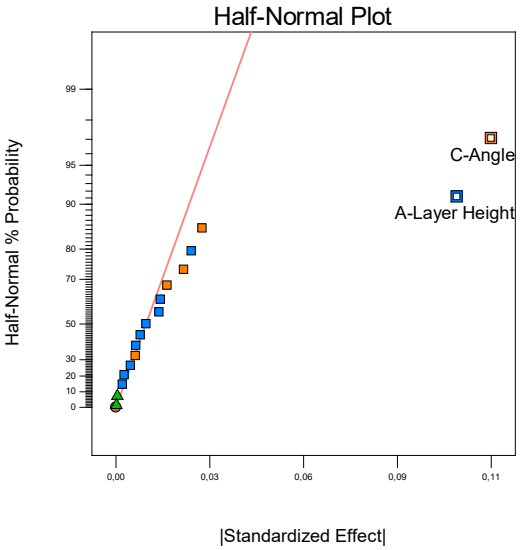


*Figure 140*

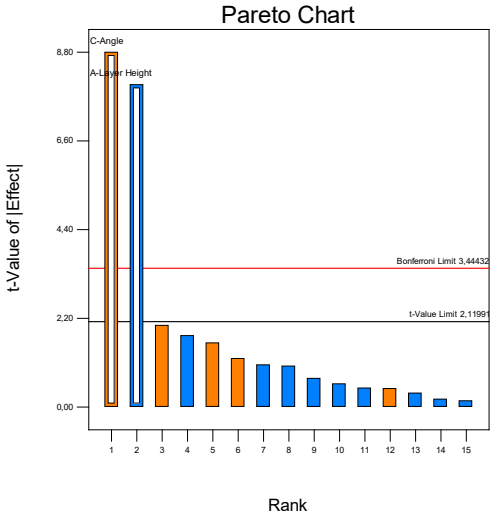


*Figure 141*

*Figure 140 Half-normal plot for Ra roughness of downward surface*

*Figure 141 Pareto chart of Ra roughness of downward surface*

| | Term | Stdized Effect | Sum of Squares | % Contribution |
|---|---|---|---|---|
| | Intercept | | | |
| M | A-Layer Height | 18,19 | 1323,14 | 53,23 |
| e | B-Speed | 2,34 | 21,86 | 0,88 |
| M | C-Angle | -13,06 | 682,52 | 27,46 |
| M | D-Line width | 0,71 | 2,03 | 0,082 |
| e | AB | 1,86 | 13,88 | 0,56 |
| M | AC | -9,04 | 326,71 | 13,14 |
| e | AD | 1,14 | 5,18 | 0,21 |
| e | BC | -1,39 | 7,70 | 0,31 |
| e | BD | 0,087 | 0,031 | 1,232E-003 |
| e | CD | -1,11 | 4,95 | 0,20 |
| e | ABC | -1,86 | 13,88 | 0,56 |
| e | ABD | 0,31 | 0,39 | 0,016 |
| e | ACD | -0,79 | 2,48 | 0,100 |
| e | BCD | 0,36 | 0,53 | 0,021 |
| e | ABCD | -0,31 | 0,39 | 0,016 |
| e | Curvature | -4,22 | 71,36 | 2,87 |
| e | Lack of Fit | | 0,000 | 0,000 |
| e | Pure Error | | 8,89 | 0,36 |
| | Lenth's ME | 3,14 | | |
| | Lenth's SME | 5,76 | | |

*Figure 142*

| | Term | Stdized Effect | Sum of Squares | % Contribution |
|---|---|---|---|---|
| | Intercept | | | |
| M | A-Layer Height | -0,10 | 0,043 | 40,44 |
| e | B-Speed | 5,918E-003 | 1,401E-004 | 0,13 |
| M | C-Angle | 0,11 | 0,052 | 48,99 |
| e | D-Line width | -4,467E-003 | 7,981E-005 | 0,076 |
| e | AB | -9,183E-003 | 3,373E-004 | 0,32 |
| e | AC | -0,013 | 6,871E-004 | 0,65 |
| e | AD | -0,014 | 7,308E-004 | 0,69 |
| e | BC | -0,023 | 2,092E-003 | 1,99 |
| e | BD | -7,434E-003 | 2,211E-004 | 0,21 |
| e | CD | 0,021 | 1,686E-003 | 1,60 |
| e | ABC | 0,026 | 2,732E-003 | 2,59 |
| e | ABD | -6,096E-003 | 1,486E-004 | 0,14 |
| e | ACD | -2,547E-003 | 2,596E-005 | 0,025 |
| e | BCD | -2,003E-003 | 1,605E-005 | 0,015 |
| e | ABCD | 0,016 | 9,651E-004 | 0,92 |
| e | Curvature | 0,017 | 1,157E-003 | 1,10 |
| e | Lack of Fit | | 0,000 | 0,000 |
| e | Pure Error | | 1,191E-004 | 0,11 |
| | Lenth's ME | 0,028 | | |
| | Lenth's SME | 0,051 | | |

*Figure 143*

*Figure 142 Numeric overview of parameters in model of upward surface*

*Figure 143 Numeric overview of parameters in model of downward surface*

*Correlation upward surface*

From the upward surface correlation analysis it was clear that layer height had the strongest positive linear relationship coefficient of 0,73 with the surface roughness values Ra and Rq.

So surface roughness Ra and Rq will both increase with an increase in layer height, which could also be seen in the screening experiment results.

For speed a small decrease in surface roughness could be seen in the screening experiment, however for the correlation experiment this effect is less noticeable. The correlation coefficient for the linear relationship with surface roughness is 0,09 for the Ra and 0,10 for the Rq. The effect of speed can not be seen a linear influence on the surface roughness values Ra and Rq for upward facing surfaces.

The angle orientation has a correlation coefficient of -0,52 for both the Ra and the Rq which indicates a moderate negative linear relationship. An increase in the angle orientation(seen from the horizontal plane) results in a lower surface roughness value Ra and Rq.

Line width shows the weakest linear relationship with surface roughness value Ra and Rq with a correlation coefficient value of 0,03. A similar effect can be seen in the results of the screening experiment for the parameter line width. So surface roughness value Ra and Rq will not increase with a change in line width.

*Correlation downward surface*

As layer height was having the strongest linear relationship for the upward facing surfaces, it does not have the strongest linear relationship for the downward facing surfaces. With a correlation coefficient of 0,50 for the Ra( 0,45 for Rq) it is the second strongest linear relationship compared with the other parameters. The linear relationship is positive which means that an increase of layer height results in an increase of roughness values Ra and Rq.

For speed a small decrease in roughness was discovered during the screening experiment for downward facing surfaces. However this effect was not evidently present in the correlation experiment. The correlation coefficient for the speed was 0,04 for the Ra(0,07 for Rq) which lies closely to a zero linear relationship between roughness values and the speed parameter.

The parameter having the strongest linear relationship is the angle orientation. With a correlation coefficient of -0,56 for Ra(-0,53 for Rq) this is a negative linear relationship of roughness and angle orientation. This means an increase of the angle orientation results in a decrease in surface roughness values Ra and Rq.

For line width the correlation coefficient is 0,20 for the Ra(0,23 for Rq) which is a stronger positive linear relationship than speed but less than the relationship of layer height and angle orientation. From the results graphs of line width the influence does not seem to be significantly, so to be sure this needs to be checked statistically.

*Parameter influence on upward facing surface roughness Ra and Rq*

In order to discover the parameters having the largest influence on the surface roughness, the half-normal plot and pareto chart have to be examined. From this it is evident that layer height has the largest

*Upward (1)*

| Roughness Ra | Roughness Rq |
|---|---|
| 31 | 35 |
| 32 | 30 |
| 32 | 31 |
| 31 | 34 |
| 31 | 31 |

*Downward (1)*

| Roughness Ra | Roughness Rq |
|---|---|
| 35 | 45 |
| 30 | 38 |
| 31 | 39 |
| 34 | 45 |
| 31 | 39 |

*Upward (2)*

| Roughness Ra | Roughness Rq |
|---|---|
| 16 | 19 |
| 13 | 16 |
| 15 | 19 |
| 15 | 19 |

*Downward (2)*

| Roughness Ra | Roughness Rq |
|---|---|
| 13 | 16 |
| 13 | 17 |
| 12 | 15 |
| 13 | 16 |

***Figure 144 Roughness Ra and Rq values of confirmation runs***

***Figure 144***

**Confirmation Report**

**Two-sided** **Confidence = 95%** **n = 5**

| Factor | Name | Level | Low Level | High Level | Std. Dev. | Coding |
|---|---|---|---|---|---|---|
| A | Layer Height | 0,15 | 0,060 | 0,20 | 0,000 | Actual |
| B | Speed | 40,00 | 20,00 | 100,00 | 0,000 | Actual |
| C | Angle | 35,00 | 30,00 | 75,00 | 0,000 | Actual |
| D | Line width | 0,35 | 0,32 | 0,38 | 0,000 | Actual |

| Response | Predicted Mean | Predicted Median[2] | Observed | Std Dev | n | SE Pred | 95% PI low | Data Mean | 95% PI high |
|---|---|---|---|---|---|---|---|---|---|
| Roughness Ra[3] | 38,1576 | 35,5223 | - | 11,7773 | 5 | N/A | 25,4585 | 32,0368 | 52,9878 |
| Roughness Rq[3] | 45,5852 | 42,2273 | - | 14,5469 | 5 | N/A | 29,9385 | 41,2073 | 63,9863 |
| Printing Time[3] | 86,0643 | 83,9693 | - | 18,9898 | 5 | N/A | 65,5532 | | 107,559 |

[1] For transformed responses the data mean is calculated on the transformed scale. See help for details.

[2] For transformed responses the predicted mean and median may differ on the original scale. See help for details.

[3] Standard error (SE) not calculated on original scale. See help for details.

***Figure 145 Confirmation report on roughness prediction by model***

***Figure 145***

influence on the roughness, followed by angle orientation and the interaction between layer height and angle orientation. The ANOVA analysis of variance confirms layer height($p< 0.05$), angle($p< 0.05$) and the interaction between these($p< 0.05$) are significant for both Ra and Rq values, see figure 146.

*Parameter influence on downward facing surface roughness Ra and Rq*

The same statistics have been used for the downward facing surfaces to investigate the parameters having the largest influence on the surface roughness. The half-normal and pareto chart clearly indicates that angle orientation has the largest effect followed by layer height. For the downward facing surface the interaction between these two parameters is not found to influence the surface roughness Ra. This also applies to the surface roughness value Rq. The ANOVA analysis of variance also confirms that angle orientation($p<0.05$) and layer height($p<0.05$) are significant, see figure 147.

*Prediction model and confirmation*

The formulas shown in the results section can give estimations for roughness values Ra and Rq based on pre set printing parameters. Multiple runs of 2 confirmation model have been printed and analysed on the surface roughness. The measured roughness values for both models were in the range of the prediction. So these formulas can give insight in the expected surface finish of the FDM printed object. If an object needs to have a desired surface finish the model can also be used for setting parameters. As a test the roughness value Ra of model A3 from the screening experiment(layer height= 0,2, speed= 60 mm/s, angle orientation= 45° and line width= 0,35 mm) has been used as input as the desired roughness value. The roughness value Ra of model A3 was 31,83 µm. One solution for accomplishing the roughness value of 31,81 µm was incorporating a layer height of 0,19 mm, printing speed of 59,88 mm/s, angle orientation of 44,8° and a line width of 0,35 mm. The overview of the optimization report can be seen in figure 148.

## Conclusion

This correlation experiment has revealed some interesting results regarding FDM surface finish. From the screening experiment 4 parameters were selected for further in depth analysis on correlation and significance. These parameters were layer height, printing speed, angle orientation and line width and acted as the input for this analysis. In total 19 upward and downward samples were printed and subjected to the optical scanner system which led to the surface roughness values Ra and Rq. With the use of Design Expert 10 this data was statistically analyzed and a prediction model created. The final formulas were confirmed with 2 models with random values printed several times.

From the correlation experiment is was clear that surface roughness Ra and Rq will both increase with an increase in layer height. This can also be seen at the downward facing surfaces but in a less stronger linear relationship than the upward facing surfaces. From the ANOVA the parameter layer height is found significant.

The effect of speed can not be seen a linear influence on the surface roughness values Ra and Rq for upward and downward facing surfaces. Both correlation

**Response 1 Roughness Ra**

**ANOVA for selected factorial model**

**Analysis of variance table [Partial sum of squares - Type III]**

| Source | Sum of Squares | df | Mean Square | F Value | p-value Prob > F | |
|---|---|---|---|---|---|---|
| Model | 2332,36 | 3 | 777,45 | 75,96 | < 0.0001 | significant |
| *A-Layer Heig* | *1323,14* | *1* | *1323,14* | *129,28* | *< 0.0001* | |
| *C-Angle* | *682,52* | *1* | *682,52* | *66,68* | *< 0.0001* | |
| *AC* | *326,71* | *1* | *326,71* | *31,92* | *< 0.0001* | |
| Residual | 153,52 | 15 | 10,23 | | | |
| *Lack of Fit* | *144,64* | *13* | *11,13* | *2,50* | *0,3213* | *not significant* |
| *Pure Error* | *8,89* | *2* | *4,44* | | | |
| Cor Total | 2485,89 | 18 | | | | |

The Model F-value of 75,96 implies the model is significant. There is only a 0,01% chance that an F-value this large could occur due to noise.

*Figure 146 ANOVA analysis of variance output for upward surface*

*Figure 146*

**Response 1 Roughness Ra**

**Transform: Inverse Sqrt Constant: 0**

**ANOVA for selected factorial model**

**Analysis of variance table [Partial sum of squares - Type III]**

| Source | Sum of Squares | df | Mean Square | F Value | p-value Prob > F | |
|---|---|---|---|---|---|---|
| Model | 0,094 | 2 | 0,047 | 67,64 | < 0.0001 | significant |
| *A-Layer Heig* | *0,043* | *1* | *0,043* | *61,18* | *< 0.0001* | |
| *C-Angle* | *0,052* | *1* | *0,052* | *74,11* | *< 0.0001* | |
| Residual | 0,011 | 16 | 6,961E-004 | | | |
| *Lack of Fit* | *0,011* | *14* | *7,871E-004* | *13,22* | *0,0725* | *not significant* |
| *Pure Error* | *1,191E-004* | *2* | *5,953E-005* | | | |
| Cor Total | 0,11 | 18 | | | | |

The Model F-value of 67,64 implies the model is significant. There is only a 0,01% chance that an F-value this large could occur due to noise.

*Figure 147 ANOVA analysis of variance output for downward surface*

*Figure 147*

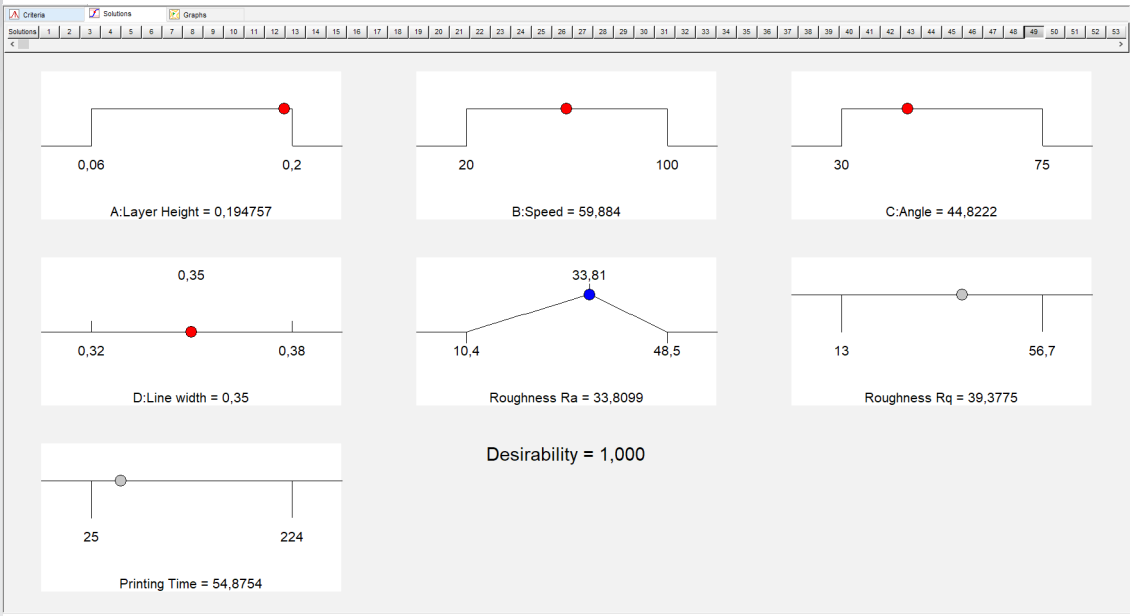


*Figure 148 Optimization solution for Ra= 33,81 micrometers*

*Figure 148*

coefficients are close to zero which means there is no linear relationship between speed and roughness values Ra and Rq.

The angle orientation has a moderate negative linear relationship for upward facing surfaces. An increase in the angle orientation(seen from the horizontal plane) results in a lower surface roughness value Ra and Rq. This same effect can be seen for the downward facing surfaces but has a stronger linear relationship.

Line width shows the weakest linear relationship with surface roughness value Ra and Rq for upward facing surfaces. However this linear relationship was stronger for the downward facing surfaces. With the use of statistical analysis and ANOVA the line width was not found to be significant.

Two formulas for the prediction of surface roughness have been generated and tested with confirmation runs. These formulas have proven their accuracy with the confirmation and optimization. It can be used for prediction and optimizing of roughness when printing polycarbonate on the Ultimaker 3 desktop printer.
For the upward facing surface prediction model the layer height, angle orientation and their interaction are taken into account and resulted in the following formulas:

Ra= 0,512046 + 280,536 * Layer Height + 0,0826984 * Angle + -2,86905 * Layer Height * Angle

Rq= 2,37525 + 310,595 * Layer Height + 0,0896032 * Angle + -3,15079 * Layer Height * Angle

For the downward facing surface prediction model the layer height and angle orientation are taken into account and resulted in the following formulas:

1/Sqrt(Ra)= 0,190008 + -0,737027 * Layer Height + 0,00252369 * Angle

1/Sqrt(Rq)= 0,167806 + -0,601067 * Layer Height + 0,00217834 * Angle

According to the models which fit the data the lowest possible roughness values Ra and Rq are 10,6 µm and 13,6 µm respectively for the upward facing surfaces. For the downward facing surfaces the lowest roughness values Ra and Rq obtainable are 9,1 µm and 11,7 µm respectively.

# 12. Mitutoyo measurement comparison

To compare the results gathered with the optical scanner system, measurements have been performed with a contact based surface roughness measuring device; the Mitutoyo Surftest SJ 210. This device is specially made for surface roughness examination and measures the profile of the surface with a fine stylus with a radius of 2 micrometers(Mitutoyo, 2017). These additional measurements act as a control experiment to investigate the suitability of the optical scanner system to be used for surface roughness measurements. Both the screening and correlation experiment are performed with the Mitutoyo surftest SJ 210 buth without the downward facing surface of the correlation samples. Some downward facing surfaces of the correlation samples show detached printing lines or large inconsistencies which might cause serious damage the measuring stylus and are therefore excluded.

## Method

For the measurements of the control experiments the only aspect which changed was the measuring device. This change also allowed for faster surface roughness measurements as the device instantly calculates the required surface roughness components Ra and Rq. No further processing of the measurements files was necessary.

*Surface roughness measurement device*

As mentioned in the first section the Mitutoyo Surftest SJ 210 was used for the surface roughness measurements. Figure 149 presents the Mitutoyo surface roughness device which is used for this control experiment. What can be seen is that the measuring unit is fixed on a specially designed holder which can move up and down. In order to measure the surface profile, the stylus needs to be positioned on the surface of the sample. The stylus partly rests on the surface without applying too much pressure to damage the stylus tip. Pressing the start measurement button will move the stylus with a distance of 6.4 mm over the sample surface following the boundary layer surface profile. The on screen reproduction of the surface profile gives an indication on the success of the measurement, see figure 149. In the case of bend samples the surface measurement will go out of range and has to be restarted and lowering the stylus more. A successfull can will immediately calculate the surface roughness components Ra and Rq.

*Sample design*

The same samples are used for the control experiment as for the optical scanner systems experiments. The width of the samples allowed for suitable placement on the measuring platform of the Mitutoyo stand. A metal plate prevented the sample from moving along with the stylus movement, see figure 149.

*Procedure*

The procedure for the control experiments was straightforward as the samples needed to be placed on the metal strip against the fixed metal plate. Followed by lowering the measuring unit until the point was reached at which the stylus tip was raised upward by the pressure of the stylus on the surface. At this point the machine was set to begin measurement by pressing start in the control panel.

The stylus tip moves with a constant speed of 0.5 mm/s along the surface profile with a scanning distance of 6.4 mm. During this scanning the stylus tip will move inwards to the measuring device. After scanning a distance of 6.4 mm the stylus will move back to its starting position and calculate the surface roughness

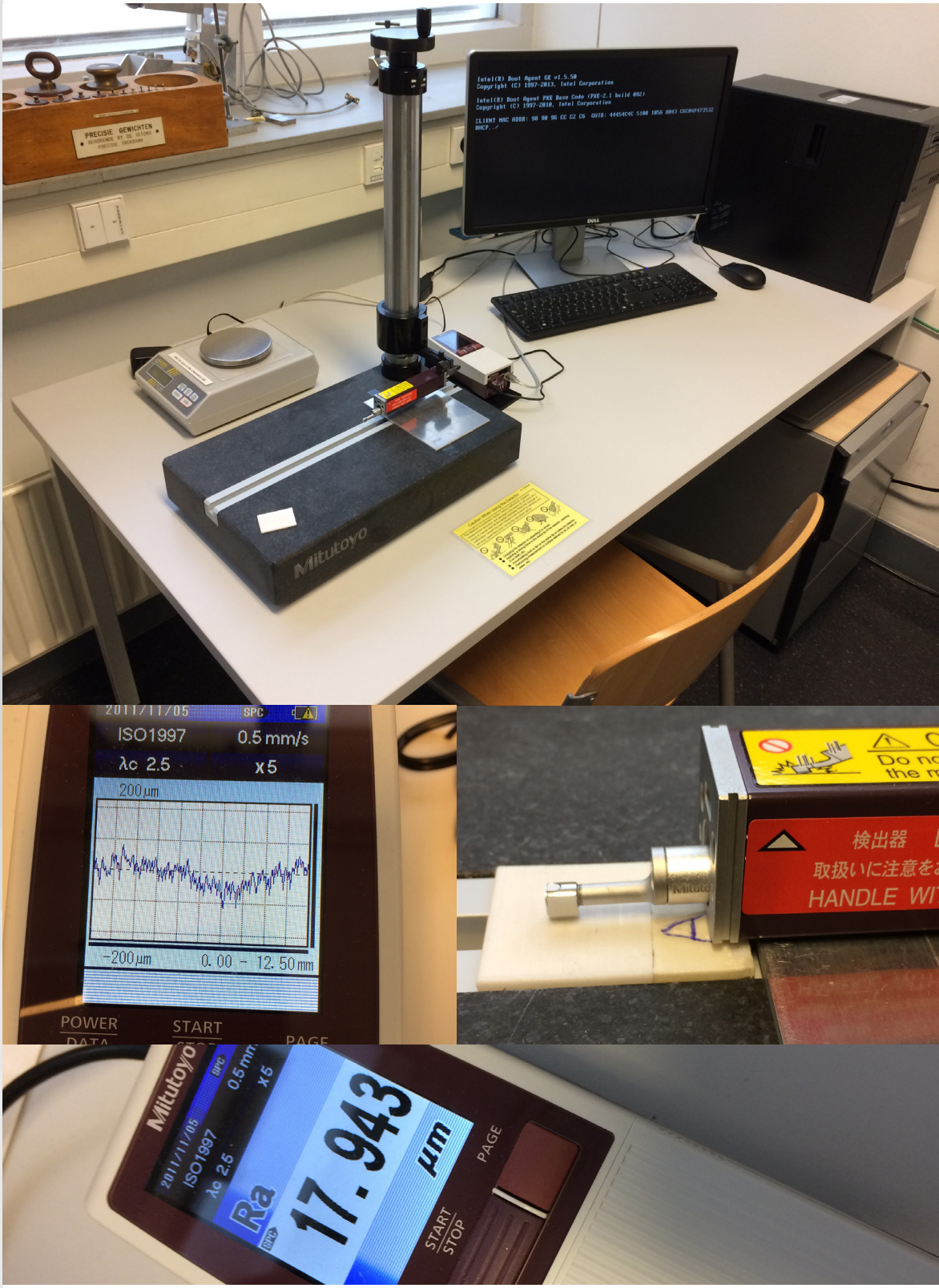


*Figure 149 Overview Mitutoyo surftest SJ-210*

*Figure 149*

components Ra and Rq. Other desired roughness components can be set in the control panel.

The results of the roughness scans are registered in excel for the screening sample results and in Design expert 10 for the correlation sample results. After collecting the data it is processed in the same manner as the results from the optical scanner system experiments.

## Results

Both the screening and correlation results will be presented in this section. The results of the screening experiment will be presented in the form of excel graphs similar to the screening results of the optical scanner. For the correlation experiment results will be presented in statistical graphs from design expert 10 software.

*Screening experiment*

The results from the measurements with the Mitutoyo measuring device can be found in figure 150 for the upward facing surfaces and figure 151 for the downward facing surfaces. This figure gives an overview of the values obtained, the values have also been plotted in graphs in order to compare them with the screening results with the optical scanner system, see figures 152 to 179.

| Sample nr. | Setting | Ra [µm] | Rq [µm] | Rq:Ra ratio |
|---|---|---|---|---|
| A1 | 0,06 mm | 9,404 | 11,462 | 1,219 |
| A1/2 | 0,1 mm | 13,775 | 16,83 | 1,222 |
| A2 | 0,13 mm | 18,064 | 22,329 | 1,236 |
| A2/3 | 0,17 mm | 20,986 | 25,075 | 1,195 |
| A3 | 0,2 mm | 23,859 | 28,852 | 1,209 |
| B1 | 250 °C | 18,673 | 22,876 | 1,225 |
| B2 | 260 °C | 17,678 | 21,83 | 1,235 |
| B3 | 270 °C | 17,873 | 21,968 | 1,229 |
| B4 | 280 °C | 17,943 | 22,114 | 1,232 |
| B5 | 290 °C | 18,157 | 22,707 | 1,251 |
| C1 | 20 mm/s | 18,832 | 20 | 1,062 |
| C2 | 40 mm/s | 17,231 | 22,753 | 1,320 |
| C3 | 60 mm/s | 18,006 | 22,275 | 1,237 |
| C4 | 80 mm/s | 18,363 | 21,03 | 1,145 |
| C5 | 100 mm/s | 16,412 | 23,035 | 1,404 |
| D1 | 0% | 18,522 | 22,068 | 1,191 |
| D2 | 25% | 18,449 | 22,966 | 1,245 |
| D3 | 50% | 18,108 | 22,407 | 1,237 |
| D4 | 75% | 18,35 | 22,76 | 1,240 |
| D5 | 100% | 17,939 | 22,186 | 1,237 |
| E1 | 15 ° | 22,169 | 26,36 | 1,189 |
| E2 | 30 ° | 24,266 | 27,416 | 1,130 |
| E3 | 45 ° | 16,605 | 20,216 | 1,217 |
| E4 | 60 ° | 13,795 | 16,702 | 1,211 |
| E5 | 75 ° | 11,157 | 13,659 | 1,224 |
| E6 | 90 ° | 9,078 | 10,883 | 1,199 |
| F1 | 0,32 mm | 18,593 | 23,064 | 1,240 |
| F2 | 0,35 mm | 17,876 | 21,905 | 1,225 |
| F3 | 0,38 mm | 17,727 | 21,856 | 1,233 |
| O | Center | 19,615 | 24,426 | 1,245 |
| O | Center | 17,454 | 21,531 | 1,234 |
| O | Center | 18,61 | 23,047 | 1,238 |
| O | Center | 18,013 | 22,143 | 1,229 |
| | | | Average | 1,22 |
| | | | Average dev | 0,03 |
| | | | std. | 0,05 |

***Figure 150***

| Sample nr. | Setting | Ra [µm] | Rq [µm] | Rq:Ra ratio |
|---|---|---|---|---|
| A1 | 0,06 mm | 13,828 | 16,458 | 1,19 |
| A1/2 | 0,1 mm | 11,898 | 14,231 | 1,20 |
| A2 | 0,13 mm | 15,032 | 18,247 | 1,21 |
| A2/3 | 0,17 mm | 18,503 | 21,953 | 1,19 |
| A3 | 0,2 mm | 22,5 | 27,177 | 1,21 |
| B1 | 250 °C | 15,305 | 18,442 | 1,20 |
| B2 | 260 °C | 14,698 | 17,732 | 1,21 |
| B3 | 270 °C | 15,014 | 18,308 | 1,22 |
| B4 | 280 °C | 15,151 | 18,338 | 1,21 |
| B5 | 290 °C | 15,559 | 18,73 | 1,20 |
| C1 | 20 mm/s | 14,872 | 18,145 | 1,22 |
| C2 | 40 mm/s | 16,487 | 19,973 | 1,21 |
| C3 | 60 mm/s | 14,641 | 17,794 | 1,22 |
| C4 | 80 mm/s | 15,007 | 17,981 | 1,20 |
| C5 | 100 mm/s | 14,452 | 17,305 | 1,20 |
| D1 | 0% | 15,486 | 18,836 | 1,22 |
| D2 | 25% | 15,24 | 18,507 | 1,21 |
| D3 | 50% | 15,012 | 18,125 | 1,21 |
| D4 | 75% | 15,608 | 18,973 | 1,22 |
| D5 | 100% | 14,815 | 17,922 | 1,21 |
| E1 | 15 ° | 51,065 | 57,108 | 1,12 |
| E2 | 30 ° | 20,477 | 24,531 | 1,20 |
| E3 | 45 ° | 14,733 | 17,674 | 1,20 |
| E4 | 60 ° | 12,873 | 15,587 | 1,21 |
| E5 | 75 ° | 11,174 | 13,594 | 1,22 |
| E6 | 90 ° | 9,684 | 11,651 | 1,20 |
| F1 | 0,32 mm | 15,232 | 18,361 | 1,21 |
| F2 | 0,35 mm | 15,427 | 18,796 | 1,22 |
| F3 | 0,38 mm | 14,864 | 17,867 | 1,20 |
| O | Center | 15,408 | 18,561 | 1,20 |
| O | Center | 14,28 | 17,106 | 1,20 |
| O | Center | 14,778 | 17,799 | 1,20 |
| O | Center | 14,821 | 17,561 | 1,18 |
| O | Center | 15,527 | 18,823 | 1,21 |
| O | Center | 15,316 | 18,451 | 1,20 |
| | | | Average | 1,20 |
| | | | Average dev | 0,01 |
| | | | std. | 0,02 |

*Figure 150 Results of Mitutoyo experiment for upward facing surfaces*

*Figure 151 Results of Mitutoyo experiment for downward facing surfaces*

*Figure 151*

This spread visualizes the difference between the Mitutoyo measurements and the optical scanner measurements of the upward facing surfaces. These graphs show the results of the samples of the screening experiment with varying parameters.

*Mitutoyo surftest SJ 210*

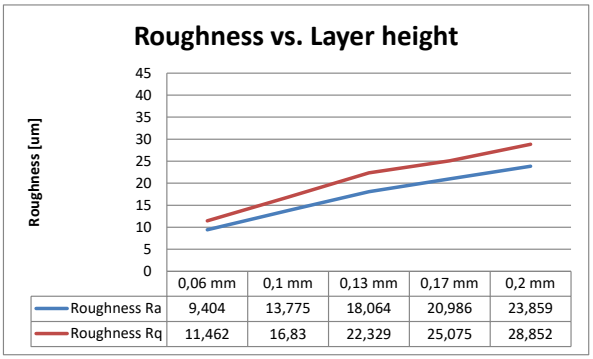


***Figure 152***

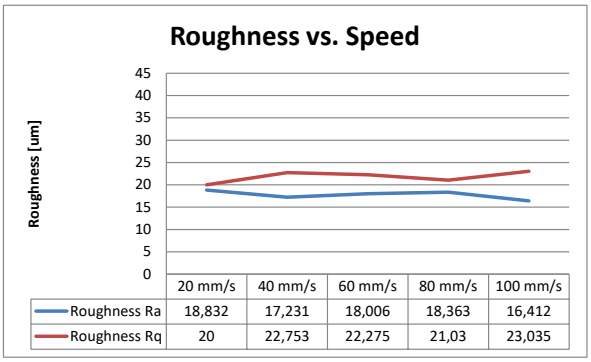


***Figure 154***

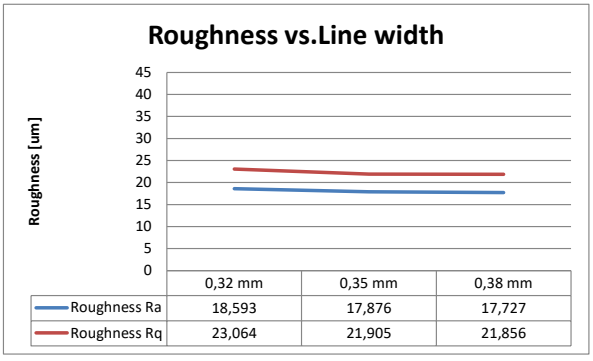


***Figure 156***

*Ultimaker optical scanner system*

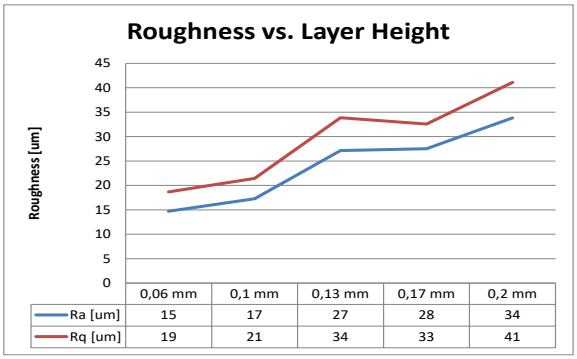


***Figure 153***

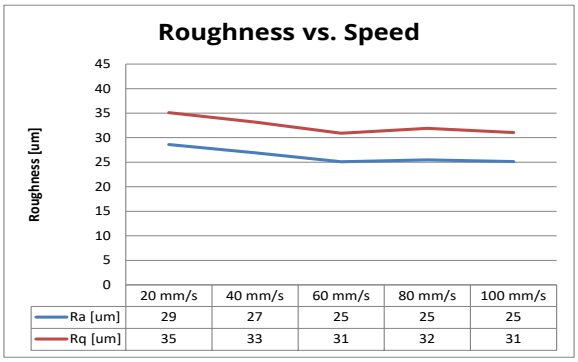


***Figure 155***

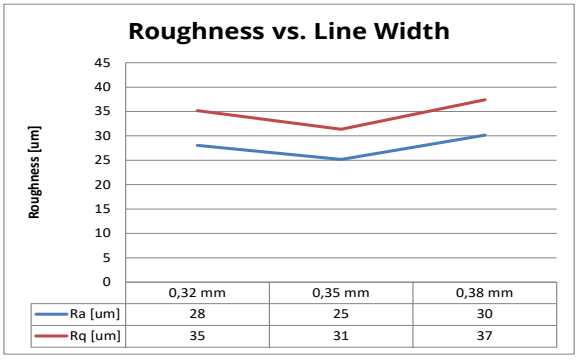


***Figure 157***

*Mitutoyo surftest SJ 210*

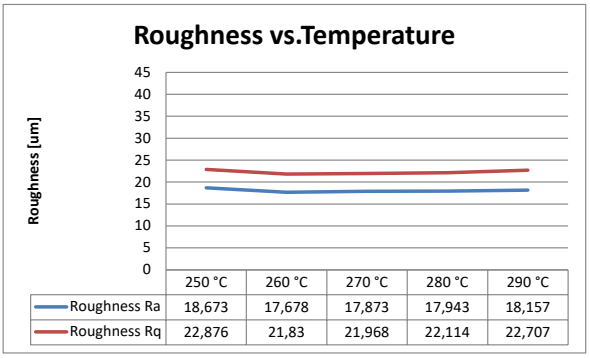


| | 250 °C | 260 °C | 270 °C | 280 °C | 290 °C |
|---|---|---|---|---|---|
| Roughness Ra | 18,673 | 17,678 | 17,873 | 17,943 | 18,157 |
| Roughness Rq | 22,876 | 21,83 | 21,968 | 22,114 | 22,707 |

***Figure 158***

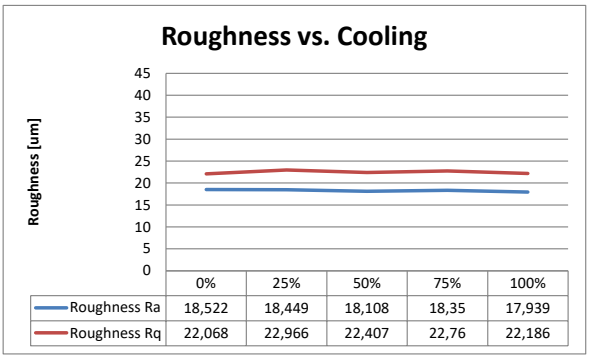


| | 0% | 25% | 50% | 75% | 100% |
|---|---|---|---|---|---|
| Roughness Ra | 18,522 | 18,449 | 18,108 | 18,35 | 17,939 |
| Roughness Rq | 22,068 | 22,966 | 22,407 | 22,76 | 22,186 |

***Figure 160***

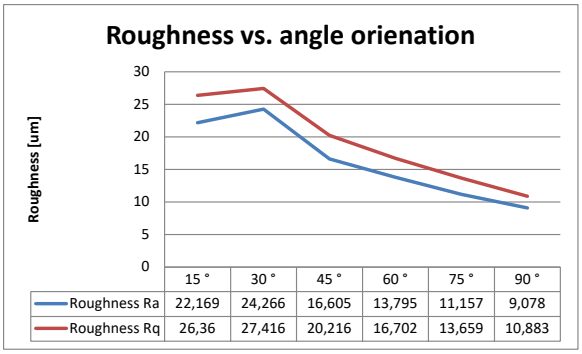


| | 15 ° | 30 ° | 45 ° | 60 ° | 75 ° | 90 ° |
|---|---|---|---|---|---|---|
| Roughness Ra | 22,169 | 24,266 | 16,605 | 13,795 | 11,157 | 9,078 |
| Roughness Rq | 26,36 | 27,416 | 20,216 | 16,702 | 13,659 | 10,883 |

***Figure 162***

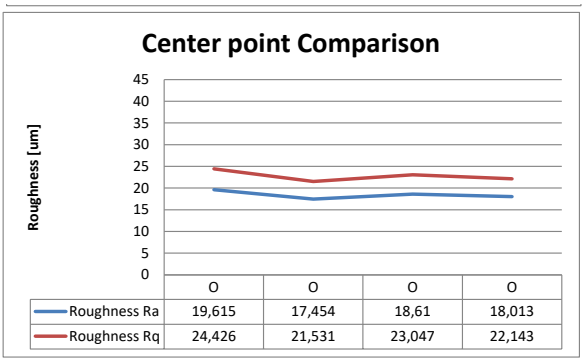


| | O | O | O | O |
|---|---|---|---|---|
| Roughness Ra | 19,615 | 17,454 | 18,61 | 18,013 |
| Roughness Rq | 24,426 | 21,531 | 23,047 | 22,143 |

***Figure 164***

*Ultimaker optical scanner system*

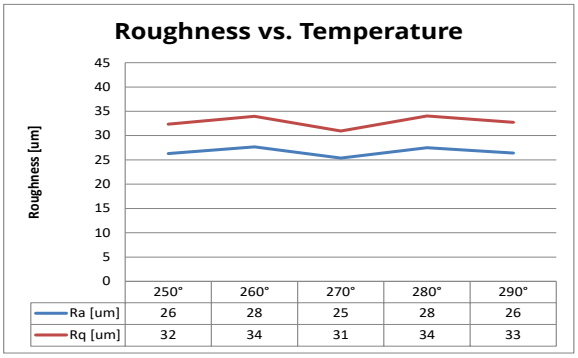


| | 250° | 260° | 270° | 280° | 290° |
|---|---|---|---|---|---|
| Ra [um] | 26 | 28 | 25 | 28 | 26 |
| Rq [um] | 32 | 34 | 31 | 34 | 33 |

***Figure 159***

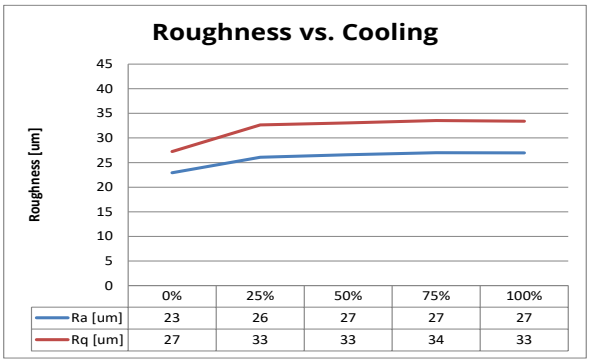


| | 0% | 25% | 50% | 75% | 100% |
|---|---|---|---|---|---|
| Ra [um] | 23 | 26 | 27 | 27 | 27 |
| Rq [um] | 27 | 33 | 33 | 34 | 33 |

***Figure 161***

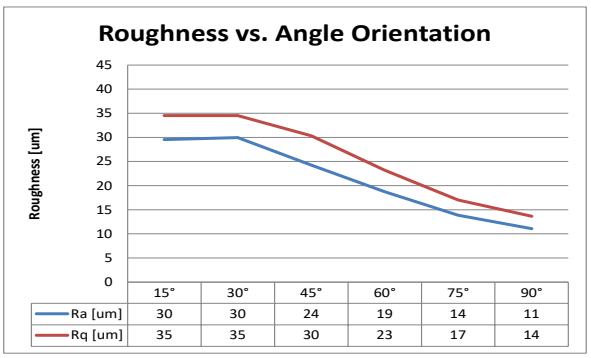


| | 15° | 30° | 45° | 60° | 75° | 90° |
|---|---|---|---|---|---|---|
| Ra [um] | 30 | 30 | 24 | 19 | 14 | 11 |
| Rq [um] | 35 | 35 | 30 | 23 | 17 | 14 |

***Figure 163***

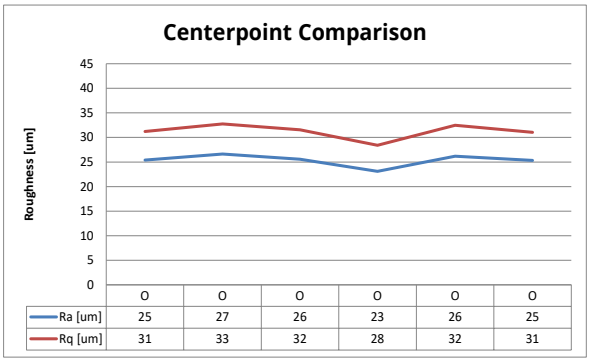


| | O | O | O | O | O | O |
|---|---|---|---|---|---|---|
| Ra [um] | 25 | 27 | 26 | 23 | 26 | 25 |
| Rq [um] | 31 | 33 | 32 | 28 | 32 | 31 |

***Figure 165***

This spread visualizes the difference between the Mitutoyo measurements and the optical scanner measurements of the downward facing surfaces from the screening samples.

*Mitutoyo surftest SJ 210*

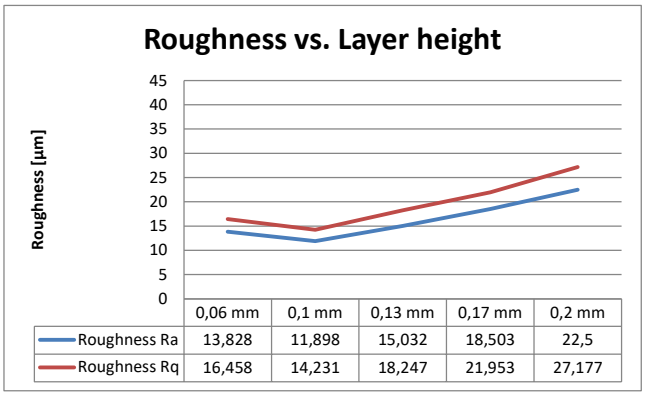


| | 0,06 mm | 0,1 mm | 0,13 mm | 0,17 mm | 0,2 mm |
|---|---|---|---|---|---|
| Roughness Ra | 13,828 | 11,898 | 15,032 | 18,503 | 22,5 |
| Roughness Rq | 16,458 | 14,231 | 18,247 | 21,953 | 27,177 |

***Figure 166***

*Ultimaker optical scanner system*

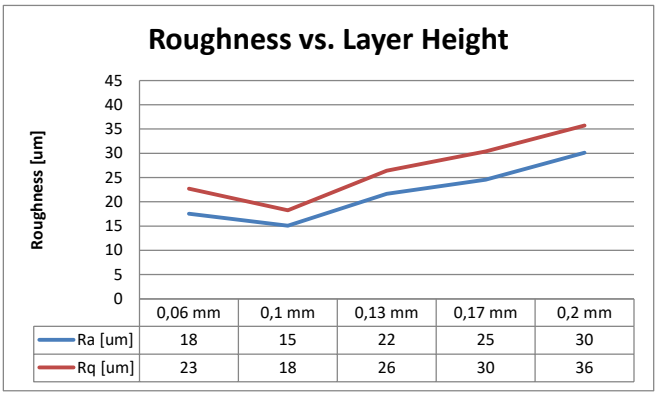


| | 0,06 mm | 0,1 mm | 0,13 mm | 0,17 mm | 0,2 mm |
|---|---|---|---|---|---|
| Ra [um] | 18 | 15 | 22 | 25 | 30 |
| Rq [um] | 23 | 18 | 26 | 30 | 36 |

***Figure 167***

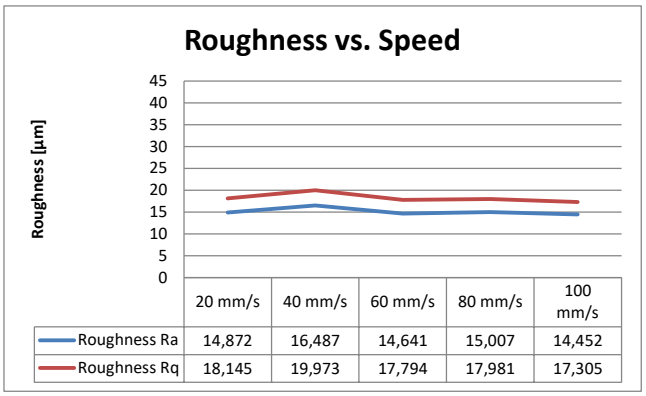


| | 20 mm/s | 40 mm/s | 60 mm/s | 80 mm/s | 100 mm/s |
|---|---|---|---|---|---|
| Roughness Ra | 14,872 | 16,487 | 14,641 | 15,007 | 14,452 |
| Roughness Rq | 18,145 | 19,973 | 17,794 | 17,981 | 17,305 |

***Figure 168***

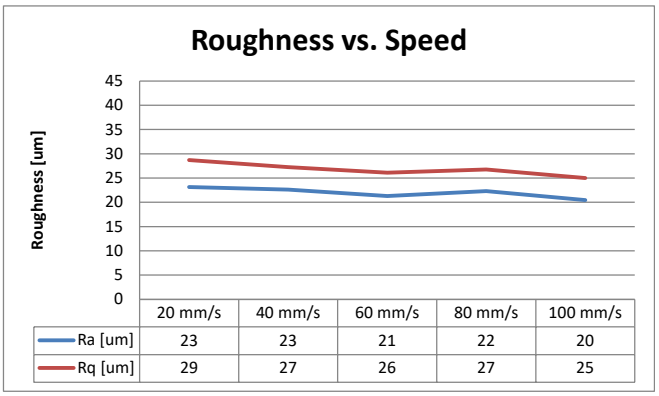


| | 20 mm/s | 40 mm/s | 60 mm/s | 80 mm/s | 100 mm/s |
|---|---|---|---|---|---|
| Ra [um] | 23 | 23 | 21 | 22 | 20 |
| Rq [um] | 29 | 27 | 26 | 27 | 25 |

***Figure 169***

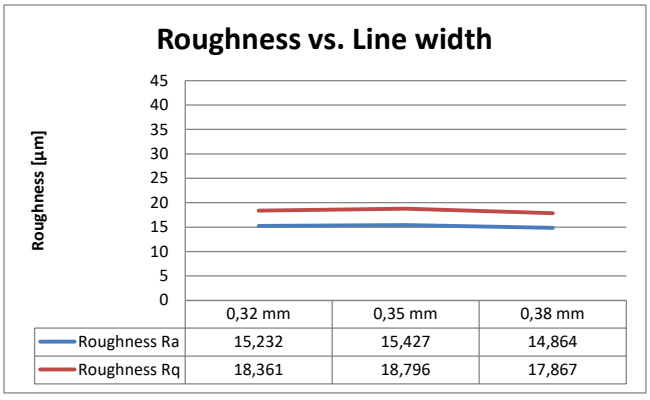


| | 0,32 mm | 0,35 mm | 0,38 mm |
|---|---|---|---|
| Roughness Ra | 15,232 | 15,427 | 14,864 |
| Roughness Rq | 18,361 | 18,796 | 17,867 |

***Figure 170***

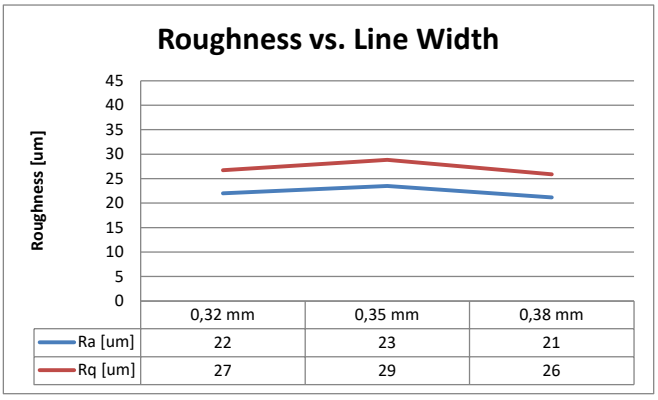


| | 0,32 mm | 0,35 mm | 0,38 mm |
|---|---|---|---|
| Ra [um] | 22 | 23 | 21 |
| Rq [um] | 27 | 29 | 26 |

***Figure 171***

*Mitutoyo surftest SJ 210*

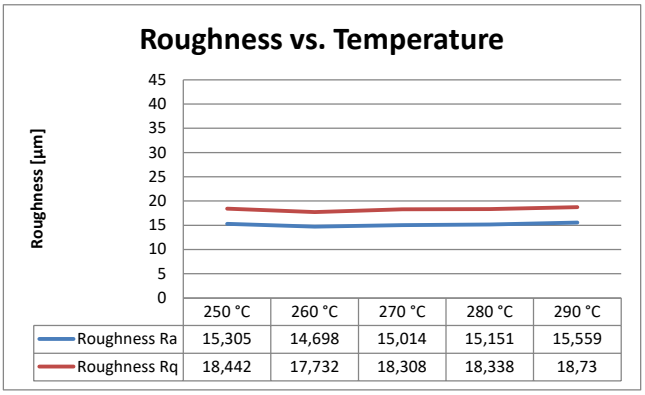


| | 250 °C | 260 °C | 270 °C | 280 °C | 290 °C |
|---|---|---|---|---|---|
| Roughness Ra | 15,305 | 14,698 | 15,014 | 15,151 | 15,559 |
| Roughness Rq | 18,442 | 17,732 | 18,308 | 18,338 | 18,73 |

***Figure 172***

*Ultimaker optical scanner system*

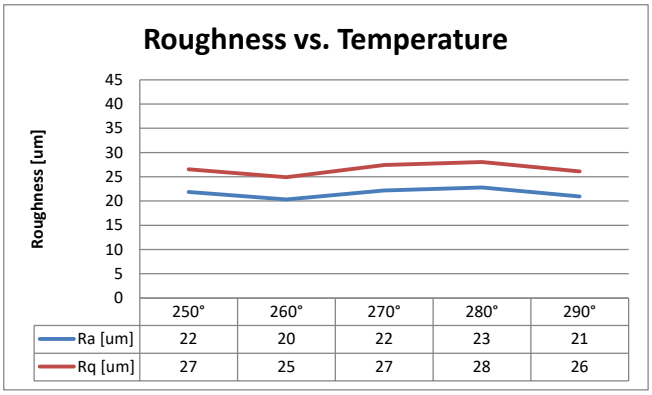


| | 250° | 260° | 270° | 280° | 290° |
|---|---|---|---|---|---|
| Ra [um] | 22 | 20 | 22 | 23 | 21 |
| Rq [um] | 27 | 25 | 27 | 28 | 26 |

***Figure 173***

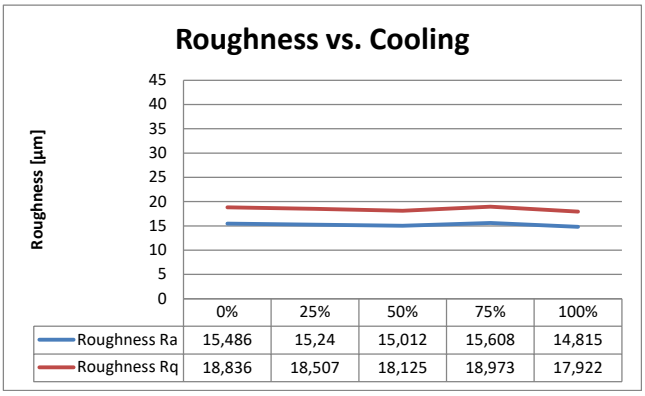


| | 0% | 25% | 50% | 75% | 100% |
|---|---|---|---|---|---|
| Roughness Ra | 15,486 | 15,24 | 15,012 | 15,608 | 14,815 |
| Roughness Rq | 18,836 | 18,507 | 18,125 | 18,973 | 17,922 |

***Figure 174***

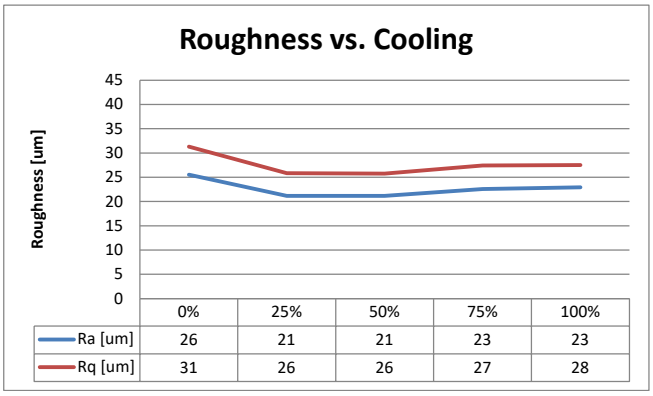


| | 0% | 25% | 50% | 75% | 100% |
|---|---|---|---|---|---|
| Ra [um] | 26 | 21 | 21 | 23 | 23 |
| Rq [um] | 31 | 26 | 26 | 27 | 28 |

***Figure 175***

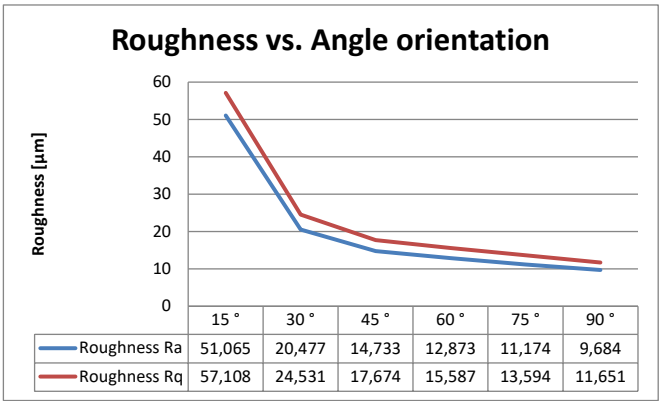


| | 15 ° | 30 ° | 45 ° | 60 ° | 75 ° | 90 ° |
|---|---|---|---|---|---|---|
| Roughness Ra | 51,065 | 20,477 | 14,733 | 12,873 | 11,174 | 9,684 |
| Roughness Rq | 57,108 | 24,531 | 17,674 | 15,587 | 13,594 | 11,651 |

***Figure 176***

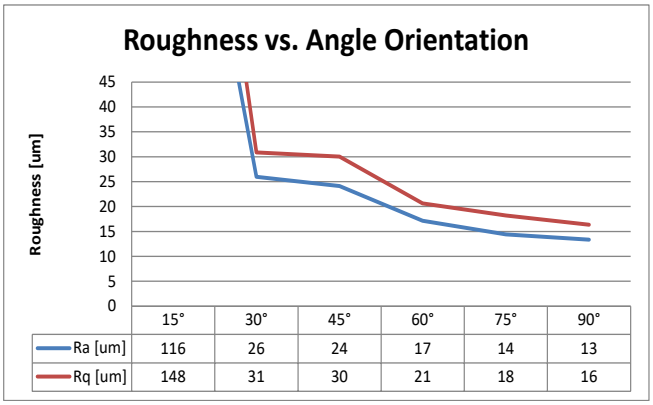


| | 15° | 30° | 45° | 60° | 75° | 90° |
|---|---|---|---|---|---|---|
| Ra [um] | 116 | 26 | 24 | 17 | 14 | 13 |
| Rq [um] | 148 | 31 | 30 | 21 | 18 | 16 |

***Figure 177***

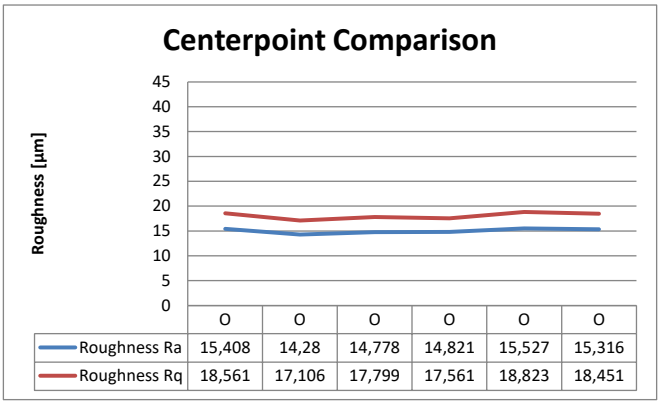


| | O | O | O | O | O | O |
|---|---|---|---|---|---|---|
| Roughness Ra | 15,408 | 14,28 | 14,778 | 14,821 | 15,527 | 15,316 |
| Roughness Rq | 18,561 | 17,106 | 17,799 | 17,561 | 18,823 | 18,451 |

***Figure 178***

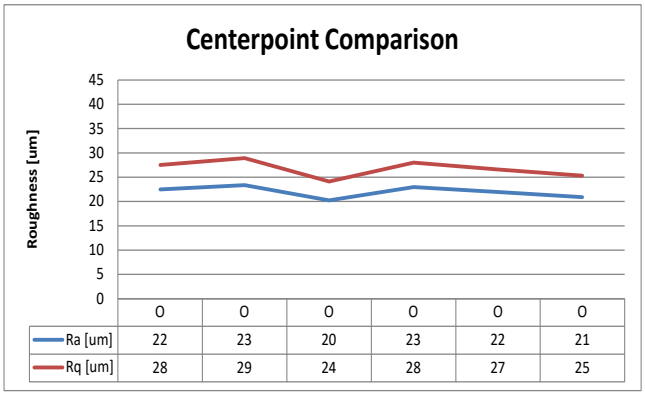


| | 0 | 0 | 0 | 0 | 0 | 0 |
|---|---|---|---|---|---|---|
| Ra [um] | 22 | 23 | 20 | 23 | 22 | 21 |
| Rq [um] | 28 | 29 | 24 | 28 | 27 | 25 |

***Figure 179***

## Discussion

So all of the samples created for the screening experiment have been scanned by the optical scanner in the objective characterization study and measured with the Mitutoyo contact type roughness profilometer. What can be seen in general for both the upward and downward facing surface is the difference in roughness value. For all samples the roughness values for the contact type measurements are lower than the optical scanner type. This could be caused by several factors including the resolution of the laser measurement sensor(1 micrometer), the refraction of the laser light on the material and material properties such as shininess or translucency. Figure 180 shows the difference when shining the laser beam at the surface onto two material; left Polycarbonate(PC) and right ABS. The comparison of different materials with respect to the roughness has been investigated separately in appendix 13 p.154.

As mentioned the resolution of the micro epsilon laser module is 1 micrometer which is less precise when comparing it to the resolution of the Mitutoyo namely 1 nanometer. This means that probably the space between printed layers will be measured more accurately. To compare the output of the two measuring methods results of a specific sample has been measured. The two outputs of the measurements can be seen in figure 181. The upper surface profile is gathered with the Mitutoyo and the lower is from the optical scanner. This figure clearly shows the difference in measuring quality which can influence the final outcome as well.

Even though the roughness values of the mitutoyo measurements are lower than the optical scanner system, the results show the same trend with respect to decrease or increase in roughness for printing parameters.

*Upward facing surfaces result comparison*

Layer height shows the same trend for both measuring types. The increase of the contact type is more stable than the optical scanner. The results of the optical scanner for speed showed a decrease in roughness with an increase in speed. The contact type measurement shows no significant difference in roughness. Linewidth shows a decrease and then an increase in roughness for the optical scanner, the contact type measurements shows no difference and resulted in a flat line. The results for temperature show no significant effect with the optical scanner which can also be seen for the contact type, the deviation is even less. For cooling there was an increase in roughness when enabling the cooling fan after which there was no change with an increase in cooling percentage. For the mitutoyo contact type measurement the effect can not be seen and shows a flat line. The trend for roughness for an increase in angle orientation can be seen in the results for both measurement types. An increase in angle orientation from the horizontal plane results in a decrease in roughness.

The centerpoint comparison show no major deviations for the contact type measurements as well as the optical scanner measurements.

*Downward facing surface result comparison*

For layer height the two trends are similar, an increase of layer height will result in an increase of surface roughness. Speed showed a small decrease in roughness for the optical scanner results, however the contact type measurement reveals there is no significant increase or decrease. Even though the optical scanner results for linewidth show some increase and decrease, the mitutoyo measurement shows no difference. Both the measurement types for the temperature show no difference in roughness with varying temperatures. The contact type measurements show less deviation than the optical scanner. For cooling the initial thought was that there was a difference between enabling and disabling the cooling fan which can be seen in the results from the optical scanner system. But comparing the results with the contact type results it reveals no change for enabling and disabling the fan for cooling. Angle orientation was the last parameter investigated and revealed a similar trend, and increase in printing angle from the horizontal plane results in a decrease in surface roughness.

The centerpoint samples have been compared to see if there is a significant difference between the two measurement types. Both show no significant difference and as expected the results of the contact type are more consistent with less deviation.

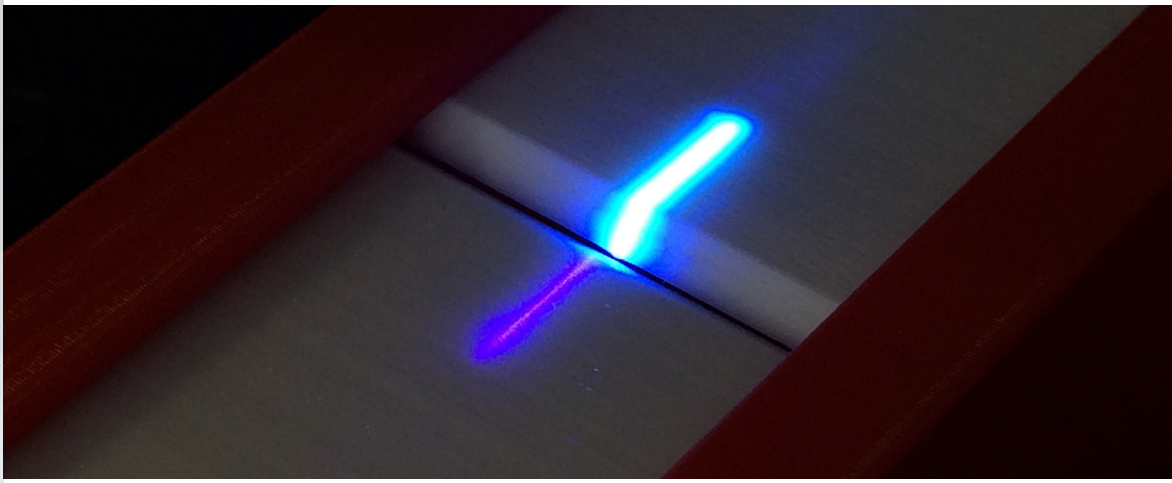

***Figure 180***

***Figure 180 Difference in refraction between PC and ABS material***

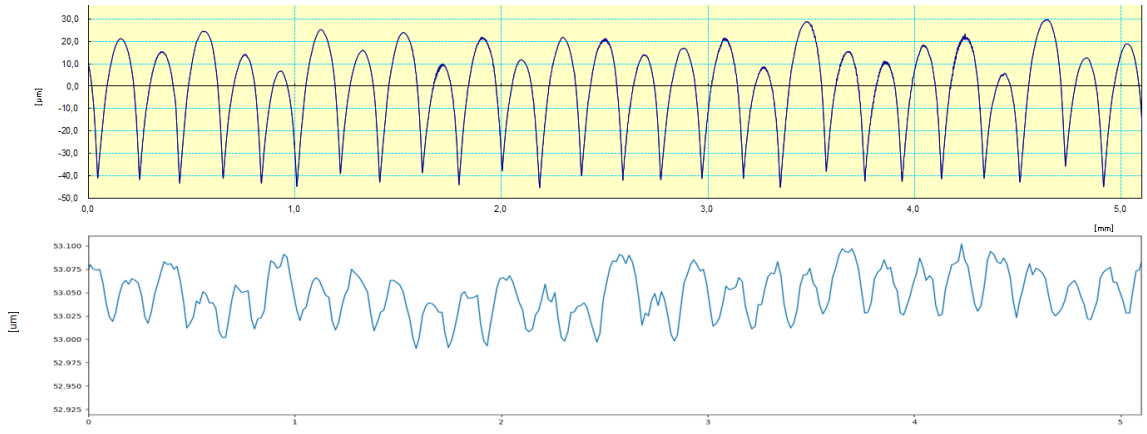


***Figure 181***

***Figure 181 Roughness profile comparison Mitutoyo (upper) and micro epsilon (lower)***

# 13. Material type and color comparison

## Introduction

Besides the control experiment with the Mitutoyo surftest contact type surface roughness meter, different materials have been explored as well. As the question raised if the same trends in roughness are visible when printing different materials or colors. The main material used for the project is polycarbonate(PC) as this was a material which has not been studied before in previous literature on surface roughness of FDM printed surfaces. Other filaments available for 3D printing are mentioned before such as PLA, ABS, TPU 95A, Nylon, PP and also some other materials with additives as carbon, wood and metal.

## Method

For the comparison of different materials PLA and ABS have been chosen as these materials are popular in FDM printing(Floor, 2015). As the objective experiment resulted in the conclusion that angle orientation from the horizontal plane and layer height were influencing surface roughness, these parameters have been chosen to be investigated in combination with PLA and ABS. The whole procedure for the creation, printing and scanning of the samples was the same as for the PC experiment. Only the printing temperature was different as PLA, ABS and PC print at different temperatures. PLA is printed at lower temperatures ranging from 195 °C-210 °C, ABS 225 °C-240 °C and PC 260 °C-280 °C (Ultimaker, 2017). The centerpoints of these ranges are chosen for the printing temperatures of the materials.

For all materials the white color version filament has been used for the printing of the samples. Also, to compare different colors on the effect on surface roughness the PLA samples have been printing in white and red.

ABS could easily be separated from PC and PLA samples as ABS has a matt finish after printing. For PC and PLA this difference is less significant as both are semi shiny, however the different material samples were stored separately with labels. Coding was the same for all samples, A series for layer height variation and E for angle orientation.
After printing the samples, they were placed in the sample holder to be scanned with the optical scanner system and processed according to the same procedure as the objective experiment with PC.

## Results

Following, the results of the different materials presented in figures 182 to 189 with respect to layer height and angle orientation for upward facing surfaces.

*Upward facing surface*

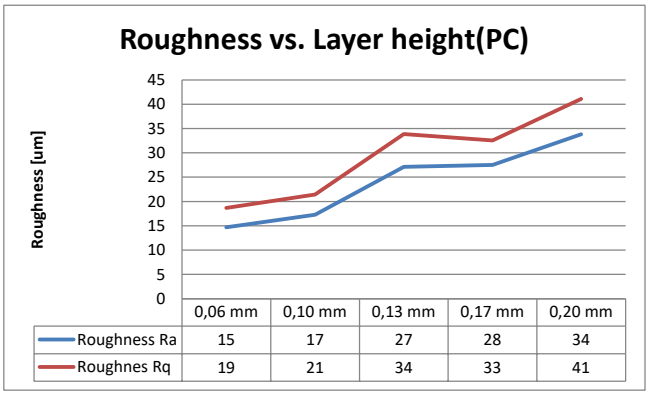


***Figure 182***

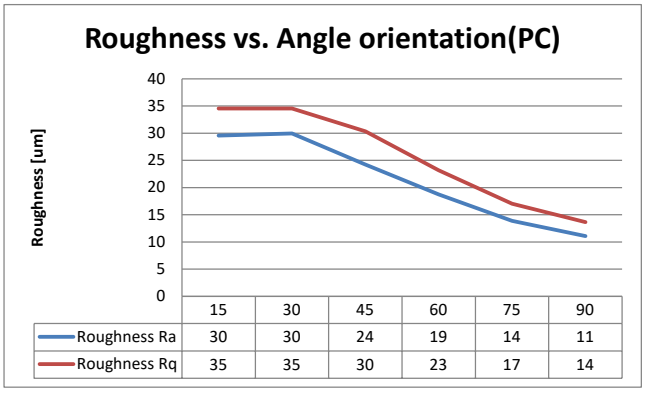


***Figure 183***

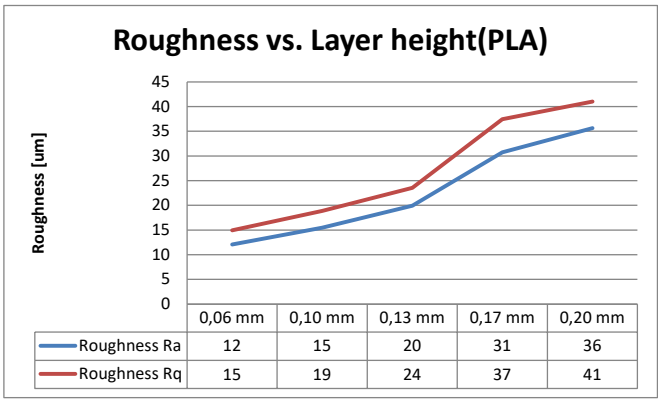


| | 0,06 mm | 0,10 mm | 0,13 mm | 0,17 mm | 0,20 mm |
|---|---|---|---|---|---|
| Roughness Ra | 12 | 15 | 20 | 31 | 36 |
| Roughness Rq | 15 | 19 | 24 | 37 | 41 |

*Figure 184*

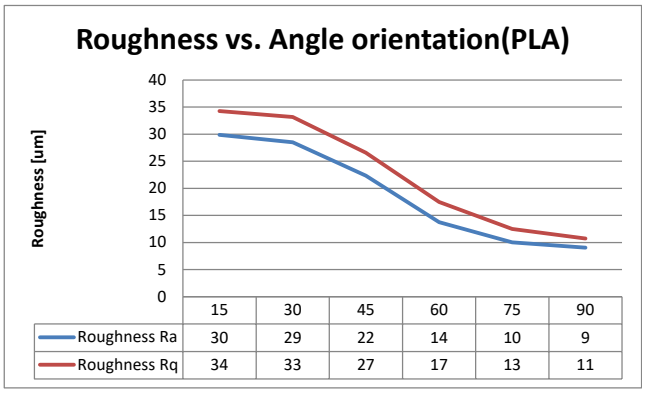


| | 15 | 30 | 45 | 60 | 75 | 90 |
|---|---|---|---|---|---|---|
| Roughness Ra | 30 | 29 | 22 | 14 | 10 | 9 |
| Roughness Rq | 34 | 33 | 27 | 17 | 13 | 11 |

*Figure 185*

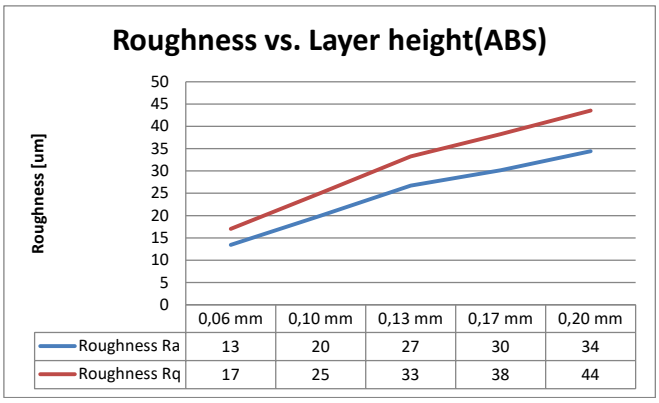


| | 0,06 mm | 0,10 mm | 0,13 mm | 0,17 mm | 0,20 mm |
|---|---|---|---|---|---|
| Roughness Ra | 13 | 20 | 27 | 30 | 34 |
| Roughness Rq | 17 | 25 | 33 | 38 | 44 |

*Figure 186*

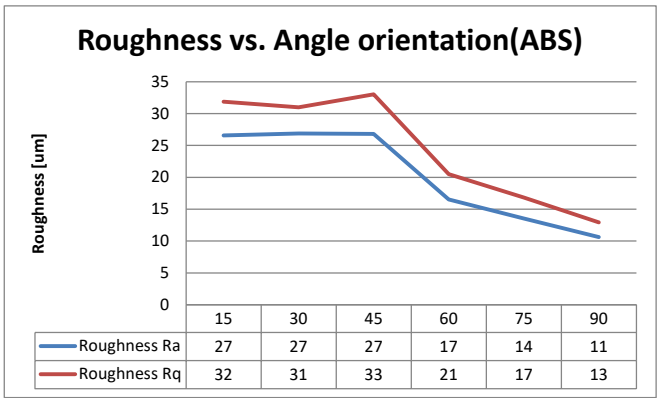


| | 15 | 30 | 45 | 60 | 75 | 90 |
|---|---|---|---|---|---|---|
| Roughness Ra | 27 | 27 | 27 | 17 | 14 | 11 |
| Roughness Rq | 32 | 31 | 33 | 21 | 17 | 13 |

*Figure 187*

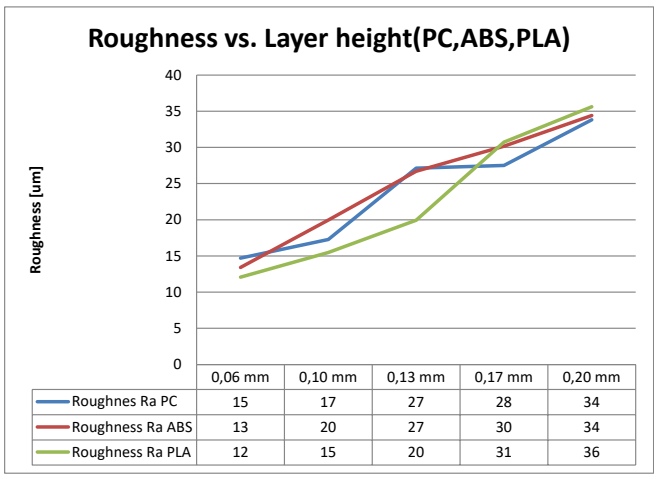


| | 0,06 mm | 0,10 mm | 0,13 mm | 0,17 mm | 0,20 mm |
|---|---|---|---|---|---|
| Roughnes Ra PC | 15 | 17 | 27 | 28 | 34 |
| Roughness Ra ABS | 13 | 20 | 27 | 30 | 34 |
| Roughness Ra PLA | 12 | 15 | 20 | 31 | 36 |

*Figure 188*

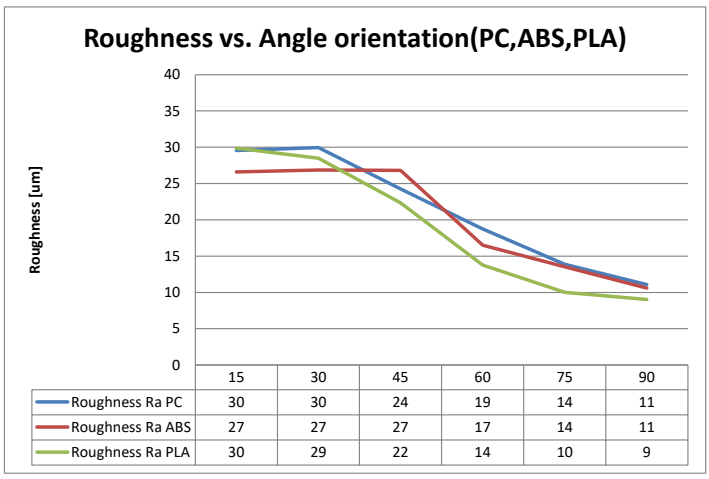


| | 15 | 30 | 45 | 60 | 75 | 90 |
|---|---|---|---|---|---|---|
| Roughness Ra PC | 30 | 30 | 24 | 19 | 14 | 11 |
| Roughness Ra ABS | 27 | 27 | 27 | 17 | 14 | 11 |
| Roughness Ra PLA | 30 | 29 | 22 | 14 | 10 | 9 |

*Figure 189*

The results for the downward facing surfaces can be found in figure 190 to 197 with respect to change in layer height and angle orientation.

## Discussion

In this section the results of the different materials will be discussed with respect to similarities or major differences in the surface roughness behaviour. First the upward facing surfaces will be discussed and afterwards the downward facing surfaces. Also, the influence of color on the surface roughness will be described at the end of this section.

*Upward facing surfaces*

Beginning with the polycarbonate material samples, what can be seen is that the surface roughness increases when the layer height increases. The roughness Ra increase is 19 µm for the range of 0.06 mm to 0.2 mm layer height. For the PLA material the surface roughness also increases with an increase of layer height. The increase of roughness Ra is 24 µm which is slightly more than the PC. Abs shows the same trend as PLA and PC; an increase of layer height results in an increase of roughness. The increase for ABS in the range of 0.03 mm to 0.2 mm is 21 µm which is slightly more than PC and slightly less than PLA. So for the different materials the trend of increasing surface roughness is similar.

For the angle orientation what could be seen for the polycarbonate is that the increase of the angle from the horizontal plane results in a decrease of surface roughness values Ra and Rq. The decrease in roughness Ra is 19 µm for the range of 15 degrees to 90 degrees in angular orientation. PLA shows the same trend as PC with decreasing surface roughness values Ra and Rq. The decrease for PLA is 21 µm divided over the range of angle orientations. ABS has similar results as PC and PLA as the surface roughness values Ra and Rq stay stable for the first increase of angle orientation of 15 degrees to 30 degrees and then decrease till 90 degrees is reached. The decrease of ABS is 16 µm which is less than the other materials. Comparing all 3 materials in one figure reveal that there is no significant difference in surface roughness behaviour for layer height and angle orientation.

*Downward facing surface*

For the downward facing surface there were some major differences between the surfaces. For polycarbonate samples the roughness values Ra and Rq increased with the increase of the layer height. But from 0.06 mm to 0.10 mm it showed a small decrease of 3 µm which was also present in the Mitutoyo surface measurement. The overall increase in roughness Ra was 15 µm. PLA showed the same trend as PC with first a decrease(8 µm) in roughness values Ra and Rq and then an increase. The overall increase in surface roughness Ra was 12 µm, slightly less than PC. The decrease of roughness values Ra and Rq for the change from 0.06 mm to 0.1 mm layer height was also present in the ABS samples. The roughness value Ra dropped 5 µm and the total increase was 16 µm. Which is slightly more than PC and PLA. What can be concluded is that for the downward facing surface the roughness decreases when changing from layer height 0.06 mm to 0.1 mm and then increases.

For angle orientation most samples showed signs of loose printing lines due to the steep angle(15 degrees). This could also be seen for the polycarbonate samples as the 15 degree angle resulted in a Ra roughness above 100 µm. But from 30 degrees the roughness decreases from 26 µm to 13 µm. Which is a decrease of 13 µm from 30 degrees to 90 degrees of angle orientation. For PLA the 15 degrees angle also started

## *Downward facing surface*

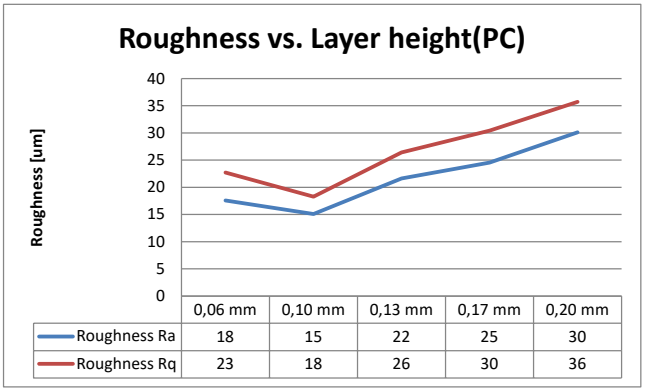


| | 0,06 mm | 0,10 mm | 0,13 mm | 0,17 mm | 0,20 mm |
|---|---|---|---|---|---|
| Roughness Ra | 18 | 15 | 22 | 25 | 30 |
| Roughness Rq | 23 | 18 | 26 | 30 | 36 |

***Figure 190***

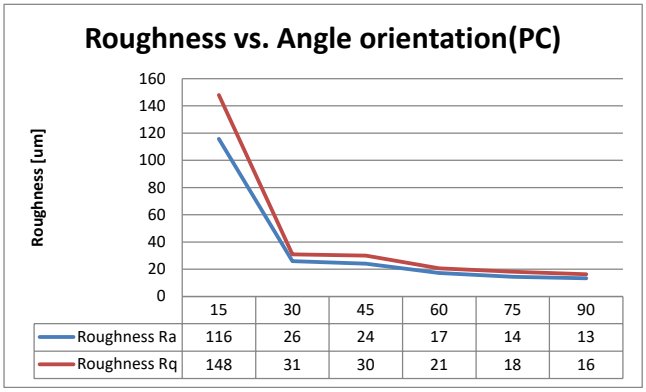


| | 15 | 30 | 45 | 60 | 75 | 90 |
|---|---|---|---|---|---|---|
| Roughness Ra | 116 | 26 | 24 | 17 | 14 | 13 |
| Roughness Rq | 148 | 31 | 30 | 21 | 18 | 16 |

***Figure 191***

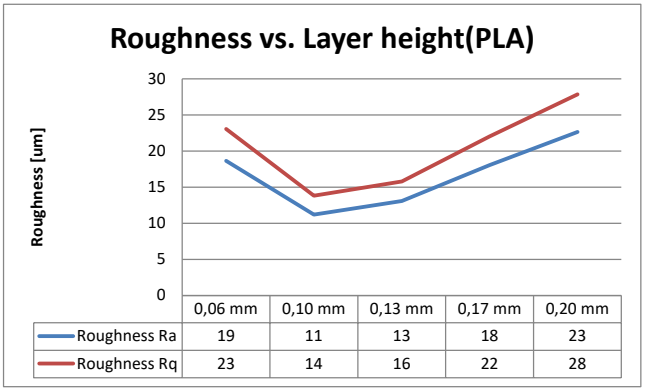


| | 0,06 mm | 0,10 mm | 0,13 mm | 0,17 mm | 0,20 mm |
|---|---|---|---|---|---|
| Roughness Ra | 19 | 11 | 13 | 18 | 23 |
| Roughness Rq | 23 | 14 | 16 | 22 | 28 |

***Figure 192***

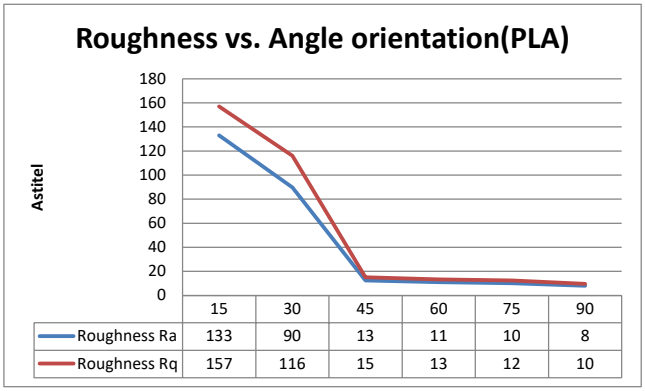


| | 15 | 30 | 45 | 60 | 75 | 90 |
|---|---|---|---|---|---|---|
| Roughness Ra | 133 | 90 | 13 | 11 | 10 | 8 |
| Roughness Rq | 157 | 116 | 15 | 13 | 12 | 10 |

***Figure 193***

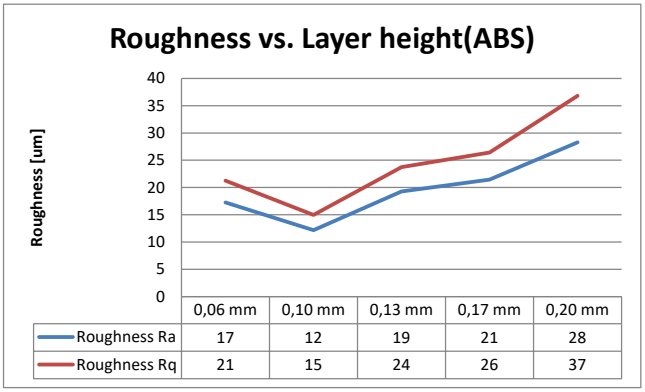


| | 0,06 mm | 0,10 mm | 0,13 mm | 0,17 mm | 0,20 mm |
|---|---|---|---|---|---|
| Roughness Ra | 17 | 12 | 19 | 21 | 28 |
| Roughness Rq | 21 | 15 | 24 | 26 | 37 |

***Figure 194***

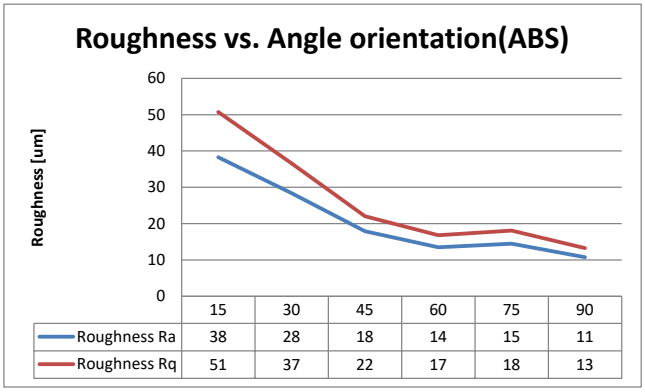


| | 15 | 30 | 45 | 60 | 75 | 90 |
|---|---|---|---|---|---|---|
| Roughness Ra | 38 | 28 | 18 | 14 | 15 | 11 |
| Roughness Rq | 51 | 37 | 22 | 17 | 18 | 13 |

***Figure 195***

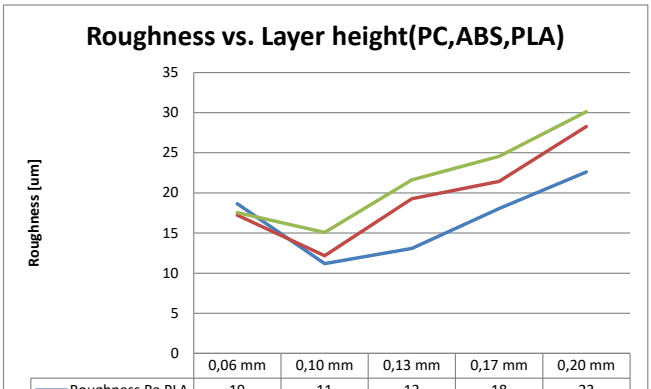


| | 0,06 mm | 0,10 mm | 0,13 mm | 0,17 mm | 0,20 mm |
|---|---|---|---|---|---|
| Roughness Ra PLA | 19 | 11 | 13 | 18 | 23 |
| Roughness Ra ABS | 17 | 12 | 19 | 21 | 28 |
| Roughness Ra PC | 18 | 15 | 22 | 25 | 30 |

***Figure 196***

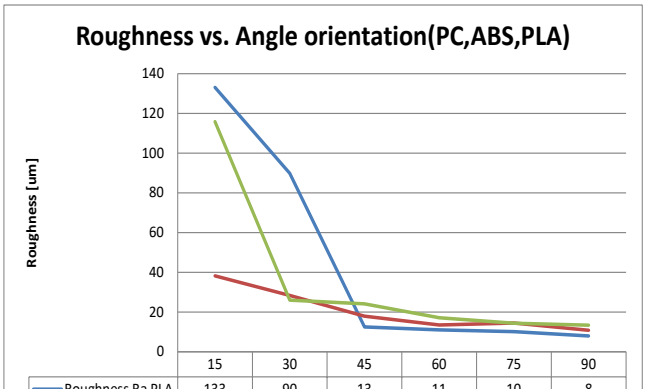


| | 15 | 30 | 45 | 60 | 75 | 90 |
|---|---|---|---|---|---|---|
| Roughness Ra PLA | 133 | 90 | 13 | 11 | 10 | 8 |
| Roughness Ra ABS | 38 | 28 | 18 | 14 | 15 | 11 |
| Roughness Ra PC | 116 | 26 | 24 | 17 | 14 | 13 |

***Figure 197***

with roughness values Ra and Rq above 100 µm. Comparing 30 degrees of angle orientation between PC and PLA results in PLA having a much higher roughness value of 90 µm compared to 26 µm. This could mean that PC has better overhang capabilities than PLA. For PLA the decrease of roughness from 45 to 90 degrees was 5 µm. ABS was the material which was having the lowest roughness values for the 15 degrees angle comparing PLA, ABS and PC. ABS printed at an angle of 15 degrees resulted in roughness values Ra and Rq of 38 µm and 51 µm respectively decreasing until the 90 degrees angle. The overall decrease in Ra roughness was 27 µm. From this comparison it is clear that the surface roughness values Ra and Rq decrease with an increase of angle orientation.
Displaying all 3 materials in one figure reveals a big difference in roughness for angles of 15 and 30 degrees but no significant difference from 45 to 90 degrees.

### Color comparison

Now the different materials have been explored on its influence on the surface roughness, the color comparison has been done with PLA. The two colors used for the comparison were PLA red and white. Similar to the previous section the layer height and angle orientation have been analyzed for the two colors.

The results for the surface roughness values Ra and Rq for layer height and angle orientation can be found in figure 198 and 199.

*Upward facing surface*
What can be seen for the layer height between the red and white PLA is that the red version shows slightly higher roughness values for Ra. Overall there is no major difference in roughness between PLA red and white.
Also for the angle orientation the roughness value Ra does not differ significantly between the red and white PLA. The red version shows slightly higher Ra values.

*Downward facing surface*
For layer height there is a large difference between the red and white PLA. The red PLA shows significantly higher Ra values than the white color.
This different behaviour is not present at the angle orientation comparison as both the red and white PLA show a similar trend. Both begin with high roughness values for steep angles as 15 and 30 degrees after which the roughness value Ra decreases. From 45 degrees both colors act similar regarding surface roughness.

Overall from the color comparison it is clear that different colors behave similarly to each other in terms of surface roughness, except for the downward facing surface layer height seems to have some influence.

## *Upward facing surface*

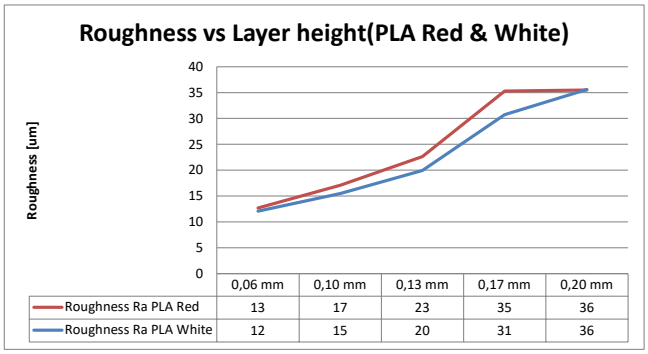


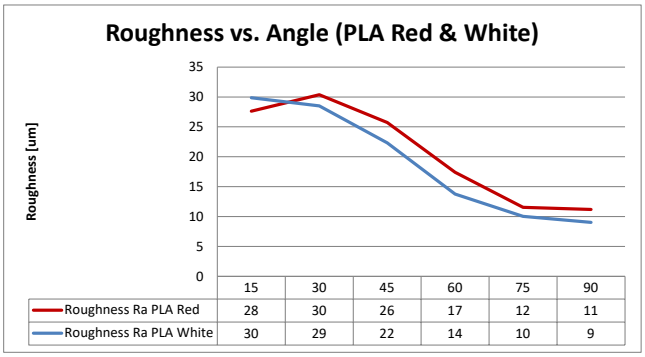


***Figure 198***

***Figure 198 Upward facing surface roughness Ra between colors***

## *Downward facing surface*

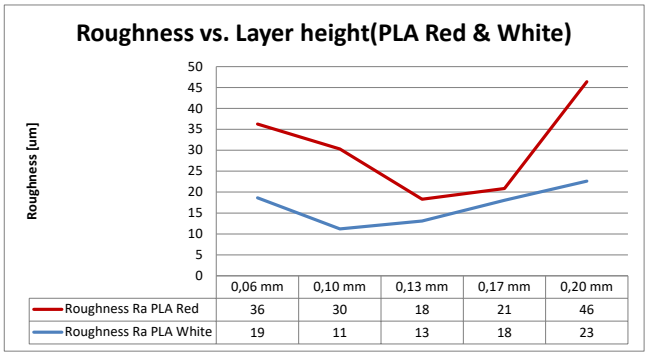


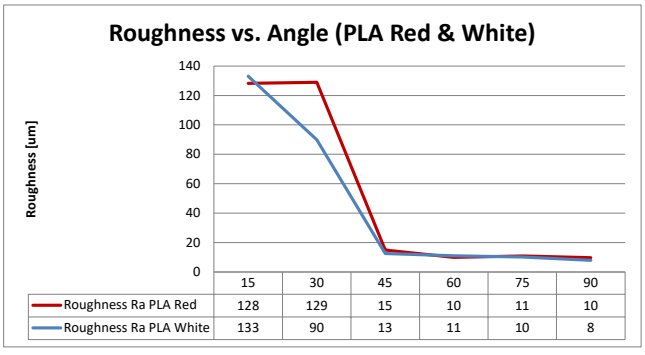


***Figure 199***

***Figure 199 Downward facing surface roughness Ra between colors***

# 14. Perception experiment

## Introduction

The second part of this project is to investigate the human perception of roughness with respect to 3D printed surfaces. The main goal of this study is to test a new haptic apparatus and collect human perception data to compare this data with the objective data. There is quite an amount of studies on the perception of surface roughness through the sense of touch. Many cover the perception of rough surfaces rather than fine texture perception. For these studies often abrasive papers are used in different grit sizes which are presented to participants. This study also aims to investigate the usefulness of 3D printed surfaces with varying roughnesses as stimuli and the perception of fine-surface textures through a new experimental apparatus.

## Literature

The literature review was performed to learn more on doing research on the topic of haptic perception of surface textures. The initial search was focussed on previous haptic research on additive manufactured surfaces especially FDM printing technology. However this kind of haptic research involving the surface texture of FDM printed surfaces has not been studied before. Only Drewing(2016) used stimuli produced by the Stratasys Objetpro printer in order to investigate low-amplitude textures and concluded that roughness is an inverted u-shaped function of texture period. However the study was not focussing on the texture due to the additive manufacturing technology but on the incorporated and modeled surface texture. Participants were free to explore the surfaces in terms of finger scanning speed with lateral movements. Other literature was studied in order to explore and establish a suitable method for FDM surface texture investigation. Unger et al. (2007) used a 6-DOF magnetic levitation haptic device to study how the just noticeable difference(JND) varies with respect to spacing and probe radius. This device could be pre-programmed to present a certain roughness and participants were able to explore the surfaces freely. The study by Libouton et al. (2010) contributed the most to the setup of the perception study on FDM printed surfaces. In the study by Libouton two samples were presented at the same time to compare and the staircase procedure was used to gather perception data. Only, in the study by Libouton sandpaper samples were used and participants were able to freely explore the samples in terms of finger scanning speed in a lateral movement.

## Experimental setup/ method

For this roughness discrimination study a new perception apparatus is designed and created in order to collect the required data for analysis. As mentioned, the goal is to compare the roughness data from the objective study with this perception study. Also the suitable methodology is determined to gather data which allows for comparison with objective roughness data.

*Apparatus*

A new apparatus was designed for this perception study as apparatuses from previous literature were not suitable. As mentioned in the literature review, most perception studies are performed with sanding paper as stimulus which required a different apparatus for presenting the sheets. The study Libouton et al.(2010) used a stimulus holder with two stimuli and the participant swiped his/her finger across these stimuli. This study was more focussed on the active scanning

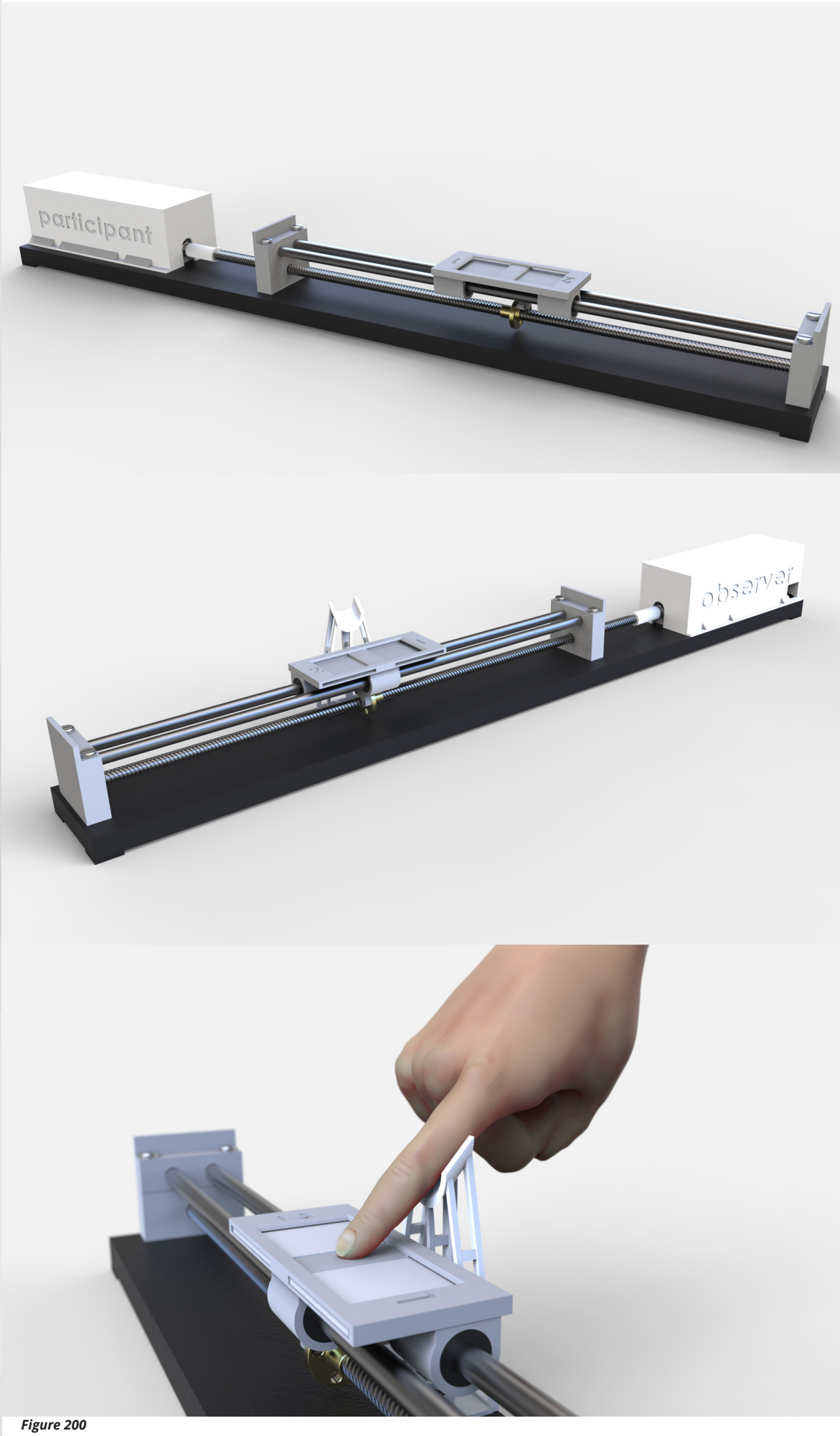


*Figure 200 Impression of the used perception apparatus*

*Figure 200*

of stimuli as participants moved their own finger with a specific speed. For this study the participant will passively scan the presented surfaces. This means the stimuli will slide across the participant's fingertip with a constant speed. The process of the creation and requirements of the used apparatus can be found in appendix 8. Figure 200 gives an impression of the apparatus used for this human perception study.

*Stimuli*

As mentioned earlier, the human perception data will be compared with obtained roughness data from the objective study. To be able to compare these two studies it is necessary to use the same samples from the objective study as different samples might have different roughness values. With the design of the samples for the objective study, the perception study was kept in mind to ensure the samples would be suitable as well. The sample design allows for enough surface area for human perception scanning with fingertips. As described in appendix 7 on the sample design, the dimensions are based on anthropometric data from dined. So even participants having a small or large fingertip length, they are able to scan the surface without touching the boundaries of the sample holder of the apparatus. The integrated coding made tracking of stimuli more convenient for the perception procedure as results could be directly linked to data from the objective study using the same coding. Figure 201 shows the sample design used for this perception experiment.

*Participants*

The participants used for this study consisted of a group of 53 people of different ages and experiences in 3D printing. The largest portion of the participants were in the range of 21 - 40 years of age with some exceeding the 50 years of age. Almost half of the participants had experience with 3D printing as these were ultimaker employees or industrial design students using 3D printing for prototyping. Right handed participants were the majority in this study.

*Methodology*

For this experiment, the staircase procedure was used to gather perception data with the apparatus, see figure 202. This procedure is a common used method for roughness discrimination in psychophysics. With this method always one centerpoint stimulus(standard) will be presented in combination with a varying stimulus. The standard was presented in each trial and switched randomly between stimuli slot. Beginning with the first staircase(roughest) and the second staircase(smoothest), then moving to the next staircase towards the second standard stimulus based on the perception response from the participants. After each trial, the participants was asked which of the surfaces was rougher. If for example the roughest is compared with the standard and the participant answeres correctly by mentioning the roughest as actual being rougher than the standard, the sample comparison will move to the next staircase towards the standard, decreasing the stimulus difference. This is the same from starting with the smoothest. At a certain comparison of stimuli the participant will not be able to correctly respond anymore. At this point the presented stimuli are perceived as having the same roughness sensation. This is referred as the threshold(mu) or point of subjective equality(PSE), which is the roughness of the comparison object that is felt as indistinguishable from the standard roughness object presented in every trial by the participant. The threshold(mu) value is the roughness value that each participant thinks is the same as

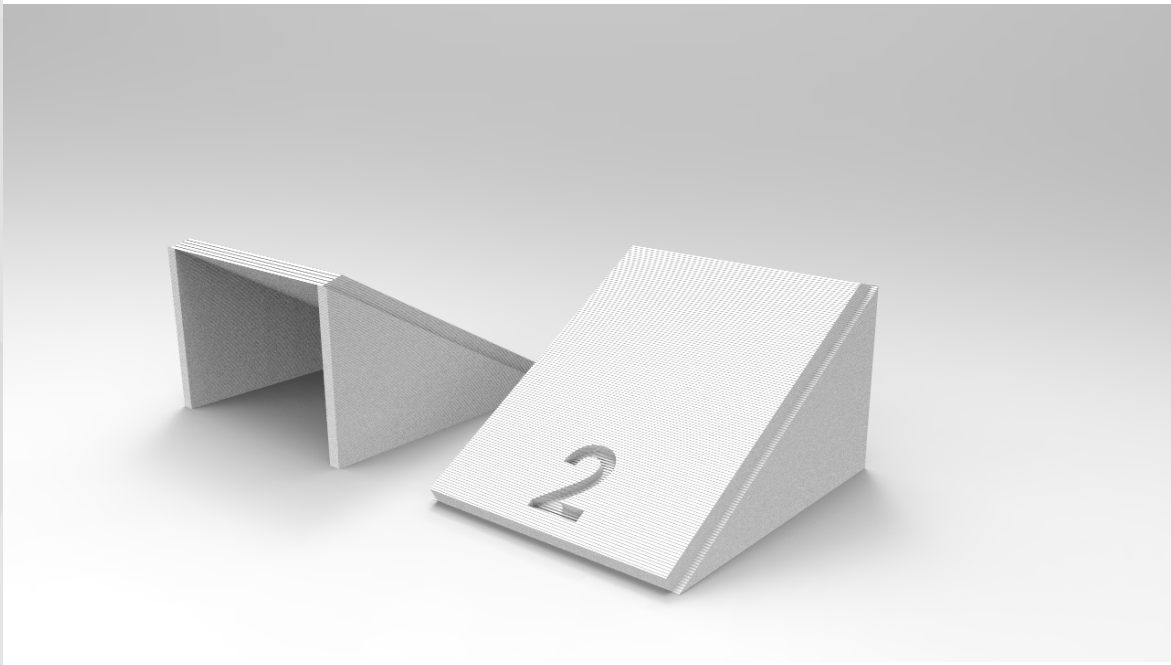


*Figure 201 Sample design used for the perception experiment*

*Figure 201*

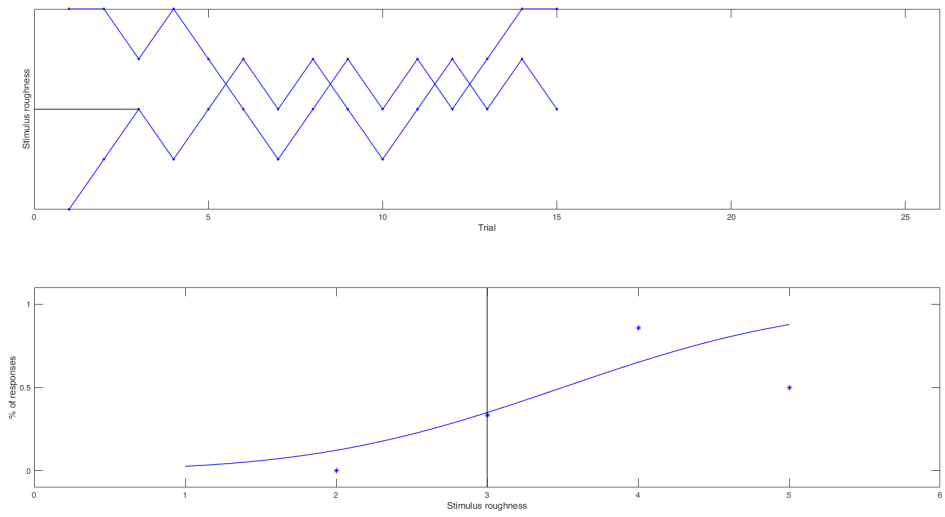


*Figure 202 Example of staircase procedure outcome of perception experiment*

*Figure 202*

the standard 50% of the time. The other gathered data is the sigma, referred to the just noticeable difference(JND) in this study. With this value we are able to describe the change in roughness needed to be able to distinguish the comparison sample from the standard sample. It is the change in the stepsize, in this study it is the change in the presented sample, that is needed to take the response proportion of 50% to 84%(on the response of which sample was rougher). It is one standard deviation from the mean (mu) of the distribution. As mentioned it is the JND - the just noticeable difference in roughness that is reliably perceivable by the participant. With this value we are able to tell in terms of 'values below this are not detectable to the participants sensing 3D printed surfaces'.

*Procedure*

Each participant was comfortably seated at the table with the designed perception apparatus. None of the stimuli were in the device when initial instructions were given. When seated, the participant was asked to put on headphones,a blindfold and position the index finger of the dominant in the finger bracket of the apparatus, see figure 203. During the experiment white noise was played to exclude external sound influence from the motor or surroundings. The blindfold in combination with closed eyes made sure visual feedback on the scanning of the stimuli did not occured. The finger bracket ensures the finger is exactly placed on the area where no surface texture was present, between the two slots for the stimuli. These precautions were incorporated to ensure the participants passively scans the stimuli and focussing purely on the receptor information of the sensation in the somatosensory system. During the instruction a dry run was observed by the participant to get familiar with the movement of the apparatus. After the dry run the participant was instructed on the desired feedback from the participant to the observer during the actual experiment. The participant was instructed to say which of the two stimuli was rougher. When the participant was ready for the scanning procedure, the white noise was started and the first two stimuli placed in the stimuli slots of the apparatus. The two stimuli required for the trial was selected with a matlab script which tracked the whole procedure as well as data collection. The apparatus is started with a button by the observer after which the apparatus will start the scanning procedure. From the middle the stimulus holder would first enable the scanning of surface 1, then return to the middle to incorporate a 90 ms rest followed by the scanning of surface 2 after which the sample holder will position itself in the starting position. During the scanning of a surface, the sample holder will move back and forth for 4 times in order to perceive the surface roughness of the surface. After feedback by the participant on the roughest stimulus, the value was filled in the matlab script and the next stimuli appeared on the screen. This process was repeated until 15 trials consisting of 2 staircases were gathered. The data was saved for further analysis and the participant thanked for their cooperation.

## Results

After collecting all responses of the perception study, the data is processed in the program Matlab with the use of scripts provided by Jess Hartcher-O'Brien. In total a number of 54 participants were performing the perception experiment. 44 participants were between the age of 20-30, 4 participants between 30-40, one participant between 40-50 and 5 participants older

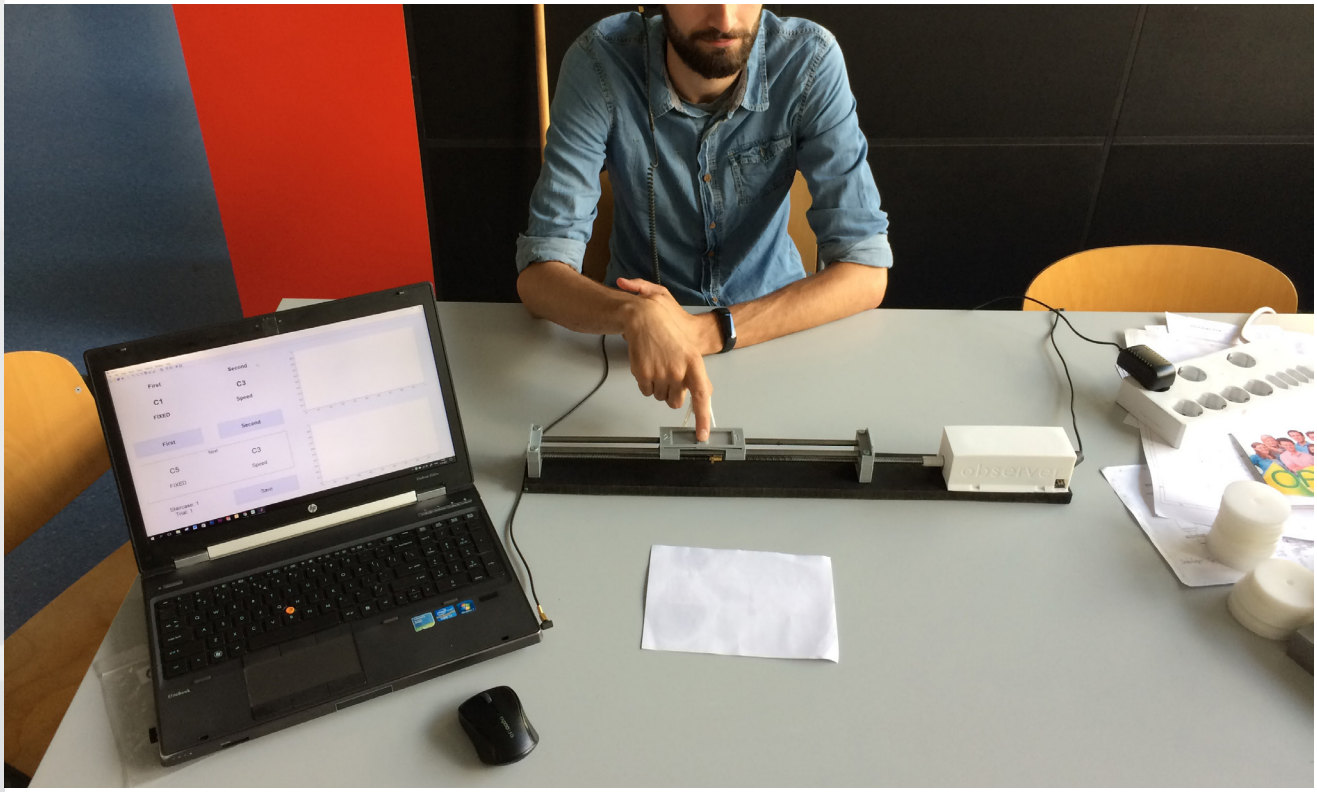

*Figure 203 Setup of the experiment*

*Figure 203*

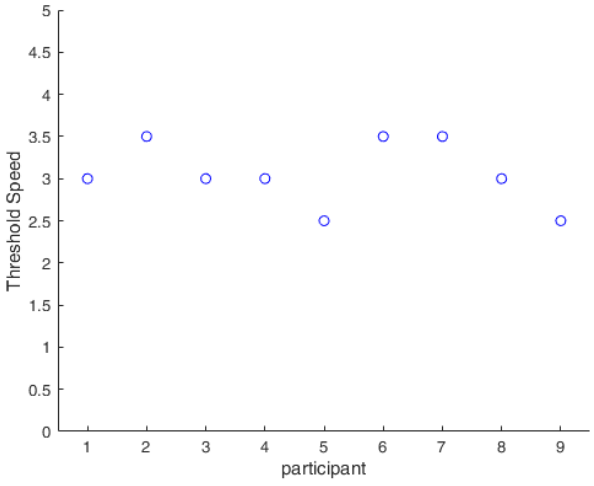


*Figure 204 Threshold/ PSE values of speed (upward)*

*Figure 204*

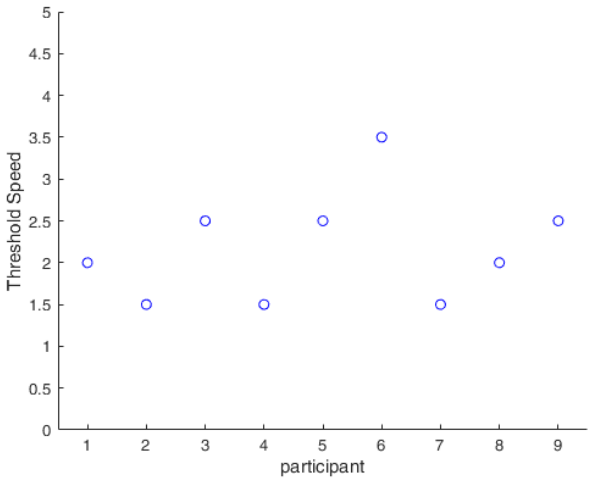


*Figure 205 Threshold/ PSE values of speed (downward)*

*Figure 205*

than 50. All measurement were successful and suitable for further analysis.

*Threshold/ Point of subjective equality(PSE)*

One response from the perception study was the stimulus threshold, otherwise know as the point of subjective equality(PSE). Which is the point the participants think the two presented stimuli are similar to each other. These threshold values have been visualized in figures to corresponding participants for each of the stimulus series, in this case 3 for the upward facing surfaces and 3 for the downward facing surfaces. The stimuli series had varying printing speeds, angle orientations from horizontal plane and layer heights incorporated.

*PSE for Speed*

Figure 204 shows the PSE values of the upward facing surfaces of the parameter speed. What can be see is that the data is quite consistent and no large deviations are present. Overall the mean PSE for the upward face of parameter speed is 3,1 (sd= 0.37). Of this speed stimuli series stimulus number 3 was present in every comparison.

The PSE values of the downward facing surface of speed can be found in figure 205 The deviation of the values from the mean of the downward facing surface is more than the upward facing surface thresholds. And the mean PSE value is 2,2 (sd= 0.62) which indicates participants finding stimulus number 2 similar to the returning stimulus number 3.

*PSE for angle orientation*

Figure 206 shows the PSE values for angle orientation of the upward facing surface. For the angle orientation quite some deviations are present in the data. This can be seen in the standard deviation of 0.82 for the mean PSE value of 3,0. The largest PSE value was 4.5 and referred to participant number 4, a 24 year old man with a year of FDM printing experience. The lowest PSE value was 2 and referred to participants 2, 6 and 9.

The deviations from the mean PSE value of angle orientation for the downward facing surface is less than the upward facing surface results. Figure 207 shows the results of the PSE values for the downward facing surface. The mean PSE value is 4,1 (sd= 0.50) with the largest PSE value being 5. The standard stimulus present in every comparison was sample number 4 for the angle orientation series.

*PSE for layer height*

Figure 208 shows the results for the upward facing surface incorporating different layer heights during testing. The PSE results are quite consistent across the participants and the mean PSE value is 2,9 (sd= 0.39). 6 of 9 participants scored a PSE value of 3 during the test.

The results of the downward facing surface can be found in figure 209 and shows some deviations around the mean value. The calculated mean PSE value is 2,7 with a standard deviation of 0,33.

*Just noticeable difference(JND)*

The other response from the perception experiment is the just noticeable difference, often referred as JND. The JND value is the change in roughness needed for the participants to be able to distinguish the varying comparison stimulus from the standard stimulus included in every comparison.

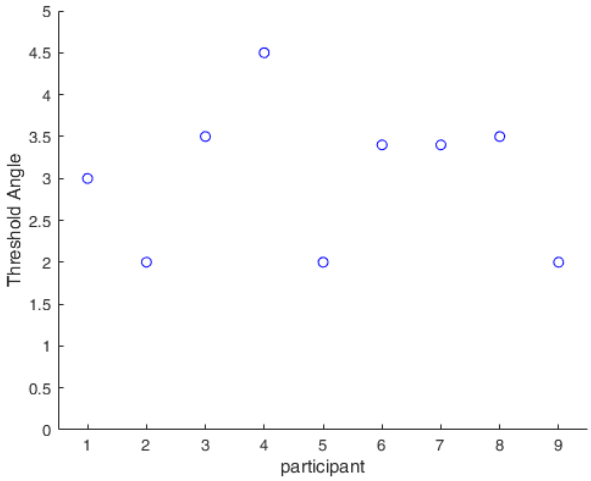


*Figure 206 Threshold/ PSE values of angle (upward)*

*Figure 206*

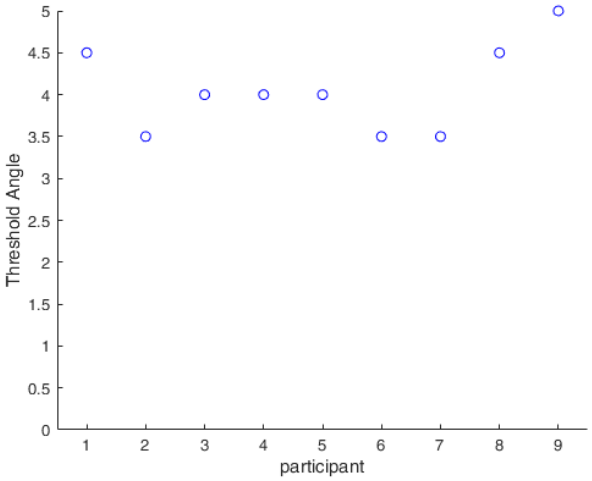


*Figure 207 Threshold/ PSE values of angle (downward)*

*Figure 207*

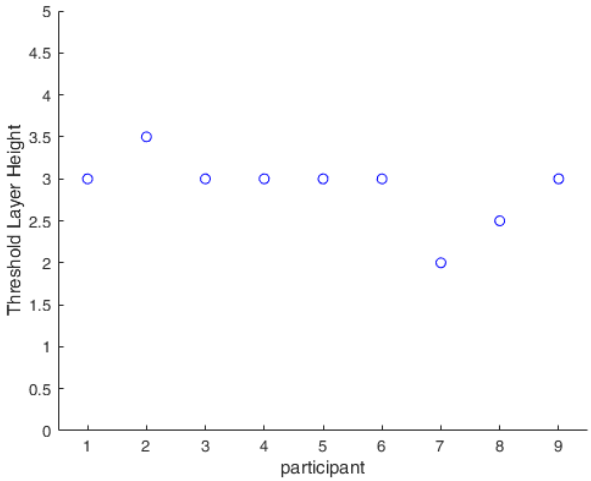


*Figure 208 Threshold/ PSE values of layer height (upward)*

*Figure 208*

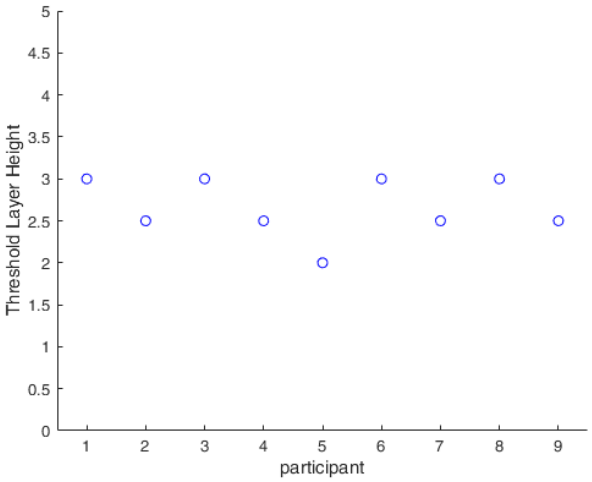


*Figure 209 Threshold/ PSE values of layer height (downward)*

*Figure 209*

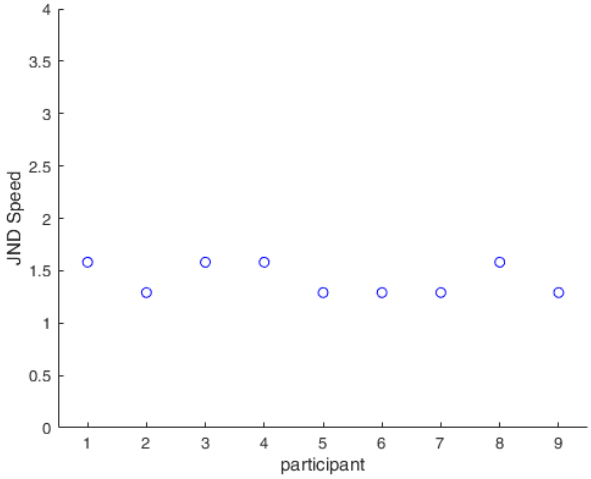


*Figure 210 JND values of speed (upward)*

*Figure 210*

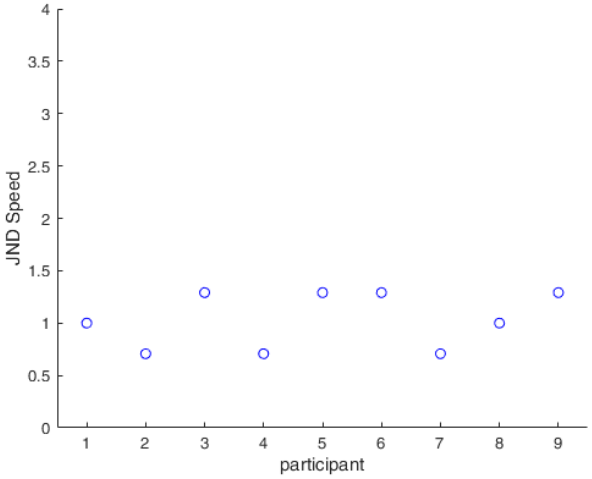


*Figure 211 JND values of speed (downward)*

*Figure 211*

*JND for speed*

Figure 210 shows the results of the JND values gathered with the perception experiment for the difference in printing speed of the upward facing surface. What can be seen is that the JND values are consistent across all participants. No major difference can be seen. The mean JND value for speed of upward facing surfaces is 1,4 with a standard deviation of 0,14. The deviation of the JND values for the downward facing surfaces is more than the upward facing surfaces. Figure 211 shows the JND values for the downward facing surface with varying printing speed. The mean JND value for the downward facing surfaces is 1 with a standard deviation of 0,26.

*JND for angle orientation*

The PSE values of the angle orientation of the upward facing surface showed quite some deviations which can also be seen in the JND values, see figure 212. This deviation can only be seen for the angle orientation. The mean JND value for the upward facing surface for a variation in angle orientation is 1,5 with a standard deviation of 0,44.

The large deviation is less present in the JND results of the downward facing surface. The results for the JND values of the downward facing surface can be found in figure 213. The mean JND value is 1,5 with a standard deviation of 0,27.

*JND for layer height*

Figure 214 shows the JND values of the layer height stimuli series for the upward facing surfaces. The values are quite consistent across the different participants. 6 of 9 participants had a JND value of 1,58. The mean JND value for this layer height comparison is 1,5 with a standard deviation of 0,20.

Also the JND values of the downward facing surface are quite consistent across the participants. The results can be found in figure 215 for the downward facing surfaces with varying layer height. The mean JND value is 1,2 with a standard deviation of 0,09 which is the smallest deviation comparing all JND standard deviations.

*Confidence intervals*

The confidence intervals have been plotted for both the upward and downward facing surface. For all JND values per parameter the means have been calculated from the sample of participants, this in order to approximate the mean of the population. The confidence interval plot shows the range of JND values which are likely to occur in the population. Figure 216 shows the plot of the JND means with confidence interval for the upward facing surface and figure 217 for the downward facing surface.

## Discussion

In this section the results from the perception experiment will be further described in terms of interpretation of the values. The goal of the perception study was to investigate if participants were able to distinguish a change in FDM surface roughness with respect to different print parameters. Responses gathered from the perception study are the PSE and JND values.

*Threshold/ Point of subjective equality(PSE)*

As mentioned before the threshold otherwise known as the point of subjective equality(PSE) is the point the participants think the two presented stimuli are similar to each other. In terms of roughness it is the roughness value that each observer thinks is the same as the standard 50% of the time.

For the speed parameter there was a difference in the threshold/PSE values for the upward and downward

*Figure 212 JND values of angle (upward)*

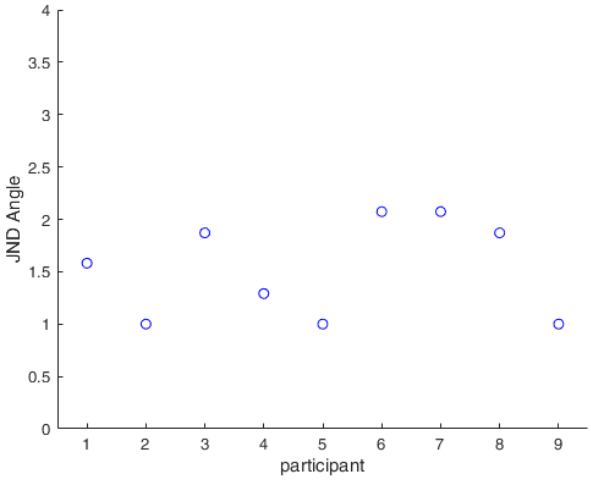


***Figure 212***

*Figure 213 JND values of angle (downward)*

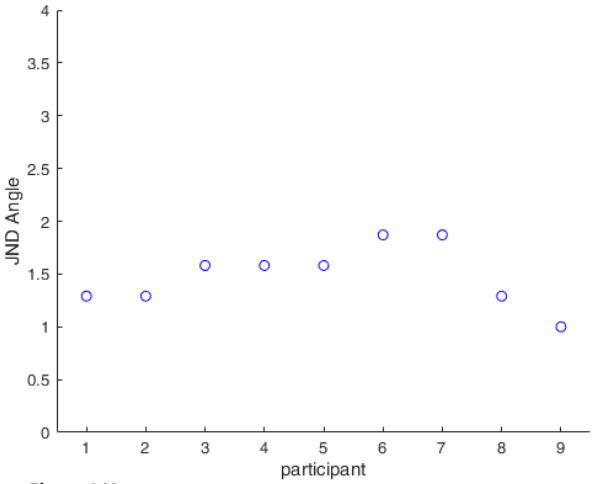


***Figure 213***

*Figure 214 JND values of layer height (upward)*

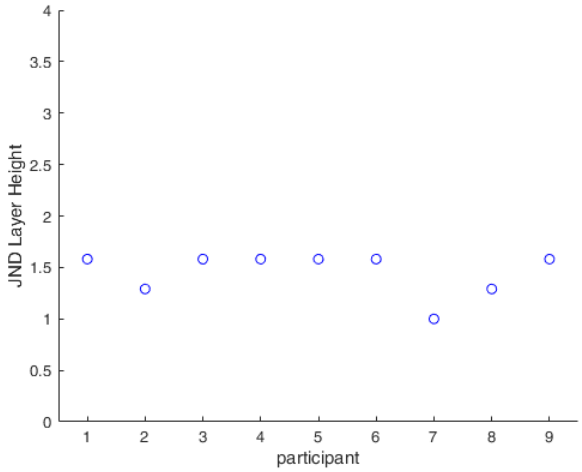


***Figure 214***

*Figure 215 JND values of layer height (downward)*

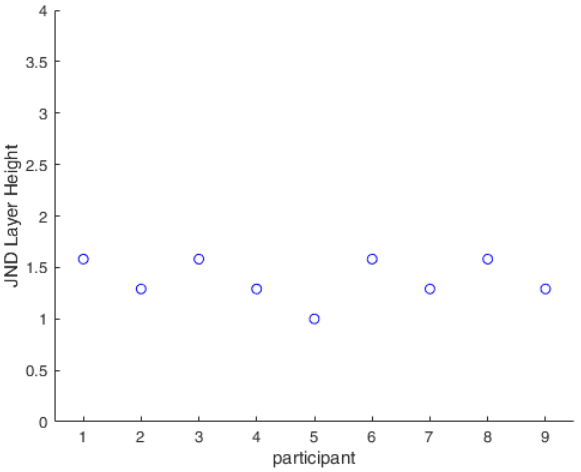


***Figure 215***

*Figure 216 Confidence intervals for upward facing surface parameters*

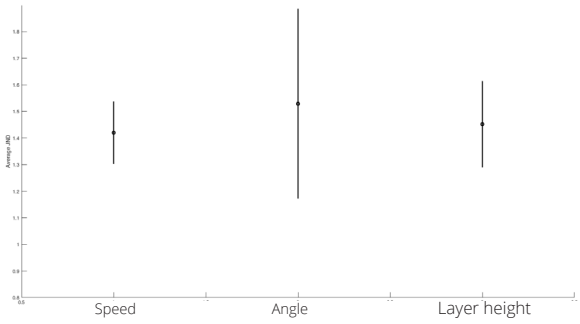


***Figure 216***

*Figure 217 Confidence intervals for downward facing surface parameters*

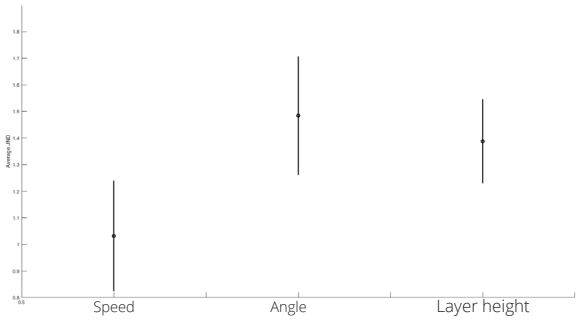


***Figure 217***

facing surface. The mean threshold for the upward facing surface was 3,1(sd= 0,37) and for the downward 2,2(sd= 0,62). During the procedure sample number 3 was present in every comparison and acted as the standard. For the upward facing surfaces on average the participants thought sample 3(Ra= 25 µm, Rq= 31 µm) was the same as sample 3(Ra= 25 µm, Rq= 31 µm) 50% of the time. For the downward facing surfaces the participants thought sample number 2(Ra= 22 µm, Rq= 27 µm) was similar to sample 3(Ra= 21 µm, Rq= 26 µm), between these samples there was 1 micrometer difference for roughness Ra and Rq.

Also between the mean thresholds/PSE values of the upward and downward facing surfaces for angle orientation there was a difference visible. The mean PSE value for the upward facing surface was 3(sd= 0,82) and 4,1(sd= 0,50) for the downward facing surface. The standard sample used in every comparison for angle orientation was sample number 4. This means that participants thought sample number 3(Ra= 19 µm, Rq= 23 µm) was similar to sample number 4(Ra= 24 µm, Rq= 30 µm) for the upward facing surface samples. For the downward facing surface samples the participants on average considered sample number 4(Ra= 23 µm, Rq= 29 µm) was similar to sample number 4(Ra= 24 µm, Rq= 30 µm) present in every comparison.

For the mean PSE values of the layer height, there was less noticeable difference between the upward and downward facing surface. The mean PSE for the upward facing surface was 2,9(sd= 0,39) and for the downward facing surface 2,7(sd= 0,33). The standard sample of the layer height comparison procedure was sample number 3. This means the participants were close to thinking that sample 3(Ra= 27 µm, Rq= 34 µm) was similar to the standard sample number 3(Ra= 27 µm, Rq= 33 µm) for the upward facing surfaces. The same phenomenon was visible for the downward facing surface of sample number 3(Ra= 22 µm,Rq= 28 µm) perceived as similar with standard sample 3(Ra= 22 µm, Rq= 26 µm).

*Just noticeable difference(JND)*

The just noticeable difference is useful to indicate the change in roughness needed for the participants to be able to distinguish the comparison from the standard. It is the difference that is reliably perceivable by human observers as the response proportion is taken from 50% to 84% for the question;"Which surface is perceived as rougher?".

For the upward facing surface the mean JND value for the speed parameter was 1,4. This means that the point at which the response rate went up from 50% to 84% between the C4(40 mm/s) and C5(20 mm/s) sample, corresponding to the 1,4 step change in sample from the standard C3. The range in roughness Ra for the varying speed samples was 25 µm to 29 µm. C1(100 mm/s), C2(80 mm/s) and C3(60 mm/s) samples had a Ra roughness of 25 µm with an increase of 2 µm per step change from C3 to C5. 1,4 step change would results in a 2,8 µm change in roughness which can be reliably perceived by human observers. For the range of printing speeds between 100 mm/s and 40 mm/s, roughness changes can not be detected reliably by observers.

The mean JND value of the downward facing surface for varying printing speeds was 1. For printing speeds the Ra roughness range was 20 µm to 23 µm with the roughest measurement belonging to the slowest printing speed of 20 mm/s. On average, considering

an increase of 3 µm over 5 different samples, one step size in samples led to an increase of 0,6 µm. With the mean JND of 1 this results in a step size of 0,6 µm needed for participants to reliably perceive a difference in roughness.

The variation of the printing angle from the horizontal plane had a calculated mean JND value of 1,5 for the upward facing surface. The range of Ra roughness values for this series of samples was 11 µm to 30 µm over 6 samples. On average, the Ra roughness increases with 3,2 µm per change in sample step. A step size of 1,5 would result in a change in Ra roughness of 4,8 µm necessary to reliably perceive a difference in roughness by observers.
For the downward facing surface the mean JND value for angle orientation was also 1,5. But there is a difference in the Ra roughness range. The Ra roughness range of the downward facing surface was 13 µm to 116 µm. The value of 116 µm(15 degree angle) is due to loose printing lines which increases the roughness significantly. Normally these steep angle orientations require support to be properly printed, howevers surfaces with support is beyond the scope of this project. As there is such a difference between the 15 and 30 degree angle orientation the unsuccessful 15 degree angle sample is excluded from this calculation for the downward facing surfaces. The other samples resulted in a Ra roughness range of 13 µm to 26 µm. One step size refers to an increase of 2,6 µm so 1,5 step size corresponds to a Ra roughness increase of 3,9 µm needed to reliably perceived by human observers.

Layer height was the last parameter which was tested perceptually and had a mean JND value of 1,5 for the upward facing surface. The range of the Ra roughness for the layer height series was 15 µm to 34 µm which is an increase of 19 µm across 5 samples. This results in a step size of 3,8 µm increase per sample. The mean JND of 1,5 results in a 5,7 µm difference in Ra roughness needed in order to reliably notice to distinguish a difference with the standard.
For the downward facing surface series the mean JND value was 1,2 calculated from the 9 participants participating in the layer height experiment. The range of the Ra roughness from the layer height samples was 18 µm to 30 µm, an increase of 12 µm Ra roughness. Divided over 5 samples results in an increase of 2,4 µm per sample step. The mean JND value of the layer height samples was 1,2 which results in a roughness change of 2,9 µm necessary in order to reliably distinguish the sample from the standard.

*Confidence intervals*
As mentioned before in the results section the JND means with confidence intervals have been plotted for all parameters of both upward and downward facing surfaces. The confidence interval plot shows the range of JND values which are likely to occur in the population. For the upward facing surface the confidence interval of speed was (1.302 , 1.537). Which is the narrowest interval of all intervals. The downward facing surface this was (0.824 , 1.24).

Compared to the other intervals, the confidence interval for the angle orientation is the largest. The upward facing surface confidence interval of angle orientation is (1.172 , 1.886). For the downward facing surface this interval is less than the upward facing surface but still the largest of the downward facing surfaces. The downward facing surface confidence interval for the angle orientation is (1.261 , 1.707).

The confidence intervals for the layer height parameter of the upward and downward facing surfaces are quite similar. The interval of the upward facing surface is (1.29 , 1.614) and for the downward facing surface (1.23 , 1.545).

## Conclusion

This second study of the surface roughness project was about the surface roughness perception of humans. For this study, a new apparatus has been designed and built in order to gather data on the perception of surface roughness as previous perceptual devices were not suitable for this study. Other apparatuses required participants to swipe across a certain surface, not taking into account the variations in speed or pressure the participant might incorporate. The new perception apparatus features a slider with a duo sample holder connected to a motorized leadscrew in order to be moved at a constant speed. During the measurements of 54 participants no immediate problems were encountered and the apparatus has proved its suitability for this experiment with the collection of successful data.

All of the results were gathered successfully the data is quite consistent even though the responses are based on people's own subjective interpretation of surface roughness. For the PSE, known as the threshold value, the participants were quite close to thinking which sample is the same as the standard 50% of the time. For both the speed and layer height the mean PSE values of both the upward and downward facing surface was around sample number 3 which correctly corresponds to the standard; sample 3. Only the mean PSE of the downward facing surface of the speed parameter was clearly lower than 3 namely 2,2. Which means that sample number 2 was found rougher than is actually was from the optical scanner data.

For the angle orientation sample number 4 was the sample with acted as the standard from the 6 different angle orientations. The angle is similar to the other standard samples of the print parameters, 45 degrees. The downward facing surface had a mean PSE value of 4,1 which is indeed similar to the standard sample 4. However for the upward facing surface the observer tend to think that sample number 3 is similar to the standard, even though sample number 3 is less rough compared to sample 4 from the optical scanner data. The difference between those two samples was 5 μm.

The mean JND values for the different parameter of the upward and downward facing surfaces showed similarities. Angle orientation had for both sides of the sample a mean JND of 1,5 similar to the JND of 1,5 of the upward facing surface of the layer height sample series. Upward facing surface for speed and downward facing surface for layer height were close with a mean JND value of 1,4 and 1,2. The only mean JND value with had a larger difference was the downward facing surface for speed, which was a mean JND value of 1.

This study explored some new and undiscovered information in the field of haptics which can be of great use for the expanding knowledge on additive manufacturing techniques as FDM printing. It shows that humans are capable to distinguish small changes in surface roughness even though this change consists of several micrometers. The study can act as a guide to enable further haptic research on different 3D printing materials, post-process techniques and also alternative additive manufacturing techniques.

# 15. Design of communication tool

The final and last part of this project is the design of a communication tool to communicate the new information of surface roughness in FDM printing technology. The new information consists of objective and perceptual data and insights gathered during the execution of the experiments.

In the objective scanning study part of the project, each printed sample was scanned in order to record the surface profile in order to calculate the surface roughness. The recorded surface profiles were three dimensional representations of the actual surface of the samples, see figure 218.

The first direction of the design of the communication tool was the recreation of specific surface roughnesses with the use of the scanned surfaces. The surface profile recordings were imported into CAD software in order to convert the point cloud of measurement points from the scans into a 3D object. These 3D objects were then imported into slicing software Cura 2.4, a program to prepare files for 3D printing, and high quality settings were incorporated to include small details of the surface scans. The final result after 3D printing is a scaled model of the surface based on the optical scanner images. Such 3D print of a surface can be found in figure 219 which clearly shows the stair stepping effect caused by the buildup of layer with FDM printing technology at an angle orientation of 15 degrees. The model is scaled 5 times in order to produce an end result which clearly visualizes the change in surface quality when changing the angle orientation. Any smaller and the surface representations would lose details and eventually the surface would not be reproducible anymore.

The next direction for the surface roughness communication tool was inspired by the current tools to communicate roughness in the industry. According ISO standard 8503-1 roughness comparators are for example used in the metal machining and injection molding industry to achieve a certain surface finish in terms of appearance and feel of an abrasive blast-cleaned surface. It is also used if an assessment has to be made of a surface. Figure 220 is an example of a roughness comparator for the surface finish of metal machining processes such as milling.

With the use of the surface profile recordings of all of the samples of the layer height, angle orientation and speed parameter such roughness comparators have been modeled. On the roughness comparator the parameter specification has been displayed as well as the measured Ra roughness from the optical scanner. Next to the specification of the settings, the modeled surface is present to enable touch and visual exploration of the surface profile. To incorporate every detail in the surface representation the connex 3 has been used for printing the roughness comparators. The connex 3 is capable of producing fine details with the resolution of 16 microns(Stratasys, 2017) by using polyjet technology, a different additive manufacturing technology. Figure 221 shows the roughness comparators produced by the connex 3 polyjet printer.

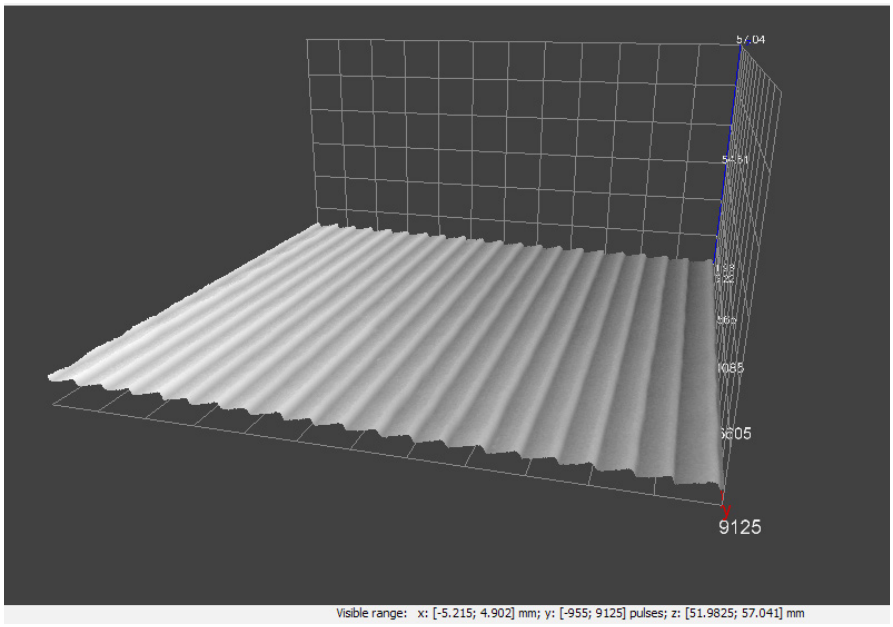


*Figure 218 3D surface profile from optical scanner*

*Figure 218*

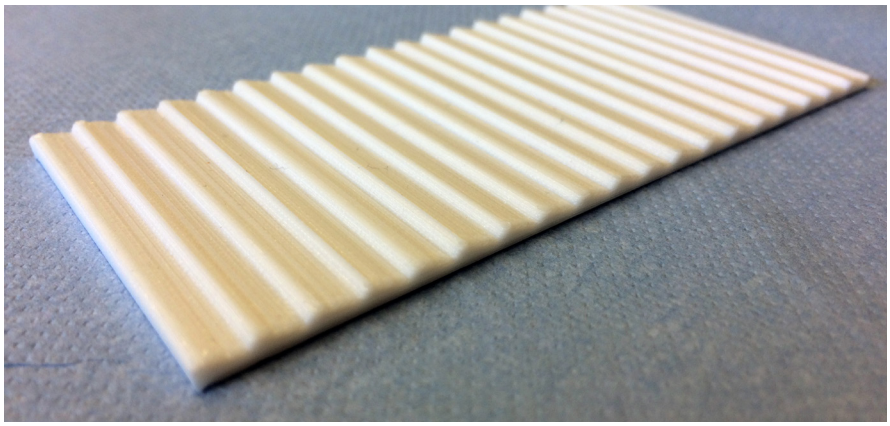

*Figure 219 FDM reproduced surface profile from optical scanner scan*

*Figure 219*


*Figure 220 Roughness comparator for surface finish of milling process*

*Figure 220*

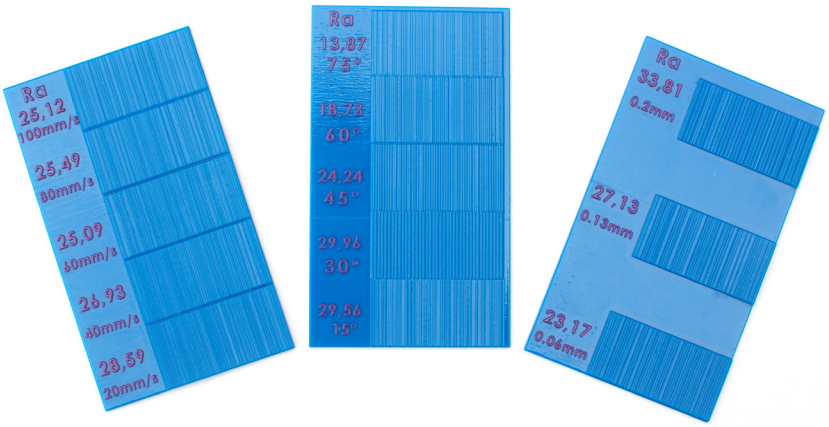


*Figure 221 FDM roughness comparators produced by connex 3*

*Figure 221*

# 16. Design iterations

The concept of creating surface roughness comparators has been chosen to be further developed as it is a clear and known tool to communicate roughness. And users of the comparators are able to explore the surface finish with their senses, which was a big part of this project. This section will describe the iteration process from the initial idea of FDM surface roughness comparators to the final model.

The surface roughness comparators produced with the connex 3 by polyjet technology was an experiment to investigate whether such micrometer details could be reproduced with additive manufacturing. As this project is about the FDM printing technology and in cooperation of the Technical University of Delft with Ultimaker BV, the final model will be produced with ultimaker 3D printers. The same roughness comparators produced by the connex 3 were printed on the ultimaker 3D printer, however the ultimaker was not capable to produce the required resolution and therefore another solution needed to be explored.

After the initial idea of the roughness comparator was not suitable for FDM printing, a different approach has been taken. In the initial idea all surfaces were printed flat even though the reproduced surfaces were taken from data of surfaces printed at a certain angle. In order to achieve the same result, the FDM printed surfaces have to be printed at the angle and settings during the printing process. Afterwards the printed surfaces could be rotated to a flat position in order to create a flat roughness comparator. To enable this rotation a hinge is required which can be directly integrated and printed without extra effort. With this idea in mind, the first prototypes were created which can be seen in figure 222. It visualizes the opportunities for this model in terms of variability in material, color and dual print possibilities. The far right model has all surfaces rotated to a flat position.

Figure 223 displays some extra viewing angles of the FDM surface roughness comparator concept. What can be seen is that the 30 degree angle orientation has side supports. These are included to enable some stability during printing of the 30 degree angle. As the supports are modeled as single walled side supports, these can be removed easily without leaving any inconsistencies to the surface. The single walled side supports have been used in the printing process of the objective experiment samples.
Also branding and secondary information of the model is possible by including letters in the CAD model. In the prototype the angle orientation is displayed in order to inform observers of the roughness comparators. And most important, the models were suitable for FDM printing technology.

In the next iteration, the idea of rotating the surfaces to a flat position has been further investigated. As the objective characterization part of the project consisted of the investigation of upward and downward facing surface, both surfaces have to be present in the roughness comparator. In the previous model the downward facing surfaces were not able to be explored by observers as the surface could not be rotated 180 degrees. In the new model created after this insight a 180 degree rotation is possible. This model can be seen in figure 224 and shows the position in which the model is printed at. After printing the surfaces can be rotated to the left to flatten all of the upward facing surfaces. In order to flatten the downward facing surfaces the surfaces have to be rotated to the right. In this position the quality of the overhanging(downward facing) surface can be inspected at different printing angles.


*Figure 222*

*Figure 222 FDM roughness comparator prototypes with hinges*

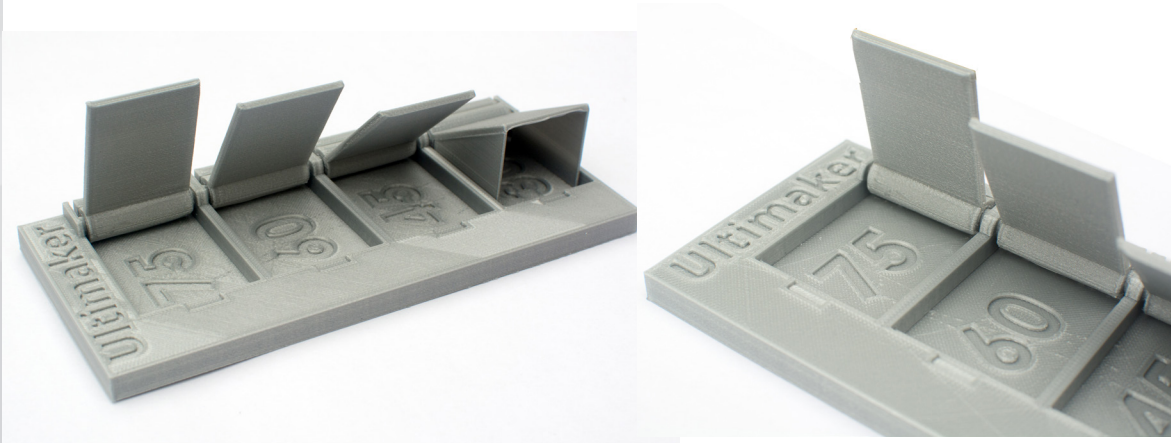


*Figure 223*

*Figure 223 Roughness comparator prototype details*

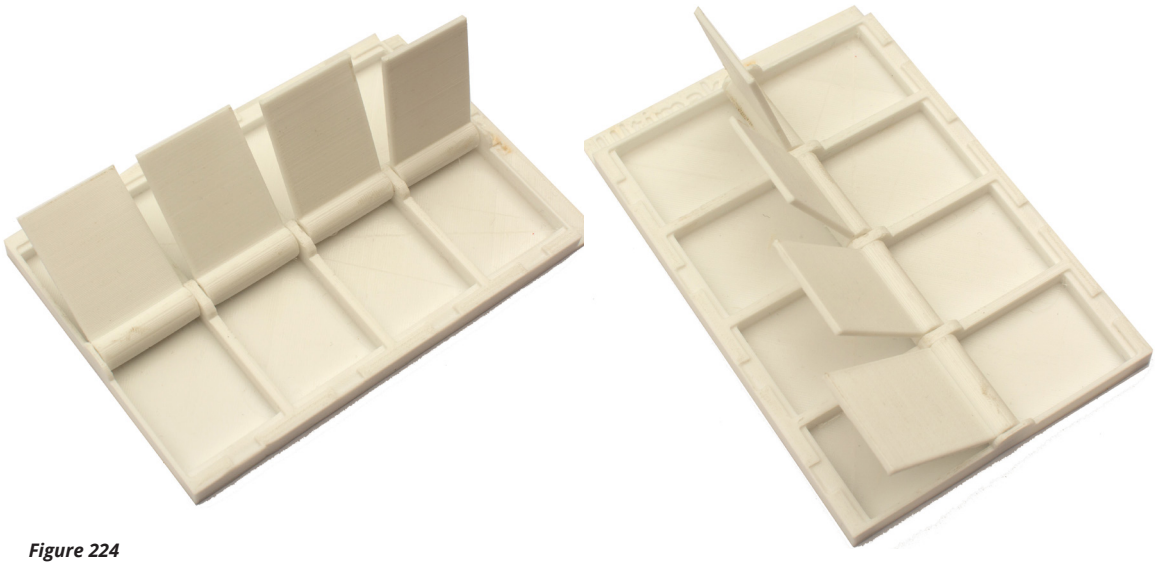

*Figure 224*

*Figure 224 Double sided roughness comparator*

This model was a big step towards the final model as it was printed successfully with the FDM printing technology using ultimaker 3D printers. It also incorporates the insights from the two studies of this project, as the model can be printed with different printing parameters and explored perceptually by the users of the model. The standard model included 75, 60, 45 and 30 degree angle orientations however this can be changed for the demands of the users as well as layer height, speed, material etc.

Also some other versions have been tested to see the potential of the model. For example the combination of PLA and PVA, a water soluble material, can be used to let users experience the benefit of using PVA as build support. When the support material is solved, the surface shows no imperfections and otherwise non-printable steep angles can be printed without problems. Figure 225 shows the result of a PLA and PVA combination of a model which was printed at a 10 degree orientation. Both the upward and downward facing surfaces are printed successfully.

Another test which shows the opportunities of the model can be found in figure 226. It is a smaller version of the bigger model just to reduce the printing time for the exploration. The model has 4 surfaces which are printed around the critical angle when loose printing lines will appear. The range of the angles were 30, 35, 40 and 45 degrees seen from the horizontal plane. The 30 and 35 degree orientation clearly show loose printing lines for the downward facing surface. For the 40 and 45 degree orientation the loose printing lines are not present which indicates that these angle orientation would be printable without extra support. These models can also be printed with different materials, layer heights, speeds and temperatures to see the influence on the downward facing surface quality.

As mentioned earlier, the user can adjust the settings for printing the model as well as altering the angle orientation of the surfaces being printed. By altering the angle orientation the user can learn about its influence on the surface roughness and overhang properties. Also, the models can be printed with different layer heights to see the influence of that parameter on the surface roughness.

Another feature is to enable the user to insert the desired surface roughness and predescribed settings will be advised to achieve such surface roughness. Suggestions on the layer height and angle orientation can be communicated to the user of the model. With this the data gathered from the optical scanner experiment is used in the final model and with the combination of perceptual exploration of the user both aspects of the project are present in the model.

Figure 227 gives an impression on the development towards the final model.

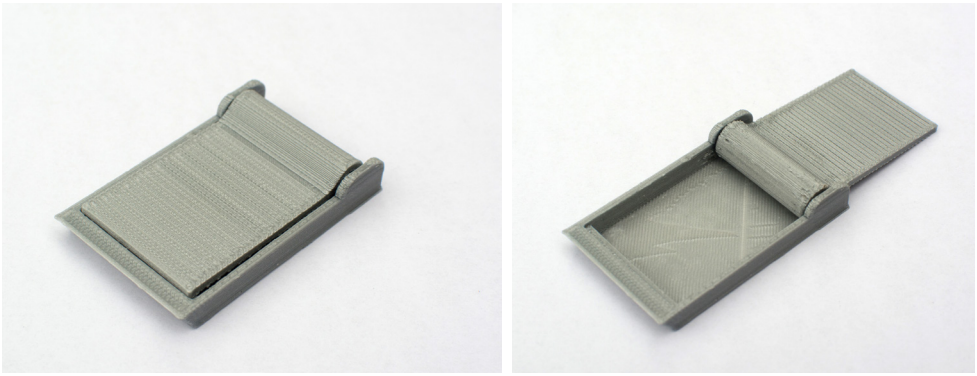

*Figure 225 PLA/PVA material combination for 10 degree angle*

*Figure 225*

*Figure 226 Critical angle visualization prototype*

*Figure 226*

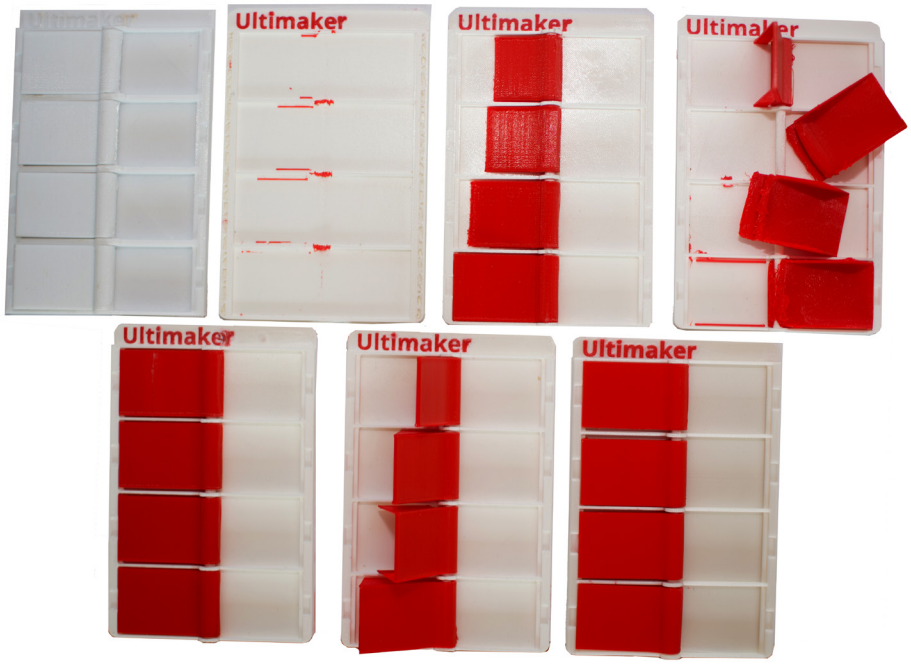


*Figure 227 Iterations of the final model*

*Figure 227*

# 17. Final Design

The final model has come together from all of the design iterations with respect to size, shape, hinge air gap, dual color opportunities and different versions for layer heights of 0.06 mm, 0.1 mm, 0.15 mm and 0.2 mm. The design iterations which were performed are described in appendix 16 p.178. Keeping the design vision in mind and combining this with the results from the objective and perception experiments resulted in the final model to communicate roughness in FDM printing, see figure 228.

This model is printed with the roughness surfaces in various angle orientations. For the displayed model these angles are 30, 45, 60 and 75 degrees but these are adjustable for specific needs. After printing the angles in the desired angles the single walled side walls can be easily removed. By pressing the roughness surfaces to the other side the side walls and bottom surface at the hinge will be separated from the base of the model without any marks due to the specified air gap. This air gap has been investigated and specified by 3D printing different spaces between the parts and tested its adhesion. When all of the parts are separated and able to rotate freely, the single side walls can be removed. This can be done by hand or with the use of pliers for best result. Now the roughness surfaces can be flatten and rotated along the 3D printed hinges and used for exploration of surface roughness of FDM printing technologies.

With this model users of FDM printers can experience the influence of layer height and angle orientation on the surface roughness perceptually by printing different models with other settings. As these parameters were most significant in influencing the surface roughness.

The model can be printed in different color and material combinations to explore various configurations as some materials have different properties regarding overhang quality for example.

Another feature could be the integration in Cura slicing software in which the user can specify the desired surface roughness. The program will advise the user on the parameter combinations suitable for obtaining such desired surface roughness. Giving the user some influence on the surface roughness.

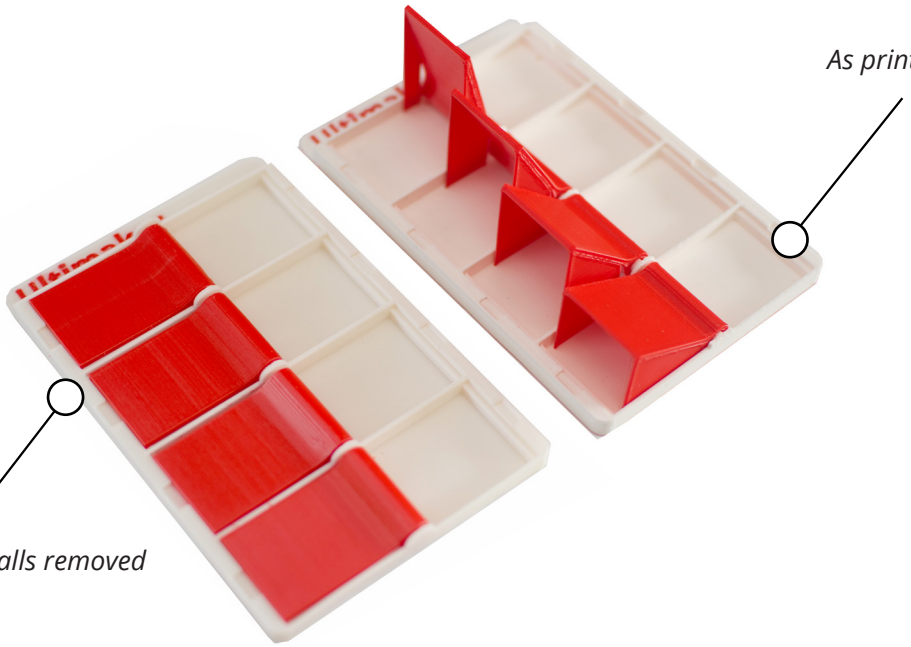

*As printed on buildplate*

*Model after support walls removed*


*Figure 228 Overview final model for roughness communication*

*Figure 228*